Investigations on the formation of linear poly(2-oxazolidinone)

Dissertation

With the Aim of Achieving the Doctoral Degree at the Faculty of Mathematics, Informatics and Natural Sciences

Submitted to the Department of Chemistry

Institute of Technical and Macromolecular Chemistry

University of Hamburg

Fabian Benedikt Ratzke

Hamburg 2025

Date of Disputation:

21.11.2025

Evaluation:

1st Evaluator: Prof. Dr. G. A. Luinstra

2nd Evaluator: Prof. Dr. B. Eling

Examination commission:

1st Prof. Dr. G. A. Luinstra

2nd Prof. Dr. M. Fischer

3rd Priv. Doz. Dr. C. Wutz

Table of Contents

List of abbreviations

[A-A]	Concentration of monomer A-A
[B-B]	Concentration of monomer B-B
BADGE	Bisphenol A diglycidyl ether
BMIM	1-Butyl-3-methyl-imidazolium
BMPC	1-Butyl-1-methyl piperidinium chloride
$\boldsymbol{b}_\mathrm{p}$	Boiling point
$\boldsymbol{b}_{NCO}$	Molality of isocyanate
BzCl	Benzoyl chloride
CDI	Carbodiimide
DCC	Dicyclohexyl carbodiimide
DCM	Dichloromethane
DIBIS	Diglycol bischloro formiate
DMAP	4-(Dimethylamino)-pyridine
DMC	Double metal cyanide
DMF	Dimethyl formamide
DMI	Dimethyl imidazolidinone
DMPU	Dimethyl propylene urea
DMSO	Dimethyl sulfoxide
DSC	Differential scanning calorimetry
EEW	Epoxide equivalent weight
EMIM	1-Ethyl-1-methyl imidazolium
ESI-MS	Electro spray ionisation mass spectrometry
FT	Fourier transformation
HMBC	Heteronuclear multiple bond correlation
HPLC	High-performance liquid chromatography
$\boldsymbol{I}$	Integral
IGATED	Inverse-gated
Index	Measure for stoichiometry used in PU chemistry.
$\boldsymbol{I}_{\mathrm{per\_proton}}$	Integral per proton
IR	Infrared
$\boldsymbol{k}$	Rate constant
K	Equilibrium constant
LC-MS	Liquid chromatography mass spectrometry
MALDI	Matrix-assisted laser desorption ionisation
MDI	Methylene diphenyl diisocyanate
MEKO	Methyl ethyl ketoxime
$\boldsymbol{M}_\mathrm{n}$	Number-average molar mass
MPPO	3-methyl-1-phenyl-2-phospholene-1-oxide
$\boldsymbol{M}_\mathrm{w}$	Weight-average molar mass
MWD	Molecular Weight Distribution
NCO	Isocyanate
NHC	N-heterocyclic carbenes
$\boldsymbol{n}$**-mer**	Oligo- or polymer with n repeating units

NMP	N-methylpyrrolidone
NMR	Nuclear Magnetic Resonance
OCGE	*o*-Cresyl glycidyl ether
o-**DCB**	*o*-Dichlorobenzene
OXA	Oxazolidinone
p	Conversion
PDI	Polydispersity index
Ph4PBr	Tetraphenyl phosphonium bromide
Ph4PCl	Tetraphenyl phosphonium chloride
PIR	Polyisocyanurate
POX	Poly(oxazolidine-2-one)
PP	Polypropylene
p-**TI**	*p*-Tolyl isocyanate
PU	Polyurethane
PVC	Polyvinyl chloride
PXRD	Powder X-ray diffraction
r	Reaction rate
$r_{A\text{-}A,B\text{-}B}$	Ratio of A-A to B-B monomer
$r_{average}$	Averaged rate of epoxide and isocyanate conversion and oxazolidinone formation
r_c	Rate of cyclisation
r_g	Rate of chain growth
R_p	Rate of polymerisation
s.c.	Solid content
SEC	Size exclusion chromatography
TBPO	Tributyl phosphine oxide
TDI	Toluene diisocyanate
T_g	Glass transition temperature
TGA	Thermogravimetric analysis
TOPO	Trioctyl phosphine oxide
TPPO	Triphenyl phosphine oxide
TPU	Thermoplastic Polyurethane
X_n	Number average degree of polymerisation
X_w	Weight average degree of polymerisation

1. Zusammenfassung

Poly(oxazolidin-2-on)e (POX)   stellen   eine   Klasse   von   vielversprechenden Hochleistungspolymeren dar, die im Vergleich zu herkömmlichen Polyurethanen eine bessere mechanische   und   thermische   Stabilität   aufweisen.   POX   wurden   durch Lösungsmittelpolymerisation von 4,4'-Methylendiphenyldiisocyanat (MDI) und Bisphenol-A-Diglycidylether (BADGE) dargestellt. Hohe Umsätze der Reaktanten sind erforderlich, um thermoplastisches POX mit hoher Molmasse zu erhalten, wobei die oxazolidinonbildende Reaktion hoch chemoselektiv sein muss. Die Bildung von Nebenprodukten (Chemoselektivität) und die Regioselektivität wurden in einem Modellsystem unter Verwendung von monofunktionellem Epoxid und Isocyanat untersucht, welche BADGE und 4,4' MDI ähnlich sind (*o*-Cresylglycidylether (OCGE) bzw. *p*-Tolylisocyanat (*p*-TI)). Ziel dieser Studie war es, die Grundlagen der Oxazolidinon-Chemie zu erforschen. Die Reaktion wurde in Lösung und in Gegenwart eines Halogenidkatalysators durchgeführt. Isocyanurat und Oxazolidinimin wurden mittels Spektroskopie und Spektrometrie als wichtigste Nebenprodukte identifiziert. Isocyanurat wurde teilweise durch das Alkoxid zersetzt, das in einer Ringöffnungsreaktion des Epoxids und des Halogenidkatalysators gebildet wurde, wodurch Oxazolidinon erhalten wurde. Die Bildung von Oxazolidinimin war irreversibel. Die Reaktionsbedingungen beeinflussten die Regioselektivität und die Bildung von Nebenprodukten erheblich.

Das Parameter-Screening verdeutlichte den wesentlichen Einfluss der Temperatur, des Lösungsmittels und des Katalysators auf den Verlauf der Reaktion. Hohe Reaktionstemperaturen verringerten den Isocyanurat-Anteil im Endprodukt sowie die Selektivität zum 3-(*p*-tolyl)-5-((*o*-tolyloxy)methyl)oxazolidin-2-on. Die Verwendung eines hochpolaren Lösungsmittels, wie Sulfolan oder Dimethylenpropylenurea (DMPU), reduzierte ebenfalls die Isocyanuratbildung sowie die Regioselektivität. Zinkchloridkomplexe, Ammonium- und Phosphoniumchloride als Katalysatoren führten zu einer geringeren Nebenproduktbildung im Vergleich zu ähnlichen Eisen (III)- und Bismut (III)chloridkomplexen. Die Zugabe von monofunktionellem Harnstoff mit aktiven N-H-Gruppen, wie z.B. 1,3-di-*p*-Tolylharnstoff, erhöhte die Chemoselektivität bezüglich des Oxazolidinons. Die Bildung von Oxazolidinimin war weitgehend unabhängig von den gewählten Reaktionsbedingungen.

Die kinetische Analyse, auf Basis von BADGE und 4,4'-MDI, ergab Reaktionsordnungen bezüglich der Katalysator- und Isocyanatkonzentration von 0.73 bzw. 0.25. Der geschwindigkeitsbestimmende Schritt ist demnach die Bildung des Alkoxids, was mit der Literatur übereinstimmt.[1]

Die Bedingungen der Polymerisation wurden auf der Grundlage der aus dem Modellsystem und der kinetischen Analyse gewonnenen Erkenntnisse optimiert. Höhere Molekulargewichte wurden durch das Lösen des Katalysators in einer initial minimalen Menge Sulfolan und die Zugabe der verbleibenden 85 bis 95% Sulfolan zusammen mit den Monomeren im Semi-Batch-Verfahren erreicht. 1-Butyl-1-methylpiperidiniumchlorid (BMPC) und Tetraphenylphosphoniumchlorid erwiesen sich als die meistgeeigneten Katalysatoren, insbesondere in der Kombination mit 1,3-di-*p*-Tolylharnstoff als Co-Katalysator.

Es wurde ein Scale-up auf einen 1 L Edelstahlreaktor durchgeführt. Das durchschnittliche Molekulargewicht des Produkts war innerhalb des untersuchten Bereichs weitgehend unabhängig von der Reaktionstemperatur. Lediglich die Menge des zyklisierten Polymers mit niedrigem Molekulargewicht nahm bei höheren Temperaturen zu. Die Stöchiometrie zwischen den AA/BB-Reaktanden korreliert mit dem mittels CAROTHERS-Gleichung berechneten M_n unter der Annahme eines Umsatzes p von 98 %.

Feste Polymere mit hohem Molekulargewicht wurden durch Ausfällung der Polymerlösungen in einem Nichtlösungsmittel gewonnen. An den erhaltenen amorphen, beigen Pulvern wurden DSC- und TGA-Messungen durchgeführt. Die Polymere wiesen eine amorphe Struktur auf und besaßen eine Glasübergangstemperatur T_g von etwa 170 °C. Der Zersetzungsbeginn trat bei 330 °C auf, wobei die maximale Zersetzungsgeschwindigkeit bei circa 400 °C erreicht wurde.

2. Abstract

Poly(oxazolidine-2-one)s (POX) represent a class of promising high-performance polymers, exhibiting superior mechanical and thermal stability compared to conventional polyurethanes. POX was prepared by solution polymerisation of 4,4'-methylene diphenyl diisocyanate (MDI) and bisphenol A diglycidyl ether (BADGE). High conversions of the reactants are required to obtain thermoplastic, high molar mass POX and the oxazolidinone forming reaction must exhibit high chemoselectivity. The formation of side products and the regioselectivity within a model system was studied using mono-functional epoxy and isocyanate that mimic BADGE and 4,4'-MDI, viz. *o*-cresyl glycidyl ether (OCGE) and *p*-tolyl isocyanate (*p*-TI), respectively. This study aimed to elucidate the fundamental oxazolidinone chemistry. The reaction was carried out in solution and in the presence of a halide catalyst. Isocyanurate and oxazolidineimine were identified as the major side products using spectroscopy and spectrometry. Isocyanurate underwent partial decomposition by the alkoxide formed in a ring-opening reaction of the epoxide and the halide catalyst, leading to the formation of oxazolidinone. The formation of oxazolidine imine was

irreversible. The reaction conditions significantly influenced regioselectivity and side product formation.

The parameter screening revealed the substantial impact of the temperature, the solvent and the catalyst on the course of the reaction. Increasing the reaction temperature reduced the quantity of isocyanurate and the regioselectivity toward 3-(*p*-tolyl)-5-((*o*-tolyloxy)methyl)oxazolidine-2-one. The use of polar solvents like sulfolane and dimethyl propylene urea (DMPU) reduced the isocyanurate formation. Zinc, ammonium and phosphonium-based chloride catalysts exhibited a reduced formation of side products in comparison to iron (III) and bismuth (III) chloride complexes. The addition of low molecular weight urea additives bearing one or two N-H groups, such as 1,3-di-*p*-tolylurea, improved the chemoselectivity towards oxazolidinone. The formation of oxazolidine imine was largely independent of the reaction conditions.

The kinetic analysis, using bifunctional monomers (BADGE and 4,4'-MDI), proved the partial reaction orders for the catalyst and isocyanate concentration to be 0.73 and 0.25, respectively. The rate-determining step is, therefore, the alkoxide formation, which aligns with the literature.[1]

The reaction system was optimized to achieve a high molecular weight polymer in the subsequent step. Higher molecular weights could be accomplished using a minimal amount of sulfolane to initially dissolve the catalyst. The remaining quantity of solvent (85% to 95% of the total solvent) was added alongside the monomers in a semi-batch process. 1-Butyl-1-methyl piperidinium chloride (BMPC) and tetraphenyl phosphonium chloride emerged as the most suitable catalysts, particularly in combination with 1,3-di-*p*-tolylurea as a co-catalyst.

A scale-up to a 1 L stainless stell reactor was performed. The average molecular weight of the product was largely independent of the reaction temperature within the studied range. The formation of low-molecular-mass cyclic compounds increased at elevated temperatures. The stoichiometry between the AA/BB reagents correlates with the M_n calculated using the Carothers equation, assuming a conversion *p* of 98%.

Solid, high-molecular-weight polymers were obtained by precipitation of the polymer solutions in a non-solvent. The resultant powders were subjected to DSC and TGA. The polymers demonstrated an amorphous structure and exhibited glass transition temperatures of about 170°C. The decomposition onset occurred at 330 °C, with the maximum decomposition rate at about 400 °C.
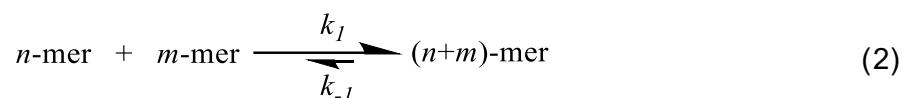
3. Introduction and background

3.1.   **Polyaddition**

The formation of poly(oxazolidine-2-one) (POX) is a step-growth polymerisation of the AA-BB type.

$$A{-}A \; + \; B{-}B \xrightarrow{\text{cat.}} {\Big[}A{-}A{-}B{-}B{\Big]}_n \tag{1}$$
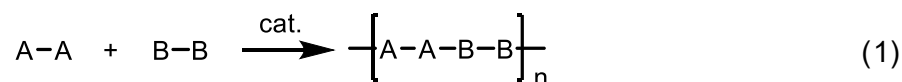
A high molar mass is achieved only at high conversions.[2]

$$n\text{-mer} \; + \; m\text{-mer} \underset{k_{-1}}{\overset{k_1}{\rightleftharpoons}} (n{+}m)\text{-mer} \tag{2}$$

No small molecule elimination occurs in the polyaddition, which results in a high atom efficiency. The collision rate and the resulting reactivity of a terminal functional group of an n-mer are assumed to be similar to those of a monomer. The diffusion rate decreases with increasing size of the *n*-mer, which could alter the reactivity.[2] This does not affect the reactivity as only one in 10^{13} collisions causes a reaction.[3]

The rate of polymerisation r_p in an AA-BB polymerisation can generically be described by a rate law containing the concentration of the monomers and, if required, a catalyst.

$$r_p = k_1 \cdot [\text{catalyst}]^x \cdot [\text{AA}]^y \cdot [\text{BB}]^z \tag{3}$$

k_1 is taken as the rate constant of the polymerisation and k_{-1} is the rate constant of the depolymerisation; *x, y* and *z* are the partial orders of the reactants. An equilibrium constant K is expressed as the quotient of k_1 over k_{-1}.

$$K = \frac{k_1}{k_{-1}} \tag{4}$$

The number-average degree of polymerisation X_n can be calculated based on the conversion *p* of the monomers (eq. 5).

$$X_n = \frac{1}{1-p} \tag{5}$$

The ratio $r_{A-A,B-B}$ of both monomers is relevant for the polymerisation grade of AA-BB systems and an extension of this equation takes that into account (eq. 6).

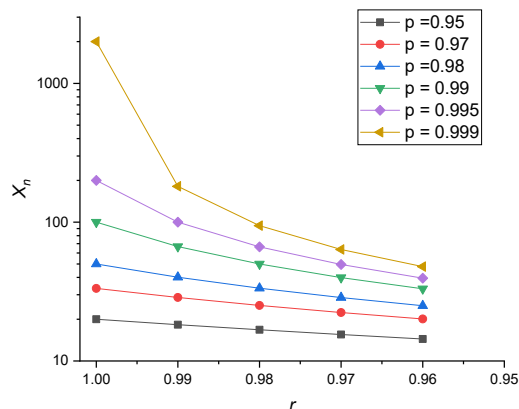$$X_n = \frac{1 + r_{A-A,B-B}}{1 + r_{A-A,B-B} - 2rp}$$

(6)

Figure 1: Dependency of X_n on the conversion p and the ratio of monomers $r_{A-A,B-B}$.[2]

High molar mass polymers in step growth polymerisations are only obtained if the reactants are used in stoichiometric amounts and high conversion is achieved (Figure 1). This contrasts with chain growth polymerisations (Figure 2).
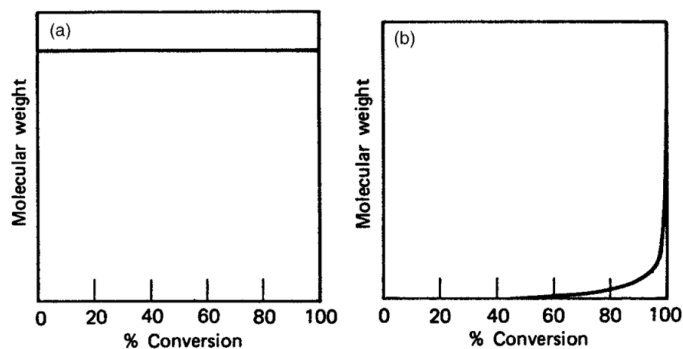
Figure 2: Molar mass evolution with increasing conversion in chain polymerisations (a) and step growth polymerisations (b).[2]

The polydispersity index (PDI) is the ratio of M_w to M_n or X_w to X_n (eq. 8). It represents the width of the molar mass distribution of the polymer. A conversion p of one results in a PDI of two in ideal step growth polymerisations of AB systems.[2]

$$X_w = \frac{1+p}{1-p}$$

(7)

$$\text{PDI} = \frac{X_\text{w}}{X_\text{n}} = 1 + p \tag{8}$$

The monomer concentration decreases with progressing polymerisation (self-dilution). Cycles may be formed at high conversions because the main active species are the chain end groups. The X_n of the cycles is determined by the cyclisation rate r_c and the growth rate r_g as an extension to Equation 5 at equimolar stoichiometry (eq. 9); α describes the ratio of r_g to r_c and X is an experimental constant larger than one. The value of X depends strongly on the reaction conditions chosen.[4]

$$X_\text{n} = \frac{1}{1 - p \cdot \left(1 - \frac{1}{X^\alpha}\right)} \tag{9}$$

The high self-dilution can lead to an increase in cyclisation in a semi-batch process under monomer-starving conditions because of the limited growth rate.

Interfacial polymerisation can be considered a subtype of step-growth polymerisations. The polymer is formed at the interface between two immiscible phases.[5] An insoluble polymer film is obtained that limits the diffusion of the monomers and catalyst across the interface. A lower polymerisation rate is the consequence. Higher space-time yields are obtained by continuously removing the film, creating a new surface. The polymer formation is essentially irreversible because of the higher enthalpy decrease chosen. The irreversibility and high probability of growing chains to react with each other result in the formation of higher molar mass polymers. Linear, high molar mass polyurethanes could be obtained using interfacial polycondensation of diamines and bischloroformates. The PDI strongly depends on the reaction conditions and PDIs from one to more than two are obtainable. Complex kinetics underlie these polymerisations depending on the concentration, reactivity, stoichiometry, solvent pH, diffusion parameters and reaction product removal.[6,7]

3.2.   **Polyurethane and isocyanate chemistry**

Aliphatic and aromatic isocyanates are commercially relevant in polyurethane (PU) production. The aliphatic isocyanates possess lower reactivity, but the PU thereof shows improved weatherability and thermal stability.[8] Aromatic isocyanates are more reactive, less expensive than their aliphatic counterparts and have a market share of more than 90% (Figure 3).[9]
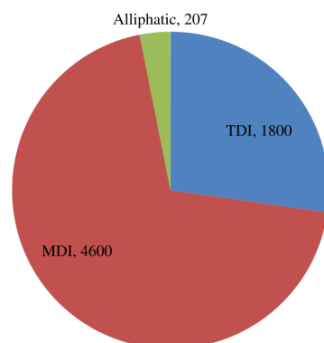
Figure 3: The production of the aromatic isocyanates TDI and MDI and aliphatic isocyanates in 2011 (values given in metric tons).[9]

The toxicity of isocyanates depends strongly on their vapor pressure. Toluene diisocyanate (TDI), hexamethylene diisocyanate (HDI) and isophorone diisocyanate (IPDI) have a high vapor pressure and high toxicity. Methylene diisocyanate (MDI) and polymeric MDI possess a low vapor pressure enabling easier and safer handling.[10]
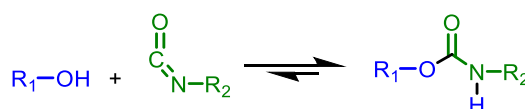
Reactions of isocyanates

The high reactivity of isocyanates can be attributed to the high electrophilicity of the central carbon atom, making it susceptible to nucleophilic attack. The delocalisation of the negative charge at the nitrogen atom in aromatic isocyanates is extended into the aromatic system (-M-effect). Their reactivity is consequently up to 100 times higher than that of aliphatic isocyanates. Isocyanates can react with compounds that contain active hydrogen atoms (e.g., -OH, -NH) according to the general scheme below.
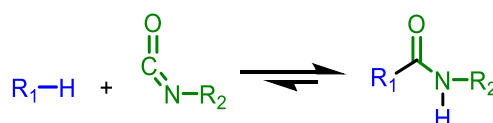
*Scheme 1: Reaction of isocyanate with a compound bearing an active hydrogen.*

The formation of urethane and urea is based on a sigma bond metathesis, in which the active hydrogens bond to the nitrogen atom.[8] Urethane groups are generated in the reaction between alcohol and isocyanate. The nucleophilic oxygen attacks the isocyanate at the electrophilic carbon atom. This reaction proceeds quickly and can take place even at room temperature.

Scheme 2: Formation of urethane by the reaction of alcohol with isocyanate, the so-called gel reaction.

The urethane formation is an equilibrium reaction. The reverse reaction dominates at higher temperatures. The rate of the reverse reaction depends strongly on the materials involved. Urethanes from aromatic isocyanates and aliphatic polyols usually start to decompose noticeably over 200 °C. The decomposition of urethanes produced from aliphatic isocyanates and polyols is observable above 250 °C.[10–12]

Isocyanates react with water as well. A carbamic acid will be formed that decomposes into an amine and carbon dioxide. Urea is formed in the reaction of the amine and a second isocyanate. The amine-isocyanate reaction is about 100 to 1000 times faster than the urethane forming reaction. The isocyanate-water reaction is referred to as the blowing reaction, whereas the urethane reaction is termed the gel reaction in PU foam reactions.[10]
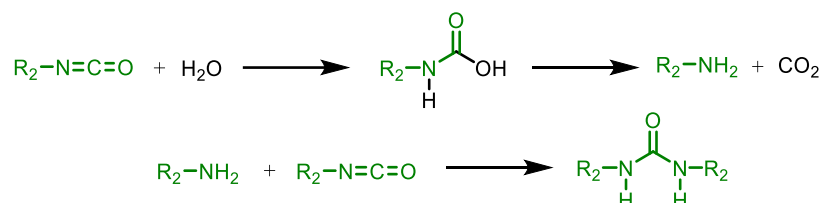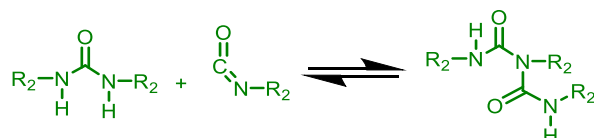

Scheme 3: Formation of an amine in the reaction of water with isocyanate releasing carbon dioxide (top). The amine formed will react with isocyanate, yielding urea (bottom).

Allophanate groups are formed in the reaction of urethane and isocyanate. The formation is also reversible and the decomposition of allophanate starts at about 150 °C in the absence of a catalyst.[10]
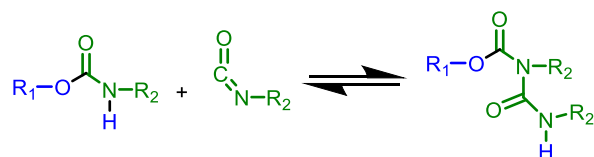
*Scheme 4: Reaction of isocyanate with the active hydrogen of a urethane to form an allophanate group.*

Biuret groups are the reaction product of isocyanate with urea, which are usually formed between 100 °C and 150 °C. Decomposition occurs at higher temperatures than that for allophanate.[10]

Scheme 5: Formation of a biuret group from the reaction of a disubstituted urea and an isocyanate function.

Isocyanates may undergo cyclisation reactions. Uretdione (dimer) can be formed in the absence of a catalyst and the reaction already takes place at room temperature.[9] They are formed

reversibly in a [2+2]-cycloaddition reaction. Nucleophilic catalysts can increase the reaction rate significantly. The decomposition of uretdione occurs at temperatures above 150°C. Nucleophilic catalysts are required for isocyanurate (trimer) formation.[13] Trimer is the most thermally stable cyclisation product. Isocyanurate formation can lead to crosslinking when using polyfunctional isocyanates.[9]
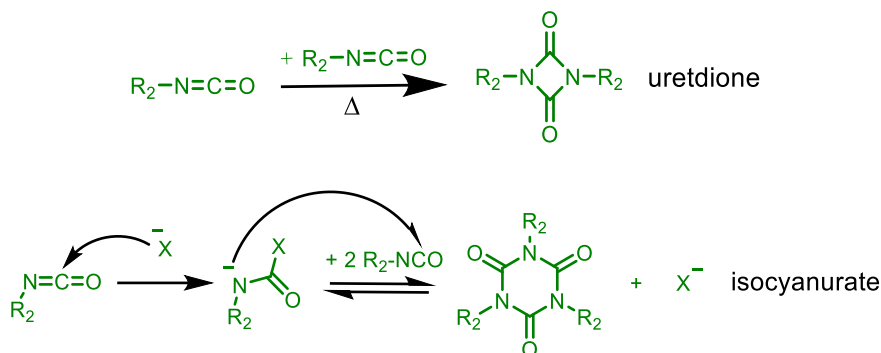
Scheme 6: The uncatalysed cyclisation of isocyanate yielding the dimer uretdione (top). The trimer isocyanurate is formed under nucleophilic catalysis conditions (bottom).

Carbodiimide formation is commercially used for the MDI modification to decrease its melting point for easier handling. A catalyst is required for the carbodiimide formation which ultimately leads to the uretonimine-modified MDI. 3-methyl-1-phenyl-2-phospholene-1-oxide (MPPO) is the most applied catalyst for carbodiimide formation, but other pentavalent phosphorous compounds can also be used.[14,15] The reaction pathway involves the oxygen atom of the catalyst attacking the isocyanate carbon atom. Carbon dioxide is released subsequently, yielding a phosphoranylidene amine as an intermediate. Carbodiimide is finally formed in the reaction with a second isocyanate, regenerating the catalyst.[16] Carbodiimide can also be formed at high temperatures in the absence of a catalyst.[17]
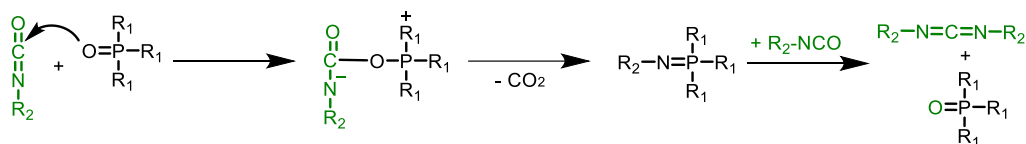
Scheme 7: Phosphine oxide catalyzed carbodiimide formation of a monofunctional isocyanate.[14]

Polyurethanes

Polyurethanes (PU) are obtained in the reaction of polyisocyanates and polyols. Otto Bayer introduced this polymerisation in 1937.[8,10] The polyols are usually polyetherols or polyesterols with a molecular weight ranging from 200 to 6000 g·mol^{-1}.[18]

Polyurethanes can be tailored to their properties for a wide range of applications. PU products are flexible foams, rigid foams, elastomers, thermoplastics, coatings, adhesives, etc. Typical PU products are mattresses (flexible and viscoelastic foams), insulation materials (rigid foams), footwear (elastomers), or artificial leather (thermoplastics). PU products are also widely used in automotive applications, such as interior trim, side panels and shock absorbers.[19] Tailoring of PU foams can be performed by adjusting the catalyst system. It balances the reaction rates of the gel and the blowing reaction. The polymer is formed in the gel reaction (Scheme 2). Carbon dioxide is released in the blowing reaction (Scheme 3). Small nuclei are generated by intense mixing of the polyol and isocyanate compound, which expand. Flexible foams contain open cells and rigid foams bear the entrapped gas in closed cells. Chemical blowing describes the use of the blowing reaction to obtain the cavities. Physical blowing is the process of the evaporation of a compound with a high vapour pressure, such as pentane. This will lead to a similar expansion of the nuclei.

The stoichiometry is highly relevant as PU formation is a polyaddition reaction. The so-called "index" is a way to express the stoichiometry. An index of 100 describes an equimolar ratio of reactants. Indices over 100 indicate an excess of isocyanate over the second reactive compound (e.g., alcohol or epoxide). Index 150 thus describes a ratio of 1.5:1 of isocyanate to the isocyanate-reactive compound.

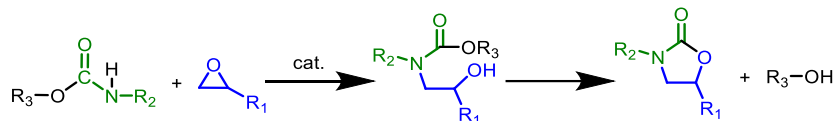## 3.3. **Poly(oxazolidine-2-one)**

1,2-Oxazolidinones, hereinafter referred to as oxazolidinone, are 5-membered rings with an internal urethane entity. They can be prepared from a wide range of starting materials. One route is the reaction of *β*-amino alcohols with phosgene, carbon dioxide, urea or isocyanates. The carbon backbone of the ring originates from the *β*-amino alcohol.[20]
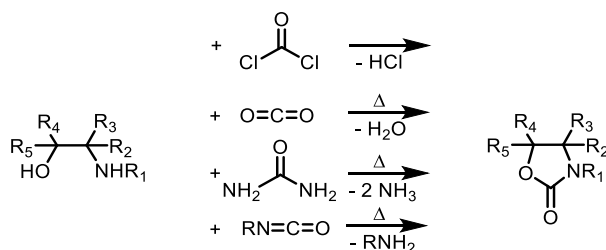
Scheme 8: Formation of oxazolidinone from β-aminoalcohols.

The reaction of a cyclic carbonate with isocyanate may yield oxazolidinones as well. Carbon dioxide is released as a side product. Oxazolidinones may also be prepared using 1,2-glycols, 1,2-dihalides, acyloins, nitrenes, oxazolines and aziridines.[20,21] These reactions often require

expensive starting materials or catalysts. The catalysed reaction of urethanes with epoxides under the release of alcohol is another pathway to oxazolidinone.[22] Nucleophiles are effective catalysts for that reaction.[20,23–25]

Scheme 9: Formation of oxazolidinone from urethane releasing an alcohol.

A common synthesis route to poly(oxazolidine-2-one)s is the reaction of bisepoxide and diisocyanate because the starting materials are readily available at low cost.[26–33] The direct reaction at temperatures between 160 and 250 °C is known.[34] Catalysis is required to achieve high oxazolidinone yields. The catalyst may be selected from LEWIS acids, such as metal halides and transition metal complexes, or amines and quaternary ammonium and phosphonium salts.[24,25,35–39] Quaternary ammonium based ionic liquids (ILs) have recently been used as catalysts. High conversion and good chemoselectivity towards oxazolidinone were obtained, for example, using 1-butyl-1-methyl piperidinium chloride (BMPC).[40] Imidazole catalysts are active at lower temperatures, which results in less trimer formation. Imidazoles, however, also catalyze the undesired homopolymerisation of epoxides.[41,42] A similar behaviour was observed for imidazolium salt catalysts.[29,43] 2-Ethyl-4-methylimidazole (EMI) as a catalyst requires a minimum temperature of 170 °C to selectively form poly(oxazolidine-2-one).[29]

Duromers based on polymers with oxazolidinone and isocyanurate moieties are known and used in (fibre-reinforced) moulding parts.[44,45] Isocyanurate-oxazolidinone copolymers containing more isocyanurate exhibited a higher glass transition temperature and a stronger shrinkage than poly(oxazolidine-2-one). High oxazolidinone contents go along with a high thermal stability of the polymer.[46]

Thermoplastic POX are prepared in bulk or in a solvent. Control over side reactions and subsequent viscosity build-up can become an issue in bulk. POX with a number-average molecular weight of about 20,000 g·mol^{-1} were reported.[47] POX prepared in bulk showed a tensile strength of 101 MPa and an elongation at break of 20%. Their tensile properties are comparable to polyethersulfones (PES) - BASF's Ultrason® E 3010 has a tensile strength of about 90 MPa and an elongation at break of about 9%.[31,48–50]

Most of the publications on POX synthesis deal with polymerisations in a solvent.[28,30,38,51,52] The glass transition temperature increases when more bulky epoxides were used.[30] The reported T_g values ranged from 156 °C to 210 °C using 1.05 equivalents bisphenol A diglycidyl ether (BADGE)

and 2,4-TDI.[50] PES, for comparison, typically possesses a T_g of about 225 °C (Ultrason® E). The formation of cyclic oligomers with molecular masses between 1,000 and 2,000 g·mol⁻¹ was observed in POX formation. The molecular mass (M_n) of the polymer calculated with and without cyclic oligomers amounted to 9,000 and 18,000 g·mol⁻¹, respectively.[30] Polymers with a molecular mass of up to 51,000 g·mol⁻¹ (M_n) were reported using stoichiometric amounts of BADGE and 4,4'-MDI. The polymerisation was performed in sulfolane using a catalytic system of an *N*-heterocyclic carbene and a LEWIS acid.[53] The suppression of branching or crosslinking reactions was essential for thermoplastic applications.

3.3.1. **General mechanism of oxazolidinone formation**

The mechanism of oxazolidinone formation involves the generation of an alkoxide from the epoxide in the first step.[1,26,54] The driving force for the ring-opening is its relatively high ring strain. The enthalpy of the ring-opening reaction is about -116 kJ·mol⁻¹.[55] Anions, cations and radicals can induce the ring-opening event. Catalysts include alkyl lithium, alkyl aluminium, alcohols, water, alkoxides, halides and phosphines.[56] Both oxirane carbon atoms of primary epoxides can be targeted by a nucleophile, leading to two differing alkoxides (Scheme 10). A secondary alkoxide (left) is formed when the least hindered carbon atom reacts with the nucleophile (pathway I). A primary alkoxide (right) is obtained if the nucleophile adds to the sterically more hindered carbon atom (pathway II).
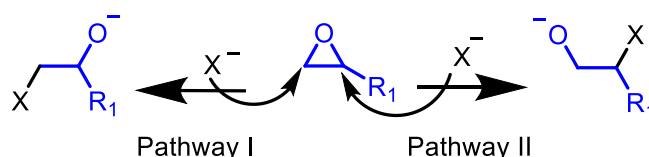
*Scheme 10: Two possible pathways of the epoxide opening by a nucleophile.*

Steric hindrance hampers the attack at the substituted carbon (pathway II) in case of a substituted epoxide and the +I-effect of an alkyl substituent R1 renders this carbon less electrophilic. Both effects tend to increase the activation energy of reaction pathway II. The nucleophilic attack is usually dominant at the sterically less hindered carbon atom, leading to a secondary alkoxide.[57]. Base-catalysed (nucleophilic) alcoholysis yields almost exclusively the product along pathway II.[58] This process may have a late transition state, in which repolarisation of the epoxide to a situation with a partial higher negative charge on the oxygen atom and consequently preferentially a partial positive charge on the secondary carbon is important.

The formation of the oxazolidinone occurs through two S_N2 -type of reactions.[30] The first step is the alkoxide formation. The intermediate alkoxide serves as a strong nucleophile, capable of reacting with the electrophilic carbon atom of the isocyanate. The resulting ionic carbamate intermediate undergoes ring closure to yield oxazolidinone, eliminating the nucleophile used to open the epoxide (X^- being a halide for example; Scheme 11).
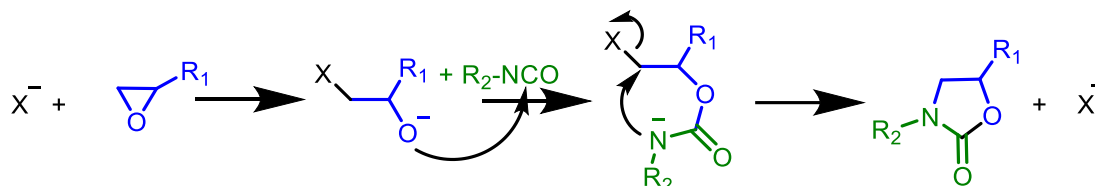
Scheme 11: Catalysed formation of oxazolidinone.[1]

An alternative pathway for the oxazolidinone formation utilises LEWIS acids as catalysts.[59] Epoxides can be opened by the action of double metal cyanides (DMC) based on zinc chloride and iron cyanide. The chloride adds to the carbon atom of the epoxide in concert with a repolarisation of the epoxide by coordination of the oxygen atom to a zinc center. A covalent bond forms between the alkoxide and the zinc atom after the opening. A formal insertion of the isocyanate into the zinc alkoxide bond yields a carbamato intermediate and oxazolidinone is obtained after ring closure under the elimination of the catalyst components.
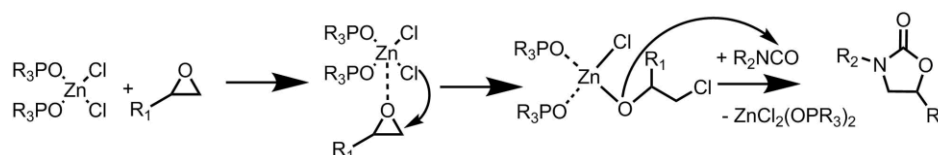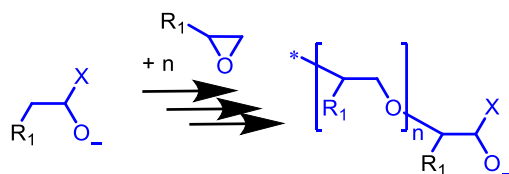

Scheme 12: Oxazolidinone formation by activation and ring-opening of epoxide by transition metal catalyst.[59]

The oxazolidinone is a 5-membered ring and more stable than a 3- or 8-membered ring.[60] Poly(oxazolidine-2-one) formation is effectively irreversible and may thus have some resemblance to interfacial polymerisations in the sense of kinetic product formation (Chapter 3.1).

3.3.2. **Known side products**

Understanding the side product formation is crucial in the successful synthesis of thermoplastic poly(oxazolidine-2-one). The primary side reactions in oxazolidinone formation from isocyanate and epoxide are (i) the formation of polyether by homopolymerisation of the epoxide and (ii) the formation of isocyanurates by trimerisation of the isocyanate. Polyether formation can be initiated by a nucleophilic attack of an intermediate alkoxide on a further epoxide (Scheme 13). Homopolymerisation of epoxides can thus occur during the oxazolidinone formation as soon as

the alkoxides are formed.[54] Epoxide homopolymerisation has been analogously reported for amine and ammonium salt catalysts.[61] The critical temperature at which polyether formation started was dependent on the catalyst: The onset temperature of a 1-Methylimidazol/BADGE system was 90 °C, appreciably higher than the 65 °C of a DMAP/BADGE system.[62] Onset temperatures as high as 340 °C were reported for phosphonium-based ionic liquid catalysts.[63]

Scheme 13: Anionic polymerisation of epoxides initiated by haloalkoxides.

Isocyanurate is formed in a trimerisation reaction of isocyanate, catalysed by a nucleophile (Chapter 3.2); in the case of oxazolidinone formation from epoxides, the alkoxide would be the nucleophile (Scheme 14).[1,64] The alkoxide-catalysed formation of the trimer is, in principle, reversible (Scheme 14). Isocyanurate formed at low temperatures can react with epoxide to form oxazolidinone upon heating.[32] This was confirmed in a study wherein oxazolidinone was formed in the reaction of isocyanurate and epoxide, catalysed by halide tetrabutyl ammonium salts. The chloride was more effective than the bromide and iodide.[57]

A trimer from bifunctional isocyanates leads to branching and potentially even to crosslinking.[65] The conversion of isocyanurate into oxazolidinone can be advantageous in the preparation of linear poly(oxazolidine-2-one). The final product may be devoid of isocyanurate pending the effectiveness of this conversion.
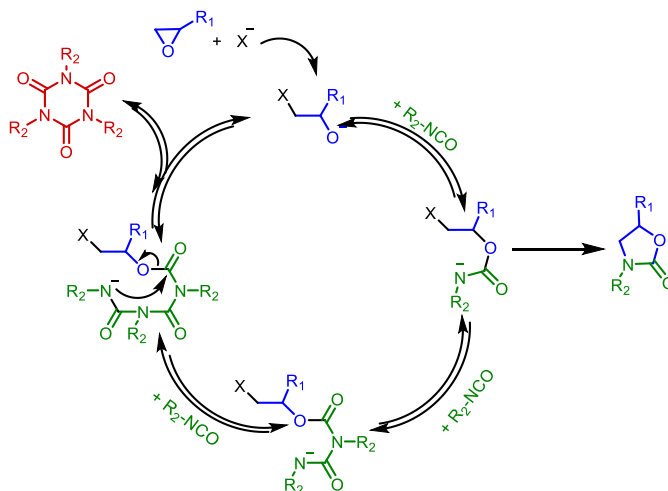
Scheme 14: Formation of isocyanurate (red) catalysed by the alkoxide formed in the ring-opening of the epoxide during oxazolidinone formation (right).

4. Motivation

The interest leading to this investigation was in developing a process for high molecular weight thermoplastic poly(oxazolidine-2-one)s (POX) utilizing bisphenol A diglycidyl ether (BADGE) and 4,4'-methylene diphenyl diisocyanate (4,4' MDI) as starting materials. The resulting polymer is reported to possess a property profile typical of engineering thermoplastic materials. It promises to provide a high added value. AABB-type addition polymerisations are also of scientific interest as the design of a high-yield, highly selective, exothermal chemical process is essential for obtaining a product with a substantial molecular weight.

Outline

The approach is divided into three sections (Figure 14). The reaction between a mono-epoxide and a mono-isocyanate was studied concerning the occurrence and extent of side reactions. The identification and quantification of side reactions, based upon the reaction conditions, are essential for determining the optimal reaction conditions for the synthesis of high molar mass polymers. The kinetics of the polymerization were mapped in the second section. The partial orders of the reactants established a basis for the polymerisation process, which constitutes the third segment. High molar mass polymers were synthesised in sample quantities of 130 g per batch under optimized conditions.
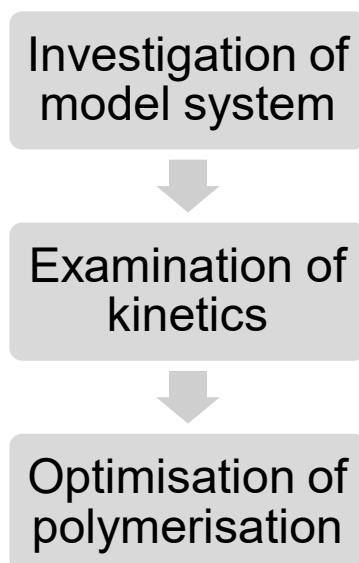

Figure 4: Approach leading to this thesis.

5. Results and Discussion

5.1. Model system

Polymer systems may be challenging to analyse at a molecular level, because their high molecular weight limits the sensitivity of the key molecular spectroscopies for detecting chemicals, i.e. mass and NMR spectroscopy. High molecular weight polymers tend to give broad NMR signals that complicate or even prevent the identification of the structure and underlying reactions. Model reactions using low molecular weight, monofunctional reactants enable an in-depth analysis of the system.

A model system based on *o*-cresyl glycidyl ether (OCGE) and *p*-tolylisocyanate (*p*-TI) was used to elucidate the reaction pathways yielding oxazolidinone. These compounds were selected due to their structural similarity to the monomers Bisphenol A diglycidyl ether (BADGE) and 4,4'-methylene diisocyanate (MDI) used in the polymerisation system (Scheme 15). OCGE was used because of the structurally identical reactive group - diglycidyl ether - and the aromatic substituent. It exhibits a lower toxicity compared to phenyl glycidyl ether. The isocyanate moiety in *p*-TI is structurally and electronically similar to that in 4,4'-MDI.
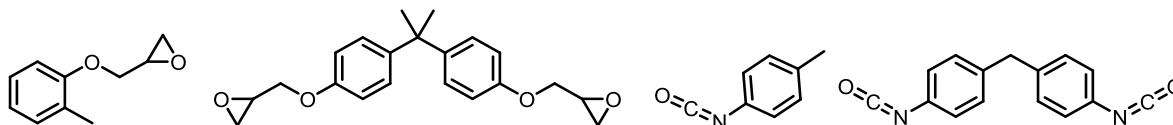
*Scheme 15: Monomers in model and polymer forming system (OCGE, BADGE, p-TI, 4,4'-MDI).*

A slight excess of epoxide was used to reduce isocyanate-isocyanate reactions such as the formation of isocyanurate. An index of 96, which corresponds to an epoxide excess of 4%, proved sufficient to reduce these isocyanate-based sid reactions.

The catalyst BMPC and the solvent sulfolane were weighed into a three-necked flask. A small amount of OCGE was added using a syringe. The monomer feed solution was prepared by weighing an index 98 mixture of OCGE and *p*-TI into a syringe. The catalyst-solvent mixture was stirred and heated to the desired temperature of 160 °C. The monomers were added over 90 min obtaining a final index of 96. This semi-batch process was employed to minimize isocyanate-related side reactions. The final solid content amounted to 67 wt%. Samples were taken from the closed vessel using a syringe for reaction monitoring and the solution was maintained for one more hour at the applied reaction temperature after the completion of the monomer addition.

The goals of this model system approach were the identification of side product formation and optimisation of the regioselectivity towards the 5-oxazolidinone.
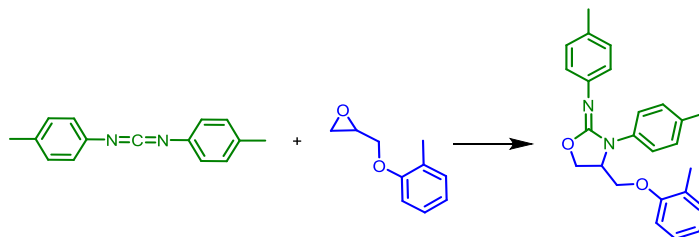
5.1.1. **Formation of oxazolidine imine**

Calculations conducted by Rebecca Sure at BASF SE provided hints for competitive carbodiimide formation in the reaction mixture. It is produced in the reaction between two isocyanate entities. The mechanistic scheme (Scheme 14) is extended to include the formation of carbodiimide and the subsequent formation of oxazolidine imine (Scheme 16).
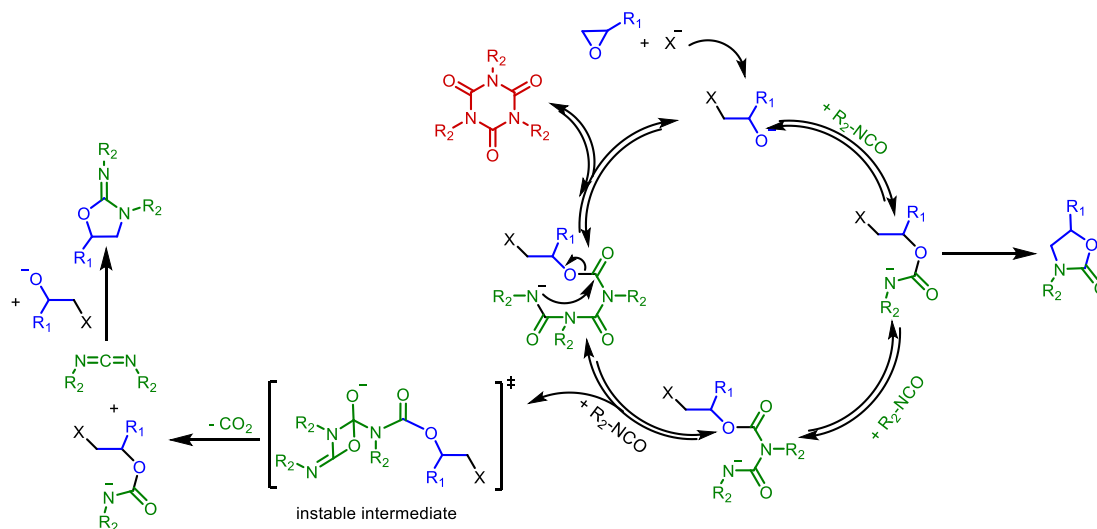
Scheme 16: Formation of the oxazolidinone (green/blue, right) and isocyanate-based side products; isocyanurate (red) and oxazolidine imine (green/blue, left).

Carbodiimide could not be detected as an intermediate product in the product mixture, because its methyl signal at 2.32 ppm overlapped with signals from other compounds in the reaction mixture. The formation of oxazolidine imine from carbodiimide and an alkoxide, as a secondary product, is consistent with the intermediate CDI formation (Scheme 17). The oxazolidine imine itself could be isolated in small quantities from the oxazolidinone forming experiment product (Figure 73 in Chapter 8).

Scheme 17: Formation of oxazolidine imine from the reaction of 1,3-di-p-tolyl carbodiimide and OCGE.

2-Imidazolidinone may be obtained from the rearrangement of oxazolidine imine at temperatures of 250 °C.[66] It was reported that 2-imidazolidinone can be formed in a direct reaction of oxazolidinone with isocyanate in the presence of 20 mol% LiCl catalyst.[67] This thermal rearrangement was not observed during the synthesis of oxazolidinone.
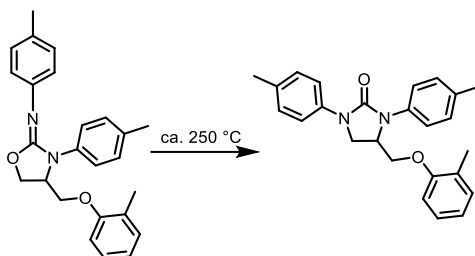
Scheme 18: Isomerisation of the oxazolidine imine to the 2-imidazolidinone at high temperatures.[66]

2-imidazolidinone and oxazolidine imine were detected in the reaction product of the epoxide-carbodiimide reaction (Scheme 17) using LC-MS. Two peaks with identical mass at different retention times indicated the presence of two isomers. ^{15}N-HMBC-NMR measurements showed that more oxazolidine imine was formed than 2-imidazolidinone.
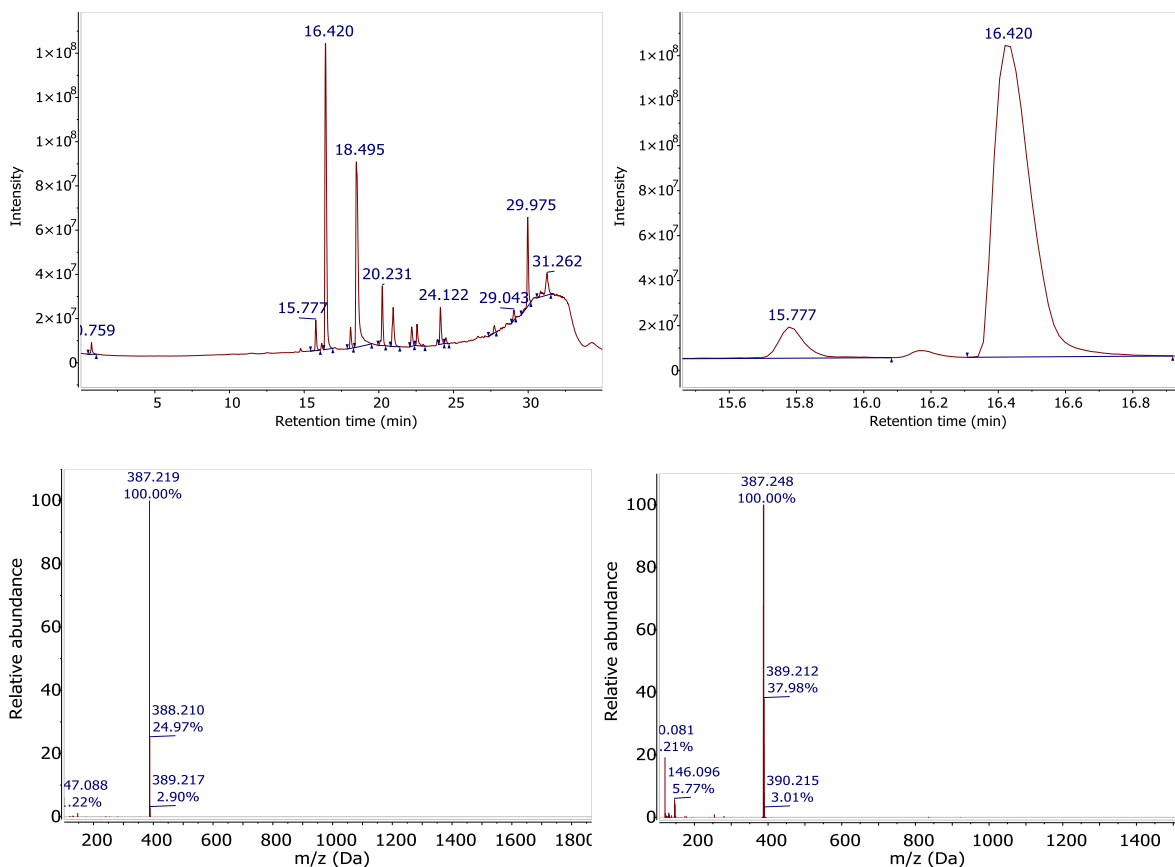
Figure 5: LC-MS trace of the oxazolidine imine reaction product (top). The product spectra obtained after retention times of 15.9 min (bottom left) and of 16.2 min (bottom right) are displayed.
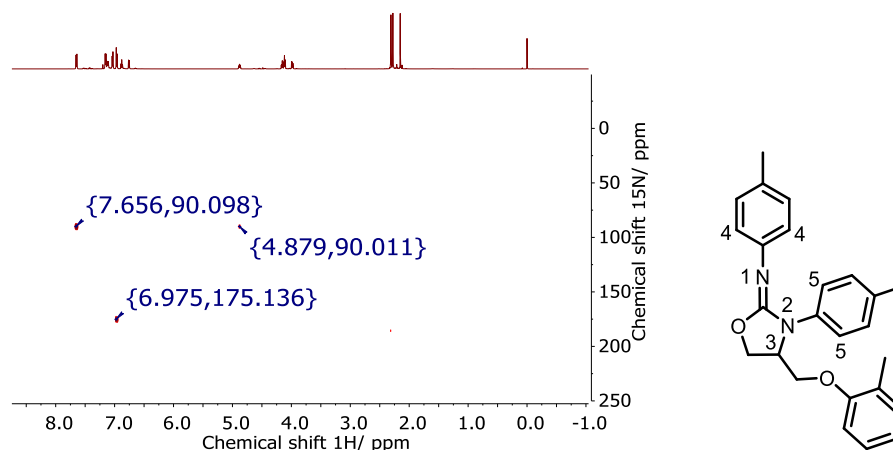
Figure 6: ^{15}N-HMBC of the reaction product from OCGE with 1,3-p-tolylcarbodiimide (scheme on the right).

The ^{15}N-HMBC spectrum shows three signals. Signals for nitrogen atoms were detected at 90 ppm and 175 ppm originating from the oxazolidine imine or 2-imidazolidinone, respectively. The signal at 90 ppm is assigned to nitrogen **2** in the five-membered oxazolidine imine ring. This nitrogen couples with its neighbouring aromatic protons ([3]J coupling, 7.66 ppm, **5**) and with the methine group within the oxazolidinone ring ([2]J coupling, 4.88 ppm, **3**). The nitrogen atom **1** at 175 ppm shows only a [3]J coupling with the aromatic protons 4 at 6.98 ppm and is assigned to the nitrogen atom of the imino group.

2-Imidazolidinone would show coupling between the nitrogen and the protons of the methylene group in the ring and the similar chemical environment of both nitrogen atoms would result in a signal for the second nitrogen atom closer to 90 ppm. Neither phenomenon was observed experimentally, confirming the predominance of the oxazolidine imine over the 2-imidazolidinone formation. The main peak in LC-MS was thus assigned to the oxazolidine imine. The presence of some 2-imidazolidinone most likely stems from a thermally initiated rearrangement of the oxazolidine imine (Scheme 18).

The IR vibration of the C=N double bond in oxazolidine imine is located at approximately 1670 cm^{-1}.[68] This band was observed in the reaction product from carbodiimide and epoxide (appendix, Figure 70). ^{1}H-NMR spectrum of this compound showed signals for three methyl groups, two of which originated from the former carbodiimide (2.31 ppm and 2.28 ppm) and one from the former epoxide (2.16 ppm, synthesis in Chapter 6.8). These methyl signals were inseparable from those of the oxazolidinone, urea and sulfolane in the NMR spectrum of the reaction mixture. The signal at 7.6 ppm originating from the aromatic protons of the imino group 4 was used for the quantification of the oxazolidine imine amount formed in the oxazolidinone synthesis (Equation 19).
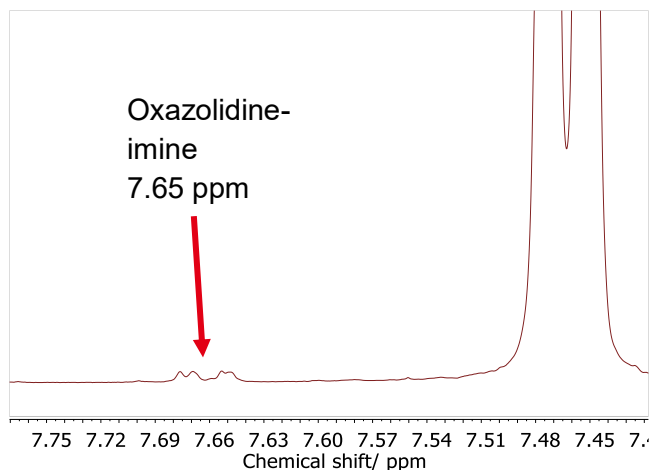
Figure 7: Detail of an NMR spectrum of a product from oxazolidinone synthesis (full spectrum in Figure 74).

5.1.2. **Identification and quantification of side products**

NMR spectroscopic analysis of the product from p-tolyl isocyanate and OCGE proved to be the most accurate and reliable method for quantifying the various reaction products. The quantity of each side product was calculated as the fraction with respect to oxazolidinone (Equation 26, method i). A strong increase in isocyanurate content occurs at the start of the reaction. The amount of isocyanurate appears to decrease and a plateau value is obtained upon continuation of the reaction (Figure 8). The amount of oxazolidine imine increases steadily with time.
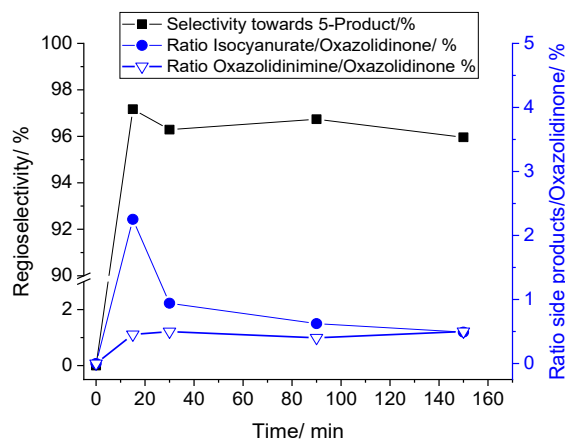
Figure 8: Time-resolved fraction of side products to oxazolidinone and the regioselectivity in a reaction using the general conditions of synthesis (Chapter 6.4).

It was uncertain whether the large amount of isocyanurate at the beginning of the reaction was genuine. An absolute quantification of the reaction products during the reaction was conducted

using phenanthrene as an internal standard (method ii). This additive is considered inert and its NMR spectroscopic signature does not interfere with the relevant oxazolidinone and isocyanurate signals (Chapter 6.3.2). This quantification method demonstrated that the amount of isocyanurate increases continuously during the addition of both monomers (addition time: 90 minutes). The decomposition of isocyanurate through a reaction with an alkoxide resulting from the excess epoxide (index below 100) became dominant after the addition was completed and prevented further isocyanurate formation (Figure 9). This result is observed in both types of quantification.

The calculation using method ii accounts for the presence of 33 wt% solvent. The oxazolidinone amount is limited to the solid content of 67 wt%, providing more accurate values for the formed isocyanurate quantity and its formation rate.

The quantification of the oxazolidine imine amount was hindered by overlapping signals with phenanthrene. The method i of evaluation of the reaction was preferred and is the basis for the analysis presented in the subsequent sections because of its ease of preparation and the ability to calculate the oxazolidine imine amount. It must, however, be noted that the formation of isocyanurate occurs continuously during monomer addition and that there is no accumulation of isocyanurate at the start of the reaction (artefact of the method i).
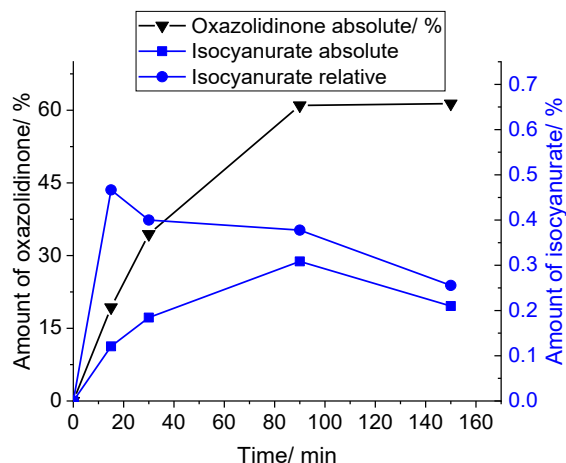

Figure 9: Time-resolved amount of isocyanurate formed during the reaction, using an internal standard.

5.1.3. **Repeatability**

The repeatability of the standard reaction (Chapter 6.4) was studied in sulfolane (Table 1) and DMPU (Table 2).
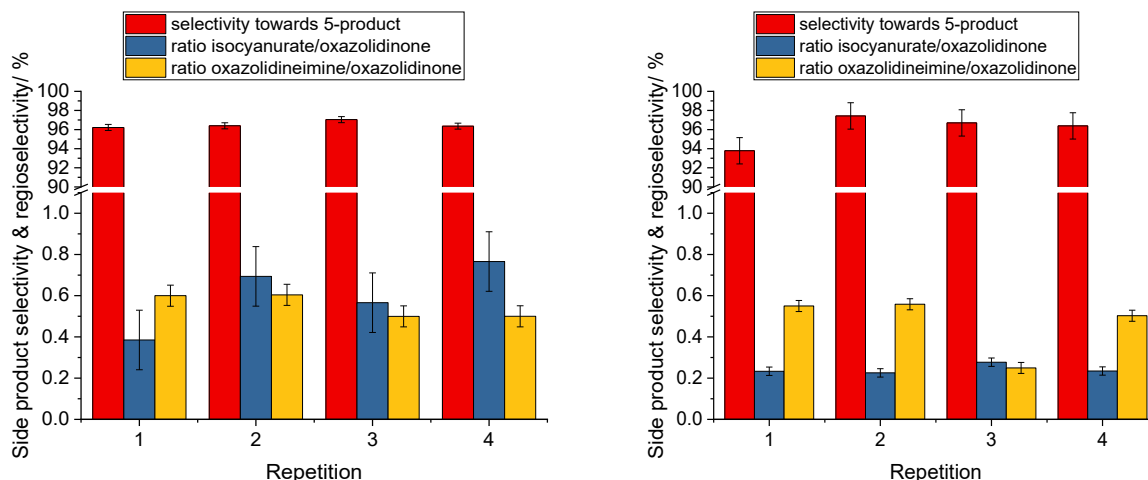

Figure 10: Repeatability of the standard reaction concerning the regioselectivity and side product formation of the final reaction products in sulfolane (left) and DMPU (right).

NMR spectroscopic analysis indicates similar regioselectivities (within 1.5% difference). The same holds true for side products (within 0.4% variation). Larger errors in the determination arise from the partial overlapping of the signals. This fact, in combination with the small integrals of the used signals, results in a higher, but still acceptable, error of maximum 9.6% from the average value.

The experimental errors from weighing, differing reaction temperatures, monomer addition and mixing were approximately 2.5 times larger than the error of the NMR analysis in sulfolane. Higher repeatability of side product formation was observed for DMPU. Its role as a co-catalyst may be the reason, as suggested by BASF SE.[40] Larger errors in regioselectivity repeatability, probably due to this co-catalyst effect, are a disadvantage of DMPU.

The error in the NMR determination was obtained from five measurements of the same sulfolane-containing product. The overall experimental error was estimated from four repetitions of the same reaction. The errors are calculated as a standard deviation from the mean value.

Table 1: Average values and the experimental error for the repeatability of standard reaction in sulfolane.

	Average value /%	Error NMR determination/%	Overall experimental error /%
Ratio isocyanurate/ oxazolidinone	0.55	0.053	0.14
Ratio oxazolidine imine/oxazolidinone	0.57	0.037	0.051
Regioselectivity	96.55	0.13	0.32

Table 2: Average values and the experimental error for repeatability of experiments in DMPU.

	Average value /%	Overall experimental error /%
Ratio isocyanurate/ oxazolidinone	0.24	0.020
Ratio oxazolidine imine/oxazolidinone	0.53	0.027
Regioselectivity	96.55	1.38

5.1.4. **Influence of solvent choice**

A series of aprotic, high boiling solvents was selected that were largely inert towards isocyanates and epoxides as potential reaction medium: sulfolane, *o*-dichlorobenzene, mesitylene and the saturated urea derivates viz. dimethyl propylene urea (DMPU) and 1,3-dimethyl-2-imida-zolidinone (DMI). NMP was also included in the study as an "unsuitable" example. NMP is not inert, as it can react with isocyanate under evolution of CO_2 to form an imine derivative that can yield at least five subsequent products with additional isocyanate.[69] The effect of the solvents on the outcome of the standard reaction procedure (Chapter 6.4) was mapped with 2% epoxide and 2.5% of the total amount of isocyanate present in the catalyst solution.
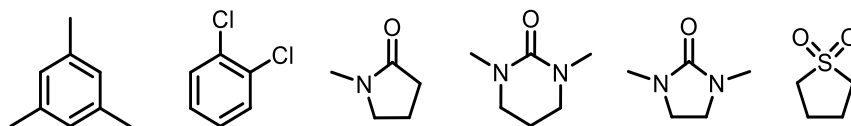
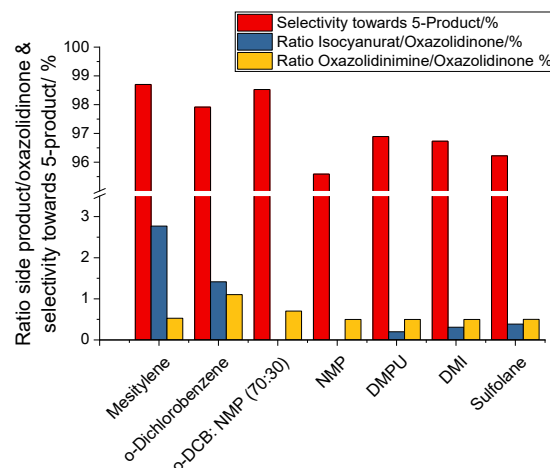*Scheme 19: Mesitylene, o-dichlorobenzene, NMP, DMPU, DMI and sulfolane (from left to right).*

Figure 11: Ratio of side products to oxazolidinone as well as regioselectivity towards the 3-(p-tolyl)-*5-((o-tolyloxy)methyl)oxazolidine-2-one (5-product) for all tested solvents.*

Sulfolane, dimethyl imidazolidinone (DMI) and dimethyl propylene urea (DMPU) are the most suitable solvents as they offer the lowest side product formation and an acceptable regioselectivity. The lowest amounts of isocyanurate formation were found using the cyclic urea solvents DMPU and DMI, which gave only slightly lower 3-(*p*-tolyl)-5-((*o*-tolyloxy)methyl)oxazolidine-2-one than the less polar solvents mesitylene and *o*-dichlorobenzene. The latter showed a high selectivity for the formation of the 3-(*p*-tolyl)-5-((*o*-tolyloxy)methyl)oxazolidine-2-one, but unfavourably, it also resulted in the highest levels of trimer formation. Another disadvantage of *o*-dichlorobenzene was the more extensive formation of oxazolidine imine. These experiments indicated that with increasing solvent polarity, the formed amount of isocyanurate and the regioselectivity decreased. The polarity of the medium may be relevant to the polar intermediates and transition states. The slower trimer formation could originate from the faster ring-closure to oxazolidinone, resulting in a lower concentration of alkoxides. The intermediate alkoxides in the oxazolidinone formation catalyse trimer formation.

5.1.5. **Influence of catalyst choice**

Several substances are known to catalyse the oxazolidinone forming reaction. This work focused on the use of organic salts such as tetrabutyl ammonium bromide (TBAB); lithium chloride and zinc chloride were evaluated as a typical LEWIS acidic catalyst as well. Triphenyl (TPPO), tri-*n*-octyl (TOPO) and tri-*n*-butyl (TBPO) phosphane oxides were used as ligands to provide sufficient solubility of the zinc salt in the organic solvents. The catalysts should not promote epoxide-epoxide and isocyanate-isocyanate reactions leading to polyether, isocyanurate and carbodiimide.
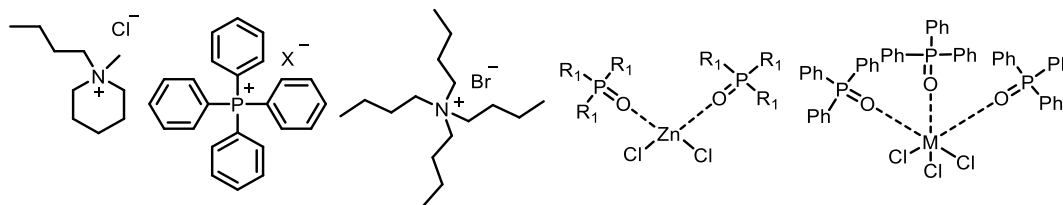
Figure 12: Structures of the catalysts; BMPC, Ph$_4$PX, TBAB, zinc, iron and bismuth chloride complexes with phosphine oxides. R$_1$ represents a phenyl, n-octyl or n-butyl group, M the iron (III) and bismuth (III) atom and X a halogenide.

The individual monomers were doped with small amounts of the salts at 160 °C for 24 h. OCGE were thus heated in the presence of 1 mol% of BMPC, Ph$_4$PCl, LiCl and ZnCl$_2$(TPPO)$_2$, respectively. It was found that Ph$_4$PCl and BMPC are the salts that give the least inter-monomer reactions. The tendency for polyether formation of these four salts can be ranked as Ph$_4$PCl < BMPC = ZnCl$_2$(TPPO)$_2$ << LiCl. The IR spectrum before and after heating using Ph$_4$PCl remained identical. A small adsorption band at 1070 cm^{-1} was observed using BMPC and ZnCl$_2$(TPPO)$_2$, which could be an indication for some homopolymerisation of the epoxy groups. The C-O-C band of monomeric bisphenol A diglycidyl ether, as a reference, was reportedly detected at 1036 cm^{-1}.[70] The band at 1070-1080 cm^{-1} was more prominent using LiCl. A broad OH band appeared between 3200 and 3600 cm^{-1}, originating from the terminal hydroxy group of the formed polyether polyol. An epoxide conversion of 95% could be calculated from the integral of the oxirane methine proton in NMR.

The conversion of *p*-TI to isocyanurate mediated by 0.5 mol% of either of the compounds BMPC, Ph$_4$PCl, LiCl or ZnCl$_2$(TPPO)$_2$ was calculated from the NMR spectra recorded after 24h at 160 °C. The isocyanurate content was 2.7% for BMPC and Ph$_4$PCl, but 2.2% for ZnCl$_2$(TPPO)$_2$. The NMR and IR spectra using LiCl before and after the experiment were identical, indicating that no reaction had occurred. The rate of isocyanurate formation equals one-third of the isocyanate consumption because three moles of isocyanate are required for the formation of one mole of trimer. The isocyanurate formation rate was calculated to 0.02%·mol%$^{-1}$·h^{-1} for BMPC and Ph$_4$PCl and 0.015% mol%$^{-1}$·h^{-1} for ZnCl$_2$(TPPO)$_2$. Isocyanates are activated by a nucleophile B, such as chlorides. The activated, charged intermediate attacks further isocyanates at the carbon atom to form uretdione and isocyanurate.[1,17,57] The thermal instability of uretdione at 160 °C (Chapter 3.2) results in the nearly exclusive formation of isocyanurate. This reaction is slower than the alkoxide-catalysed trimerisation.
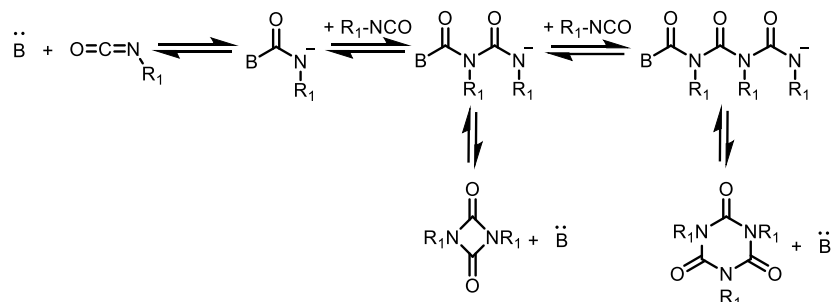
Scheme 20: Reaction pathways in the nucleophile-catalysed formation of dimers and trimers by a base B from isocyanates.[17]

The conversion of isocyanate to carbodiimide was 2.9% for Ph_4PCl and 0% for LiCl. It amounted to 6.2% for BMPC and 40.4% for $ZnCl_2(TPPO)_2$. Phosphane oxides are known catalysts for the formation of carbodiimides.[15,38,71] The rate of carbodiimide formation for $ZnCl_2(TPPO)_2$ was calculated to be 0.42% $mol\%^{-1} \cdot h^{-1}$ and it was 0.065 and 0.03% $mol\%^{-1} \cdot h^{-1}$ for BMPC and Ph_4PCl, respectively.

BMPC, Ph_4PCl, $ZnCl_2(TPPO)_2$, Ph_4PBr, TBAB, $ZnCl_2(TOPO)_2$, $ZnCl_2(TBPO)_2$, $FeCl_3(TPPO)_3$ and $BiCl_3(TPPO)_3$ were tested for catalytic activity in the standard oxazolidinone forming reaction at a concentration of 1 mol%. The highest 3-(*p*-tolyl)-5-((*o*-tolyloxy)methyl)oxazolidine-2-one selectivity (98%) was achieved using zinc (II) chloride complexes, whereas the lowest selectivity (95%) was obtained with the bismuth (III) catalyst. Lower regioselectivities of 96% were achieved using BMPC, Ph_4PCl and Ph_4PBr compared to zinc chloride complexes. The organic chloride salts and zinc chloride complexes were found to achieve the lowest amounts of side products.
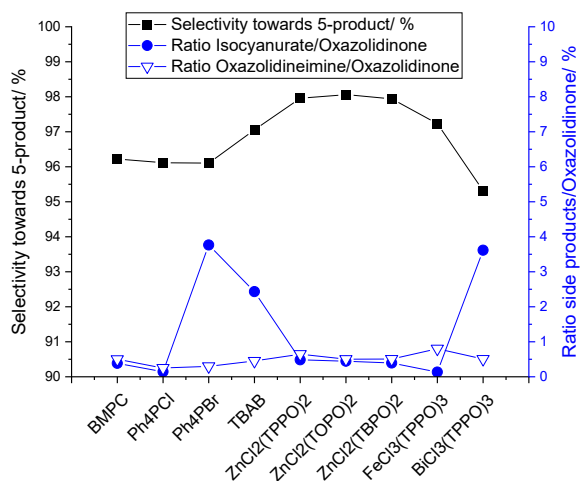
Figure 13: Ratio of side products to oxazolidinone and 3-(p-tolyl)-5-((o-tolyloxy)methyl)oxazolidine-2-one selectivity for the tested salts.

The quantity of the oxazolidine imine formed is relatively small and largely independent of the catalyst. No consecutive reactions of the oxazolidine imine were observed. The largest amount of isocyanurate was obtained using tetraphenyl phosphonium bromide (TBAB) and the bismuth catalyst. $BiCl_3$ can form a large variety of charged complexes, which may act as a basic catalyst favouring isocyanurate formation.[72] Basic catalysts, such as alcoholates or carboxylates, are effective trimer forming catalysts.[26,73] More trimer was formed using bromide catalysts (TBAB, Ph_4PBr). The lower nucleophilicity of bromide anions than chloride may be the reason for the increased isocyanurate formation. The isocyanate band at 2270 cm^{-1} was already observed during the monomer addition using bromide catalysts, whereas this was not the case in the chloride-catalysed reactions. The NCO/OXA ratio after 15 min of monomer addition was 35% for Ph_4PBr and 9% for Ph_4PCl, which indicates a faster isocyanate conversion with the chloride salt. A similar effect of nucleophilicity on the trimer formation was found in literature.[57,74]

High chemoselectivity was observed using zinc chloride complexes as catalysts. The final product contained a low amount of isocyanurate. The different reaction behaviours may be explained by the different pathway of the oxazolidinone formation (Scheme 12). Metal compounds can coordinate to the isocyanate oxygen and the epoxide oxygen, thereby increasing the electrophilicity of the isocyanate carbon.[17] No influence of the selected phosphane oxide ligands on the isocyanurate and oxazolidine imine formation was observed, suggesting that the catalytic activity was governed solely by the metal halide.

Excessive isocyanate was mainly converted into isocyanurate using BMPC and Ph4PBr as catalysts, whereas the oxazolidinone and oxazolidine imine formation were more prominent using $ZnCl_2(TOPO)_2$. The effect of isocyanate accumulation during the reaction was invoked by adding a small amount of isocyanate (10% of the total required amount) to the catalyst-epoxide system before the start of the oxazolidinone forming reaction. The monomer mixture with an index of 86 was subsequently added over 90 min to obtain the final index of 96, which is identical to the standard reaction.
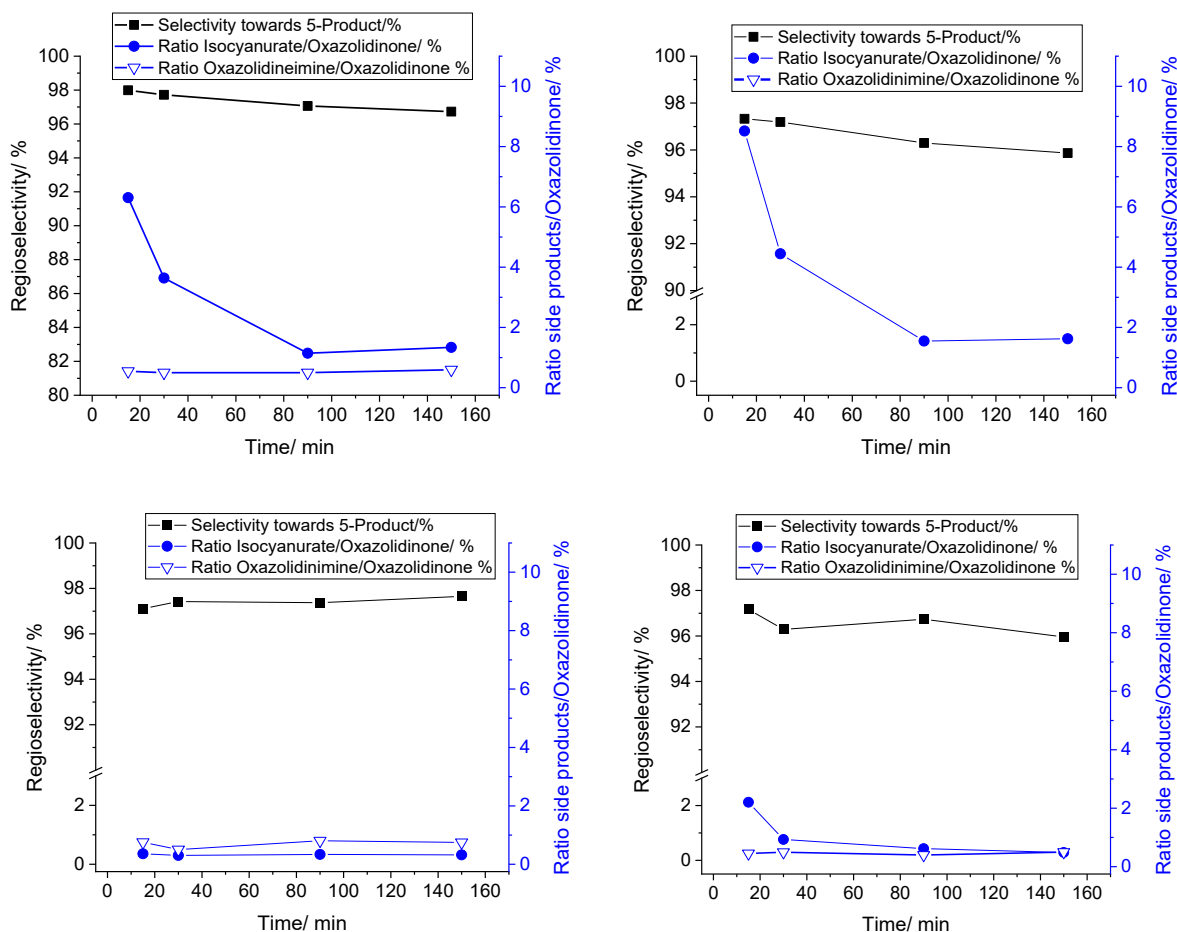
Figure 14: Comparison of the three catalysts BMPC (top left), Ph₄PBr (top right) and ZnCl₂(TOPO)₂ (bottom left) with excess isocyanate present at the start of the reaction. The standard reaction (Chapter 6.4) is shown as a reference (bottom right).

A major drawback of the potential catalyst $ZnCl_2(TOPO)_2$ is the formation of carbodiimide caused by the ligands, as well as the lower reaction rate. The OXA formation rate decreases in the order $BMPC > Ph_4PBr > ZnCl_2(TOPO)_2$, as indicated by the observed accumulation of isocyanate over the course of the reaction (Figure 15). The carbodiimide formation resulted in a higher oxazolidine imine yield than in the reference reaction. The oxazolidine imine ratio for Ph_4PBr could not be determined due to overlapping NMR signals from the oxazolidine imine and the catalytic salt.
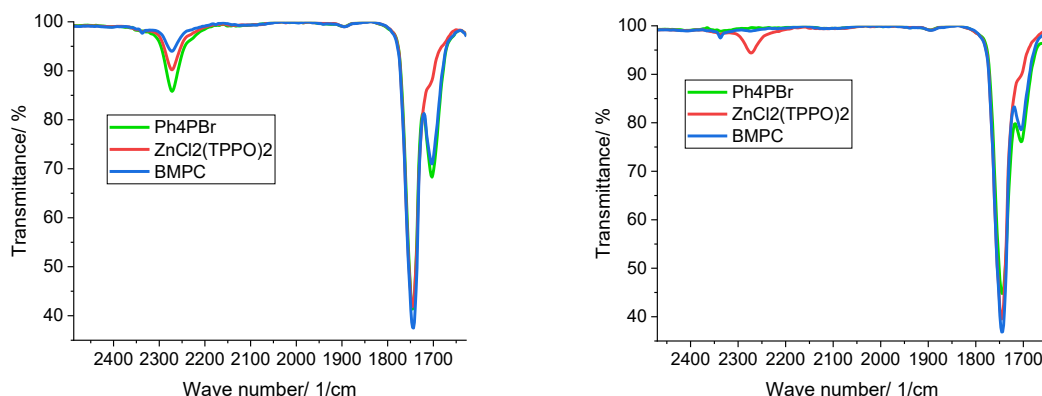
Figure 15: IR spectra of the three catalysts after 15 minutes (left) and 30 minutes (right) of monomer addition.

BMPC was identified as the best catalyst because it is least prone to induce side product formation (polyether, carbodiimide, isocyanurate) from the monomers. $ZnCl_2(TOPO)_2$, in contrast, is a better catalyst for carbodiimide and subsequent oxazolidine imine formation. Higher isocyanate concentrations should be avoided regardless of the catalyst chosen, especially when alkoxides are formed from the epoxide.
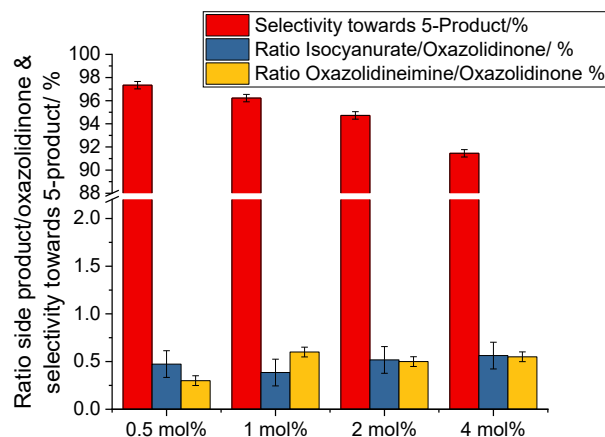
Figure 16: Regio- and chemoselectivity for diverse loads of BMPC.

The formation of isocyanurate and oxazolidine imine appeared to be independent of the BMPC catalyst concentration. Increased intermediate isocyanurate contents were observed at 0.5 mol% catalyst, likely because of higher intermediate isocyanate concentrations. The alkoxide concentration increases with higher catalyst loadings, which leads to a lower regioselectivity (Chapter 5.1.4). The optimum catalyst concentration, with respect to regioselectivity and space-time yield, lies between 1 and 2 mol%.

Urea derivatives with at least one active hydrogen, such as 1,3-di-*p*-tolyl urea, were found to act as co-catalysts and improve the regio- and chemoselectivity of the reaction toward oxazolidinone. This finding opens a path of enhancing the chemoselectivity of the OXA formation reaction. Aliphatic urea exhibited a significantly reduced co-catalysing effect. No improvements were observed for saturated urea, e.g., 1,3-diethyl-1,3-diphenylurea. It can be concluded that the active urea hydrogen atoms were fundamental for the co-catalytic action.[75]

A urea derivative was added to the catalyst solution and the monomer mixture was added faster (30 min instead of 90 min) to induce a build-up of isocyanate concentration. This was done with the objective of detecting a difference in reaction rates between those with and without the presence of the selected urea. The isocyanate was converted faster when unsaturated urea was added as a co-catalyst, resulting in lower quantities of side products. Commercially available DYHARD® amines may be used as co-catalysts for the oxazolidinone formation as well.[47].
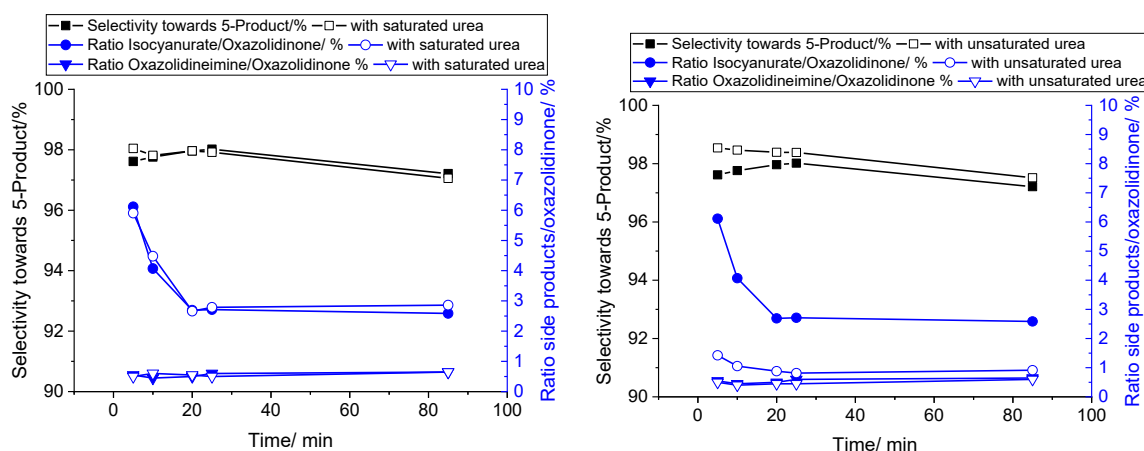
Figure 17: Identical reactions carried out using no urea (filled) and 1,3-diethyl-1,3-diphenylurea (left, open dot) and 1,3-di-p-tolylurea (right, open dot).
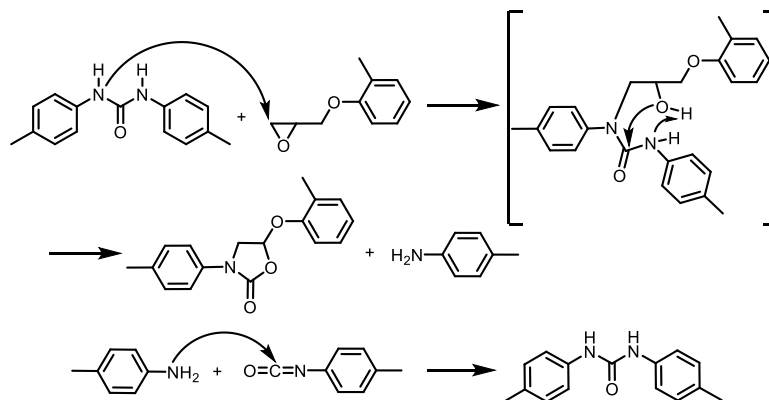
Scheme 21: Oxazolidinone formation from the reaction of an epoxide in the presence of di- or tri-substituted urea (such as 1,3-p-tolyl urea).

Oxazolidinone formation from urea and an epoxide is suggested to take place under the evolution of an amine, which is quickly converted into urea again from the amine-isocyanate reaction (Chapter 3.2). The generated urea is catalytically active again. Fully saturated urea, such as the tetra-substituted 1,3-diethyl-1,3-diphenylurea, is probably not reactive because of i) the missing active proton (Scheme 21) and ii) the generated *N,N*-Ethyl-phenyl anion, which is a poor leaving group. Calculations by BASF SE suggested a different mechanism in which the alkoxide intermediate formed in the epoxide-halide reaction (Scheme 14) was stabilized by urea. This stabilisation would influence the subsequent nucleophilic attack on the isocyanate, potentially explaining the observed higher chemoselectivity. It remained unclear which mechanism the reaction follows.

The most suitable catalysts for the oxazolidinone formation were BMPC and Ph_4PCl. They provide the best combination of high regio- and chemoselectivity. Zinc chloride complexes induced the formation of oxazolidinone with a high regio- and chemoselectivity too but additionally favoured the undesired formation of carbodiimides and consecutive products. A catalyst load of 1 to 2 mol% BMPC with respect to the molar amount of epoxide proved sufficient for high regio- and chemoselectivity. Improved regio- and chemoselectivity was achieved through the addition of urea containing N-H groups as a co-catalyst. The most suitable catalyst system was 1 mol% BMPC and 0.5 mol% 1,3-di-*p*-tolylurea.

5.1.6. **Influence of reaction temperature and monomer addition profile**

The formation of isocyanurate trimer from isocyanate was more prominent at lower temperatures, i.e., 80 °C, but decreased at higher temperatures. No significant change in isocyanurate formation was observed above 160 °C. Temperatures over 160 °C thus enable a process with a good space-time yield for oxazolidinone formation without major drawbacks of, e.g., crosslinking based on the trimer. The activation barrier for the ring formation to the oxazolidinone is higher than that for the isocyanate polymerisation after the initial nucleophilic attack and subsequent backbiting. This activation barrier seems to be mostly overcome over 120 °C, leading to final isocyanurate contents of approximately 5 %.[29,32]
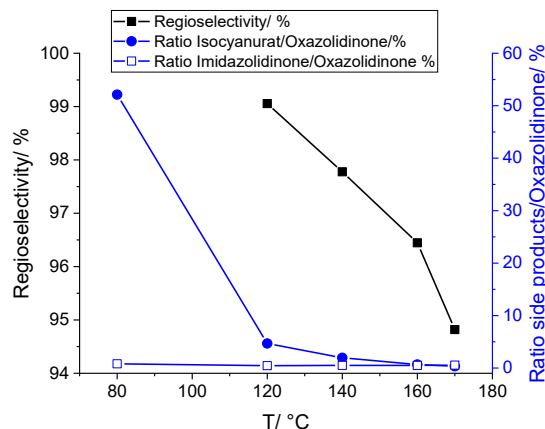
Figure 18: Temperature dependence of the ratio of side products to oxazolidinone and the 3-(p-tolyl)-5-((o-tolyloxy)methyl)oxazolidine-2-one selectivity (regioselectivity).

Higher reaction temperatures gave a lower regioselectivity for oxazolidinone formation. The reduction in regioselectivity is most likely caused by overcoming the activation barrier for the nucleophilic attack at the sterically more hindered 2-position of the epoxide. More primary alkoxide and, consequently, more 3-(p-tolyl)-4-((o-tolyloxy)methyl)oxazolidine-2-one is formed (Figure 18). A higher temperature was chosen for the addition process because of the improved space-time yield, reduced isocyanate accumulation and decreased side product formation such as isocyanurate.[46]

The best balance between high regioselectivity and low side product formation at reasonable reaction times was obtained with a monomer addition time of 90 minutes. Prevention of a build-up of isocyanate concentration during the process is essential to minimize side product formation. Accumulation of isocyanate was only observed at an addition time of 60 minutes, where the final isocyanurate concentration doubled to 0.9 %.
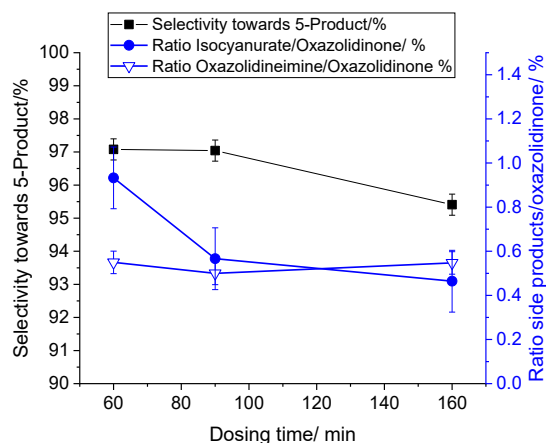
Figure 19: Ratio of side products to oxazolidinone and regioselectivity towards 3-(p-tolyl)-5-((o-tolyloxy)methyl)oxazolidine-2-one.

The addition of a 1:1 mixture of epoxide and isocyanate to the catalyst solution (option i) gave less isocyanurate and a higher regioselectivity than the addition of isocyanate to an epoxide/catalyst mixture (option ii, Figure 20). This is probably caused by a mixing issue: the reactor setup does not allow a fast mixing of the isocyanate in the medium, resulting in locally unfavourable high isocyanate concentrations.
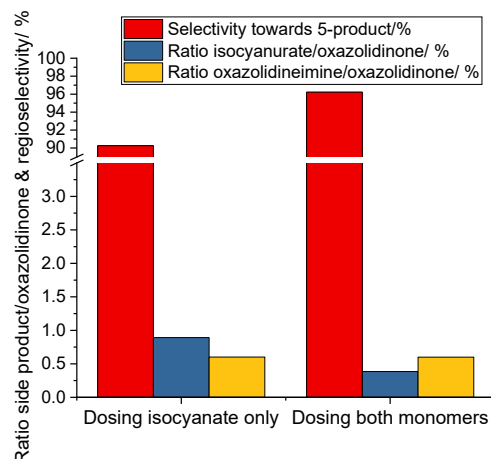

Figure 20: Comparison of the characteristics of the two possible addition methods.

The sequence of oxazolidinone formation starts with the addition of a chloride anion to the epoxide to yield the first intermediate as alkoxide. This reaction appears to occur within a minute at 160°C, indicating that the catalyst becomes active without a major induction period. The reactions were conducted according to the standard reaction procedure (Chapter 5.1), except that the epoxide and catalyst mixture was maintained at 160 °C for a specified time before the isocyanate/epoxide addition - the waiting time. The initial alkoxide content after the waiting time could not be detected by NMR directly; therefore, the final product was analysed. The activation of the epoxide to form the halo-alkoxide is fast enough under the standard reaction conditions using a one-minute waiting time. A constant feed rate without waiting time is proposed for a high space-time yield.
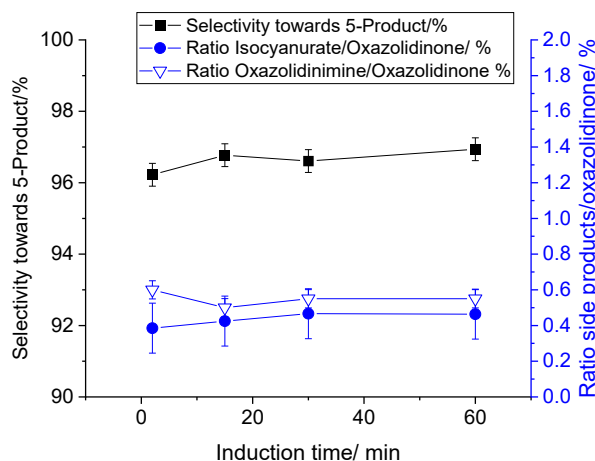
Figure 21: Ratio of side products to oxazolidinone and the regioselectivity towards the 3-(p-tolyl)-5-((o-tolyloxy)methyl)oxazolidine-2-one of the final product.

The addition of 2% epoxide to the catalyst solutions to obtain alkoxide prior to the monomer addition yielded the lowest side product formation. The combination with an additional 2% isocyanate did not exhibit any further effects. The presence of isocyanate without epoxide leads to side products (Chapter 5.1.5).
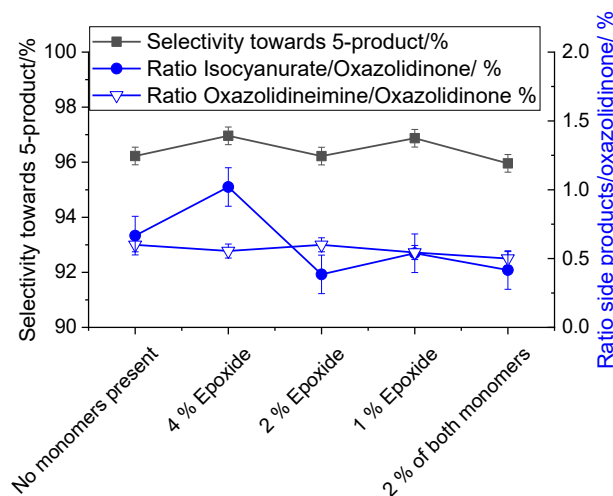

Figure 22: Ratio of final side products to oxazolidinone and regioselectivity dependent on the initial monomer amounts.

The regio- and the chemoselectivity towards oxazolidine imine were independent of the epoxide presence at the start of the reaction. The small amount of epoxide led to the formation of alkoxide (Chapter 5.1.8), reacting quickly with isocyanate. The result is a slower formation of the isocyanurate byproduct.

The best conditions for the formation of 3-(p-tolyl)-5-((o-tolyloxy)methyl)oxazolidine-2-one were found to be 2 % of epoxide in the catalyst solution, a constant monomer additon rate over

90 minutes, a reaction temperature of 160 °C and the addition of a mixture of isocyanate and epoxide one minute after reaching the desired reaction temperature.

5.1.7. **Efforts to minimize the steady state isocyanate concentration**

Minimizing the steady state isocyanate concentration during the reaction will favour the oxazolidinone formation as exemplified above (Scheme 16).

The alteration of the monomer feeding protocol to obtain an excess of epoxide in the first stage led to no significant change in the side product formation (option i) but a decrease in regioselectivity. OCGE (10% of the total epoxide) was added to the catalyst solution and two monomer addition steps were used. An epoxide/isocyanate mixture was added first, followed by the addition of isocyanate in a separate step to achieve a final index of 96. The use of initial 50 % OCGE of the total epoxide (option ii) resulted in a decrease of isocyanurate content to 0.3 % (reference ca. 0.7 %) at the cost of a 6 % reduction in regioselectivity towards the 3-(p-tolyl)-5-((o-tolyloxy) methyl)oxazolidine-2-one. The index of the following monomer addition over 90 min was changed to 146 to reach a final index of 96, as in the reference reaction. The decreased regioselectivity observed with options i) and ii) was due to the high amount of epoxide present (Chapter 5.1.4), which increased the polarity.
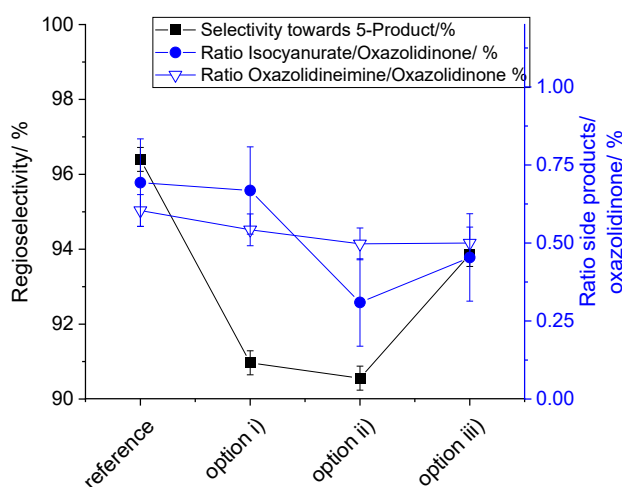
Figure 23: Influence of the dilution of isocyanate by option i), ii) or iii). The reference uses the general reaction conditions.

The addition of a previous batch of oxazolidinone product - including solvent and catalyst - to the catalyst solution led to a reduced final isocyanurate content, but also a reduction in regioselectivity by 2 % (option iii). Reduced amounts of sulfolane and BMPC were added to match the

concentrations of the reaction components used in the standard reaction. The setup of a cyclic process where a significant quantity of oxazolidinone product is consistently present may help achieve lower levels of side product formation, though this might slightly compromise regioselectivity.

Blocked isocyanates are compounds in which the NCO group is reversibly reacted with another compound. They can be used instead of free isocyanates to reduce the risk of isocyanate-based side reactions. Molecules containing active hydrogens are primarily used for blocking. The advantages include decreased reactivity of the highly reactive NCO group. The deblocking is initiated by the addition of a nucleophile, heating or a combination of both. Examples of blocked isocyanates include dimerised isocyanates (uretdiones) and ketoxime blocked isocyanates (e.g., methyl ethyl ketone oxime (MEKO) blocked MDI). Blocked isocyanates are widely used (e.g., 1K waterborne applications) and are commercially available.[11,76]
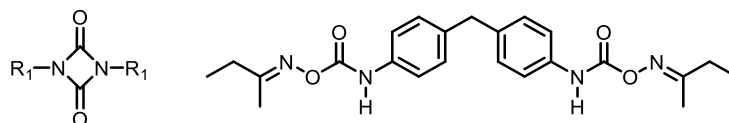
Scheme 22: Structure of two blocked isocyanates, uretdione (left) and MEKO blocked MDI (right).

There are two fundamental pathways for deblocking, the addition-elimination and the elimination-addition mechanisms. The former pathway involves the direct addition of an alkoxide to the urethane, forming the oxazolidinone, thereby eliminating the alcohol (Scheme 9). The latter would be a decomposition of the urethane, liberating the isocyanate.[11]

The *in-situ* blocking with high boiling alcohols (b_p > 180 °C) gave a reduced regioselectivity but similar chemoselectivity. The reason for this is most likely the increased polarity (Chapter 5.1.4). The alcohol (10 mol% related to the total isocyanate amount) was added to the catalyst solution prior to the addition of the monomers. A final index of epoxide and alcohol to isocyanate of 95 was calculated, provided that all the *in-situ* formed urethane decomposes again. A preliminary experiment revealed that only approximately 30% of the *in-situ* formed urethane was decomposed. A genuine index of 98 was obtained consequently.
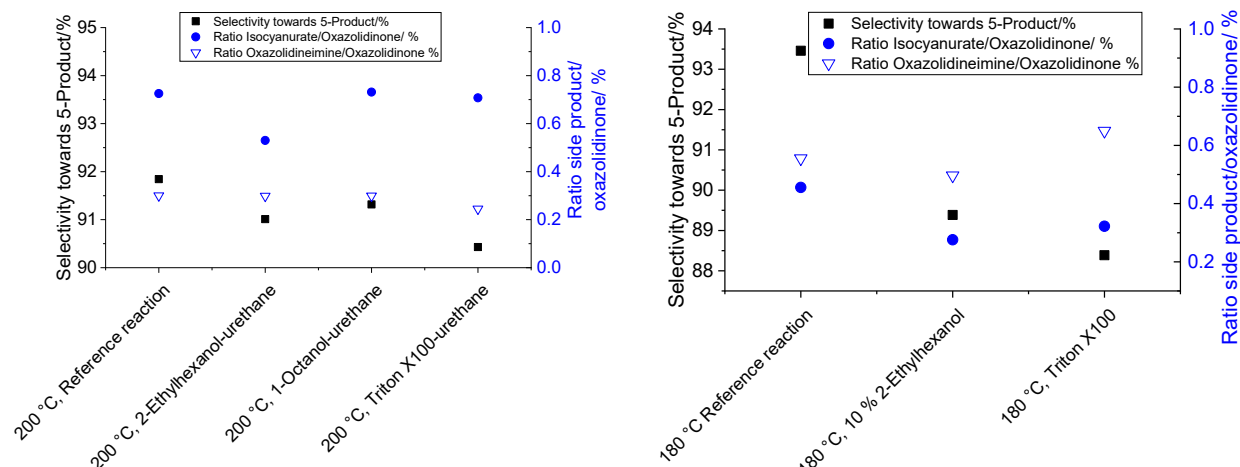
Figure 24: Ratio of side products to oxazolidinone and regioselectivity for the addition of urethanes (left) and alcohols (right)t.

The use of urethanes as blocked isocyanates did not significantly alter the side product ratio. The regioselectivity was not affected as well, although it was reported that a high regioselectivity could be obtained from the oxazolidinone formation from urethanes and epoxide[23]. Urethane (20 mol% related to the total isocyanate amount) was added to the catalyst solution. The final index would amount to 118, assuming the complete urethane degradation to isocyanate. NMR analysis revealed that only approximately 13 % of the total amount of urethane was decomposed by the end of the experiment. This implies a real index of 100. The reaction temperatures were raised to 180° C and 200 °C for the alcohol addition and urethane addition routes, respectively. The increased temperatures were taken to facilitate the decomposition of the – *in-situ* formed – urethane.
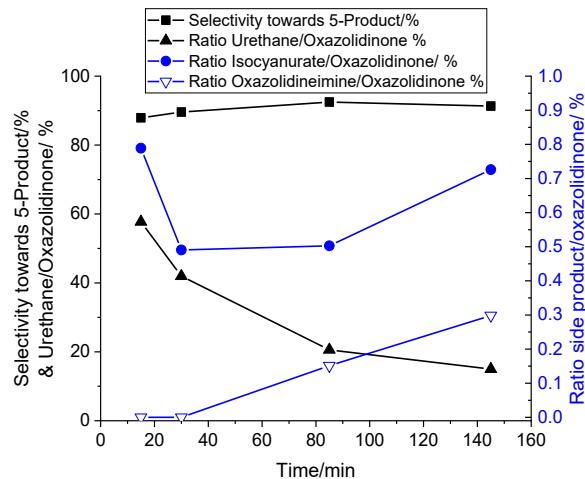
Figure 25: Monitoring of chemo- and regioselectivity using 20% of 1-Octanol-Urethane.

The added urethane is decomposed and diluted by the oxazolidinone formed during the reaction (Figure 25). The increase in isocyanurate after the completion of the monomer addition (90 min) is possibly caused by the further decomposition of urethane generating excess isocyanate.

5.1.8. **Qualitative comparison of reaction rates**

Qualitative kinetic knowledge enables process adjustments to achieve high chemo- and regioselectivity.
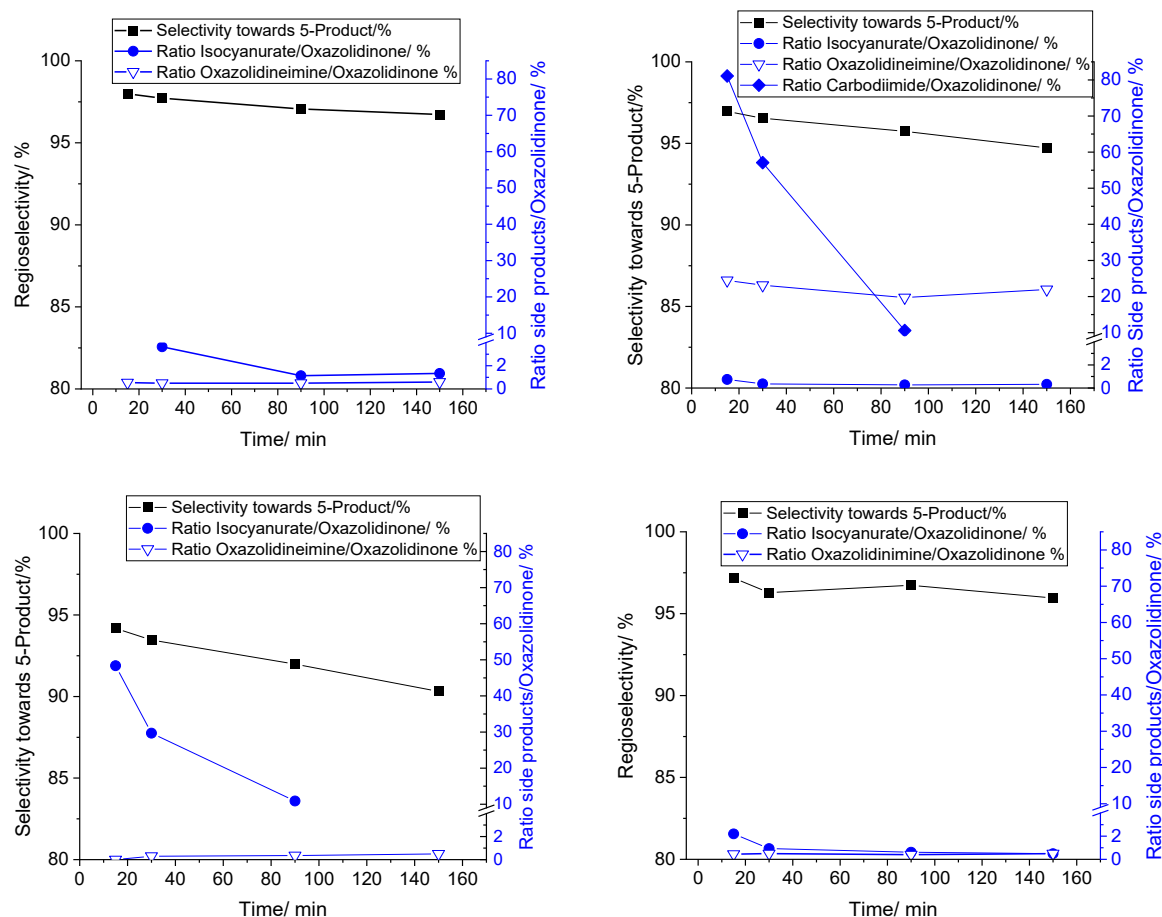
Figure 26: The use of 10% of the total isocyanate (top left), the replacement of 30% of the isocyanate by 1,3-di-p-tolylcarbodiimide (top right) or by isocyanurate (bottom left). The reference is shown at the bottom right.

The trimer formation was faster than the other reactions (top left) in the presence of alkoxide, which was provoked by the addition of isocyanate (10% of the total required amount) to the catalyst solution. No free isocyanate was detectable by IR after 30 minutes.

The formation rates of oxazolidinone and oxazolidine imine were similar because the ratio of oxazolidine imine to oxazolidinone remained approximately constant during the reference

reaction. The oxazolidine imine formation was provoked by the replacement of isocyanate with 1,3-di-*p*-tolylcarbodiimide (30 mol%). The carbodiimide NMR signal could be used for quantification; however, due to overlap with other signals, such as the methyl group of oxazolidinone, this calculation was less precise. The carbodiimide signal decreased throughout the experiment, but incomplete conversion was observed by the end of the monomer addition. This is verified by the increase in oxazolidine imine after the completion of the monomer addition. The calculated high amount of oxazolidine imine is an artefact resulting from the expression using the ratio oxazolidine imine/OXA (Chapter 5.1.2), but absolute quantification using phenanthrene was impossible due to overlapping NMR signals. Decomposition of the oxazolidine imine or oxazolidinone was not observed.

The decomposition rate of isocyanurate (10 mol%) to oxazolidinone was found to be slower than that of the other investigated reactions. Alkoxide-catalysed isocyanurate decomposition was prominent throughout the monomer addition. It became dominant after the completion of the monomer addition. A reduction in isocyanurate of only approximately 20% was estimated from NMR data, which is lower than the 50% reduction observed for the carbodiimide signal after the monomer addition was complete.

The reaction rates can be ranked as isocyanurate formation > oxazolidinone formation ≈ oxazolidine imine formation > isocyanurate decomposition. The rate of oxazolidinone and isocyanurate formation were determined using the absolute quantification method with phenanthrene as an internal standard (Chapter 5.1.2).

5.1.9. **Summary**

Monofunctional model compounds were used in oxazolidinone formation experiments. The focus was on enhancing the chemo- and regioselectivity to obtain high molecular weight thermoplastic polymers as the next step. Identification and reduction of side products were crucial in optimizing the reaction parameters toward oxazolidinone formation. Isocyanurate, oxazolidine imine and polyether formation were detected as side products. It could be concluded that:

- Solvents of high polarity (e.g., sulfolane, DMPU) increased the chemoselectivity toward oxazolidinone. Higher regioselectivity was obtained with lower polarity solvents (e.g., *o*-dichlorobenzene).

- BMPC and Ph$_4$PCl were identified as the most suitable catalysts. Their high chemoselectivity was superior to ZnCl$_2$(TPPO)$_2$, which showed a strong catalytic activity for carbodiimide formation, resulting in a higher yield of oxazolidine imine.

- Unsaturated urea bearing NH groups as co-catalysts significantly improved the chemoselectivity toward oxazolidinone.

- A minimum reaction temperature of 160 °C was necessary to minimise undesired isocyanurate formation. Temperature increase led to a reduction in regioselectivity and isocyanurate content.

- The presence of 2% of the total epoxide in the catalyst solution improved the chemoselectivity.

- An addition time of 90 minutes under the selected conditions was optimal for increasing the chemoselectivity.

- The addition of an almost equimolar epoxide/isocyanate mixture (index 98) showed the best balance between the chemoselectivity and process complexity.

- The reaction rates were qualitatively found to have the following order in the oxazolidinone formation experiment: isocyanurate formation > OXA formation ≈ oxazolidine imine formation > isocyanurate decomposition.

- No benefits were achievable by the addition of urethane or alcohol to reduce the steady-state isocyanate concentration.

The optimum reaction conditions for the oxazolidinone formation were a catalyst solution consisting of 1 mol% BMPC, 0.5 mol% 1,3-di-p-tolylurea and 2% epoxide heated to 160 °C. A mixture of isocyanate and epoxide (index 96) was added over 90 minutes and heated for another 60 minutes. This process was used as a starting point for the polymerisation reaction.

5.2.   **Rate law of the poly(oxazolidine-2-one) formation**

Knowledge about the rate law of the polymerisation to poly(oxazolidine-2-one) would enable the optimisation of chemoselectivity. The rate of the oxazolidinone formation r_{OXA} (Scheme 16) is, at least, determined by the molalities b [mol·g⁻¹] of the catalyst (BMPC) and the monomers epoxide (BADGE) and isocyanate (4,4'-MDI).

$$r_{\text{OXA}} = \frac{db_{OXA}}{dt} = k_1 \cdot b_{cat}^a \cdot b_{Epoxide}^b \cdot b_{NCO}^c \tag{10}$$

The partial orders hint towards how each reactant takes influence on the rate-determining step (Equations 3 and 10). The rate of oxazolidinone formation can be adjusted by altering concentrations or molalities of the compounds relevant to the rate-determining step. It potentially would allow the tailoring of a monomer addition profile to increase the polymer yield and reduce side product formation, such as isocyanurate. An optimised space-time yield is obtainable consequently.

The design of experiments (DoE) and the statistical evaluation were performed using DesignExpert 11 (Stat-Ease Inc). The software performs multivariate data analysis to calculate the desired coefficients, i.e. partial reaction orders. A two-factorial design was used to determine the rate law. An excess of epoxide (index below 100) was chosen for all reactions to minimize the risk of side reactions.

Table 3: Cubical experiment plan for the elucidation of the oxazolidinone formation kinetics.

Run	b_{cat}/ mol·g⁻¹	b_{Epo}/ mol·g⁻¹	b_{NCO}/ mol·g⁻¹	index	s.c./%
1	$3.0 \cdot 10^{-8}$	$1.0 \cdot 10^{-3}$	$1.5 \cdot 10^{-4}$	14	19.7
2	$1.0 \cdot 10^{-7}$	$1.6 \cdot 10^{-3}$	$1.5 \cdot 10^{-4}$	10	28.6
3	$3.0 \cdot 10^{-8}$	$1.0 \cdot 10^{-3}$	$5.0 \cdot 10^{-4}$	48	24.1
4	$1.0 \cdot 10^{-7}$	$1.6 \cdot 10^{-3}$	$5.0 \cdot 10^{-4}$	32	33.0
5	$1.0 \cdot 10^{-7}$	$1.0 \cdot 10^{-3}$	$5.0 \cdot 10^{-4}$	48	24.1
6	$3.0 \cdot 10^{-8}$	$1.6 \cdot 10^{-3}$	$1.5 \cdot 10^{-4}$	10	28.6
7	$1.0 \cdot 10^{-7}$	$1.0 \cdot 10^{-3}$	$1.5 \cdot 10^{-4}$	14	19.7
8	$3.0 \cdot 10^{-8}$	$1.6 \cdot 10^{-3}$	$5.0 \cdot 10^{-4}$	32	33.0

Equation 10 can be rearranged to Equation 11. The transformation of the used data was thus avoidable and the partial orders were easily extractable.

$$\ln\left(\frac{db_{OXA}}{dt}\right) = \ln(k_1) + a \cdot \ln b_{cat} + b \cdot \ln b_{Epoxide} + c \cdot \ln b_{NCO} \tag{11}$$

Table 4: Linearized input (cat, epoxide, NCO) and output (OXA) data into DesignExpert 11.

Run	Ln b_{cat}	Ln $b_{epoxide}$	Ln b_{NCO}	db_{OXA}/dt / mol·g^{-1}·s^{-1}	Ln db_{OXA}/dt
1	-17-32	-6.87	-8.80	$8.25 \cdot 10^{-7}$	-14.01
2	-16.12	-6.46	-8.80	$2.42 \cdot 10^{-6}$	-12.93
3	-17.32	-6.87	-7.60	$9.75 \cdot 10^{-7}$	-13.84
4	-16.12	-6.46	-7.60	$2.65 \cdot 10^{-6}$	-12.84
5	-16.12	-6.87	-7.60	$2.85 \cdot 10^{-6}$	-12.77
6	-17.32	-6.46	-8.80	$8.40 \cdot 10^{-7}$	-13.99
7	-16.12	-6.87	-8.80	$1.83 \cdot 10^{-6}$	-13.21
8	-17.32	-6.44	-7.60	$1.55 \cdot 10^{-6}$	-13.37

The conversion monitoring by NMR spectroscopy was performed on samples taken from the reactor. The isocyanate, epoxide and oxazolidinone conversions were calculated until the first 20 - 30% of isocyanate was consumed. The integral of the epoxide NMR signal was set to two in the first sample of the reaction. The obtained solvent integral was taken as an internal standard in all other spectra of the sample series of the experiment. The ratio of the obtained integral to the expected integrals (e.g. 1 for the methine moiety of the oxazolidinone) was used to obtain the corresponding conversion. The slope of the plot (conversion, time) gave the average reaction rate *r* (Figure 27).
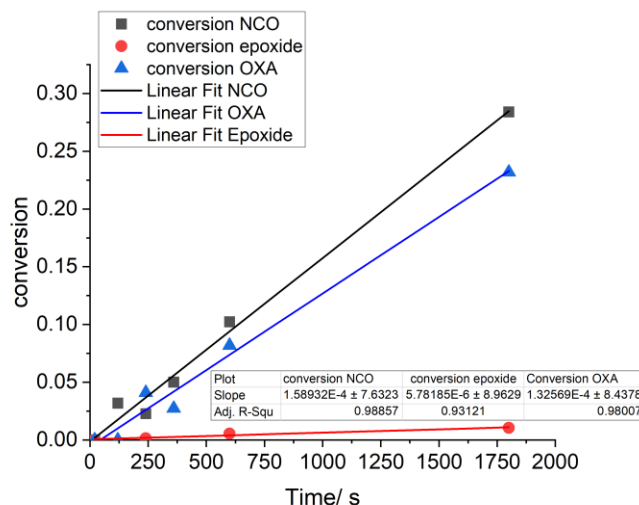
Figure 27: Plot of the conversion of the monomers and the formation of the oxazolidinone against time of an exemplarily reaction.

The molar conversion rate r_{OXA} [mol·g^{-1}·s^{-1}] (Table 4) was needed as a response value to generate the model. The conversion p is a dimensionless unit and thus, the r_{OXA} was estimated by the multiplication of the conversion rate [s^{-1}], i.e. the slope of the linear fit, with the initial molality [mol·g^{-1}] of the limiting monomer, the $b_{NCO,0}$ (Equation 12). The value in equation 12 was taken from Figure 27.

$$r_{OXA} = \frac{db_{OXA}}{dt} = \frac{d(p \cdot b_{NCO})}{dt} = \frac{1.33 \cdot 10^{-4} \cdot b_{NCO,0}}{s} \tag{12}$$

The three input concentrations were the main influences on the oxazolidinone formation rate. No significant cross-dependencies of the parameters could be found. The obtained data were subjected to ANOVA (Analysis of variance) to check for the validity and significance of the model.

Table 5: p-values from the ANOVA of the obtained model.

Factor	p-value
Model	0.005
a - Ln b_{Cat}	0.0014
b - Ln $b_{Epoxide}$	0.1948
c – Ln b_{NCO}	0.0407

The software performs tests and calculations of the variance, the F-value and gives the so-called *p*-values (probability values). Obtained *p*-values below 0.05 are regarded as statistically significant within the model. The model itself and the Ln b_{cat} have the highest significance, as seen from the

low *p*-values. The epoxide molality $b_{Epoxide}$ is regarded as insignificant, probably because of the large excess of epoxide. The isocyanate molality b_{NCO} is a significant term but has a lower influence on the model than the catalyst concentration. The quality of the fit is also calculated by the squared residuals R^2. The model obtains a high R^2 and Adjusted R^2. It has an acceptable quality of prediction as expressed by a Predicted R^2 of around 0.79 as well. Predicted and adjusted R^2 are in plausible agreement. The Adequate Precision is a measure of the signal-to-noise ratio (SNR) and should be as high as possible. Values above four are regarded as satisfactory.

Table 6: Calculated fit statistics.

Factor	Value
R²	0.948
Adjusted R²	0.909
Predicted R²	0.792
SNR (Adeq. Precision)	12.385
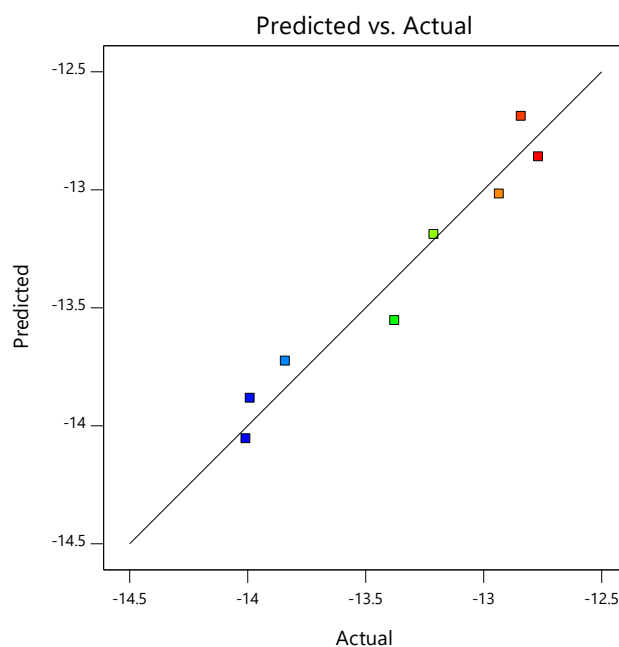
Figure 28: Plot of predicted against actual values.
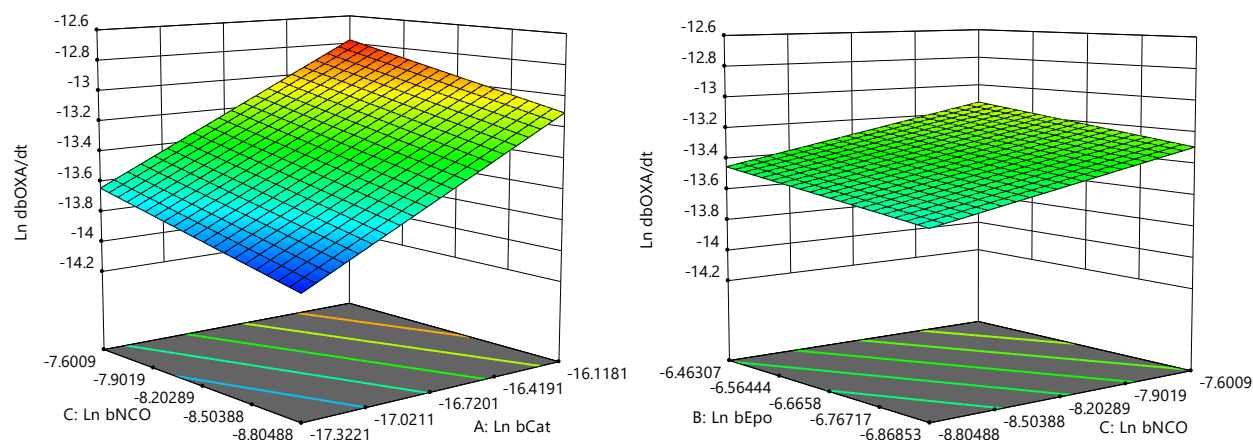
Figure 29: 3D surface graphs showing the high impact of Ln b_{Cat} and the more negligible impact of Ln $b_{Epoxidet}$ and Ln b_{NCO} on the obtained values.

The calculated coefficients of each parameter obtained from the model are the partial reaction orders (Table 7). These hint at the relevance of each compound in the elemental reaction of the rate-determining step.

Table 7: Coefficients of the parameters obtained from DoE.

Parameter	Coefficient of parameter / Partial reaction order
a	0.72
b	0.42
c	0.27

The catalyst and the epoxide concentration seem to be the most critical reactants in the rate-determining step. The alkoxide formation is therefore a good guess for the rate-determining step, because it is the only reaction that consumes catalyst. Three steps are necessary for the oxazolidinone formation (Scheme 11): the formation of the alkoxide, the nucleophilic attack of the alkoxide onto the isocyanate and the ring-closure including the release of the catalyst. The low partial reaction order of the b_{NCO} reflects that the compound is not relevant in the rate-determining step but, for example, is of importance in the next consecutive step (reducing the rate of a back reaction to the high-energy intermediate). The reaction order of the epoxide could not be established because of the excessive presence of epoxide making it readily available for the reaction in all experiments. The r_{OXA}, thus, was not altered significantly by changes in the $b_{Epoxide}$.
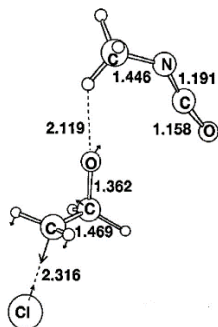
Figure 30: Rate-determining step as calculated using ab initio methods. Atomic distances [Å] are shown.[1]

The proposed rate-determining step is in accordance with former investigations based on *ab initio* calculations, wherein it was found that the transition state of the nucleophile attacking the epoxide in the ring-opening step is the rate-determining step.[1] High catalyst and epoxide molalities give fast oxazolidinone formation. Isocyanurate forms from the same intermediate as the oxazolidinone. A faster oxazolidinone formation thus might reduce the probability of isocyanurate formation, which is favourable for obtaining thermoplastic polyoxazolidinone.

5.3.   Polymerisations

The polymerisation was based on the monomers Bisphenol A diglycidyl ether (BADGE) and 4,4'-methylene diisocyanate (4,4'-MDI). They were selected due to their availability. Both compounds are thermally stable aromatics. Aromatic isocyanates offer the added benefit of significantly higher reactivity (Chapter 3.2) compared to aliphatic ones. An improved mechanical and thermal stability of the products is expected compared to analogous products based on aliphatic monomers.
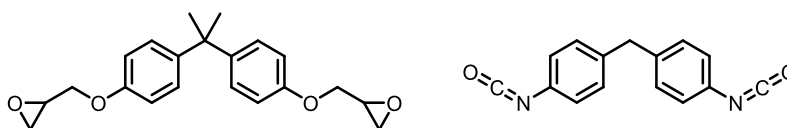
Scheme 23: Aromatic monomers: BADGE (left) and 4,4'-MDI (right).

5.3.1. Stability of reactants

The reactivity of the monomers in the presence of several catalysts and solvents was investigated at elevated temperatures, particularly to detect and quantify the extent of side reactions. These would impact the stoichiometry, resulting in lower molecular weight products. Chosen catalysts were BMPC and $ZnCl_2(TPPO)_2$, which were the most promising in the catalyst study (Chapter 5.1.5). Catalyst systems consisting of ionic liquids with metal halides, such as

BMPC with $ZnCl_2$, were also evaluated. This kind of combination was reported to be beneficial towards the oxazolidinone formation[77–79] Catalyst-BADGE mixtures were heated to approximately 190 °C and maintained at that temperature for 6 hours. The viscosity of all samples increased significantly due to polyether formation. This reaction is potentially initiated by the formation of an alkoxide following the nucleophilic ring-opening of the epoxide. The etherification of BADGE is challenging to detect in oxazolidinone formation experiments using IR spectroscopy because of the lack of discriminating vibrations.[42] The presence of ring opened products, however, can be inferred from the appearance of a broad OH-band in the range of 3200 cm^{-1} to 3600 cm^{-1}.

Table 8: Appearance of the BADGE samples after heating at 190 °C for 6 h in the presence of potential oxazolidinone forming catalysts.

Catalyst	Appearance	NMR
$ZnCl_2(TPPO)_2$	Solidified, brittle	Insoluble
BMPC	Liquid (hot), solid at room temperature	Polyether formation inferred
BMPC:LiCl (70:30)	Viscous (hot), solid at room temperature	Insoluble
BMPC:$ZnCl_2(TPPO)_2$ (70:30)	Liquid (hot), solid at room temperature	Polyether formation inferred

The solidification and insolubility of BADGE after the thermal treatment in the presence of a catalyst is likely caused by the crosslinking of the bifunctional monomer. $ZnCl_2(TPPO)_2$ and BMPC:LiCl (70:30) thus may not be suitable as catalysts. The insolubility of neat lithium chloride in BADGE excluded its use as a catalyst as well.
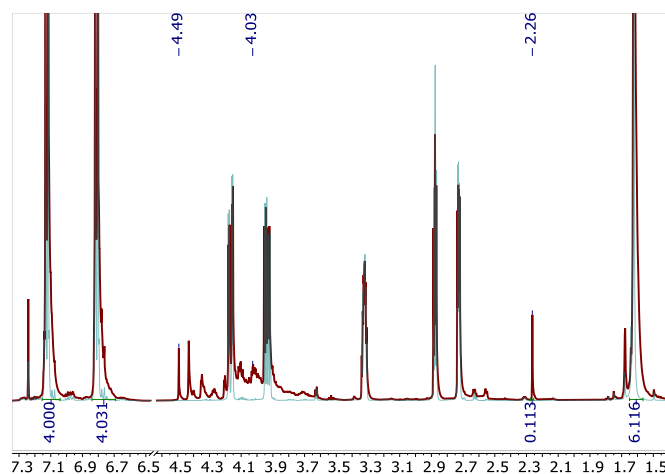
Figure 31: Zoom-in of the ^{1}H-NMR spectrum of pure BADGE (red) and the one heated to ca. 190 °C for 6 h (blue, bold line) together with 1 mol% BMPC.

BMPC and BMPC:ZnCl$_2$(TPPO)$_2$ showed the slowest polyether formation. Only the products of these combinations were soluble and could be subjected to NMR analysis. The presence of polyether was indicated by the appearance of numerous peaks in the region of the methylene protons of the glycidyl ether (4.0 to 4.5 ppm). The broadening of the aromatic peaks at approximately 6.8 ppm and 7.1 ppm suggests the formation of a component such as BADGE-polyether. The resonance at 2.3 ppm that appears after heating may originate from their methyl groups. An estimate of the polyether formation rate based on the appearance of this signal giyieldsves values of 0.30 mol$_{polyether}$·(mol$_{catalyst}$·h)$^{-1}$ for BMPC and 0.35 mol$_{polyether}$·(mol$_{catalyst}$·h)$^{-1}$ for the 70:30 mixture of BMPC:ZnCl$_2$(TPPO)$_2$, respectively.

The stability of the catalysts in 4,4'-MDI was not tested, as the isocyanate-based side reactions were already described using the model system (Chapter 5.1.5), in which BMPC and Ph$_4$PCl showed the lowest rate of side product formation.

5.3.2. **Solvent choice and concentration**

The most promising solvents identified in the model study were sulfolane, DMPU and DMI (Chapter 5.1.4). The influence of the solvents on the molecular weight distribution was investigated. DMI was excluded from further testing due to its higher hazard potential and the signals within its infrared spectrum overlapped with those of isocyanurate. The solvent removal proved to be more challenging than with the other solvents. A solvent that enables the production of linear, high molecular mass poly(oxazolidine-2-one), which can be easily removed after the reaction to isolate the synthesised polymer, was a prerequisite.

Sulfolane was identified as the more suitable solvent for the BMPC-catalysed oxazolidinone polymer formation. This insight was obtained by heating mixtures of the monomers and DMPU or sulfolane at 170 °C for 5 h. No reaction of BMPC and DMPU or sulfolane was observed within the timeframe using IR and NMR spectroscopic monitoring, indicating the solvents' inertness towards BMPC. Similar behaviour was observed for solvent-BADGE and BMPC-4,4-MDI mixtures. In contrast, the mixture of DMPU with 4,4'-MDI solidified in such experiments. DMPU is a cyclic urea derivate (Scheme 19). Its intrinsic basicity, particularly in contact with water, results in a pH-value of approximately 11 at a concentration of 100 g·L^{-1} in water.[80] Isocyanates undergo trimerisation in alkaline media.[9,81] The trimerisation took place even though DMPU was dried over molecular sieves. Acidic compounds, such as benzoyl chloride and diethylene glycol bis-chloroformate (DIBIS), were added to suppress this base-catalysed reaction. DIBIS proved to be the most effective. Benzoyl chloride inhibited the reaction, although higher concentrations were

necessary to achieve the same effect. Mixtures of DMPU and 4,4'-MDI were doped with increasing amounts of DIBIS and stored at room temperature as well as at 50 °C. Samples with DMPU solidified upon standing because of polyisocyanurate (PIR) formation. The time to solidification was longer when the DMPU was drier and more DIBIS was added. Higher temperatures resulted in faster solidification. The high dependence on the conditions of DMPU was found challenging in the preparation of the oxazolidinone polymers. Sulfolane possesses a low BRØNSTED acidity and needed no additional treatment to avoid trimerisation.[82]
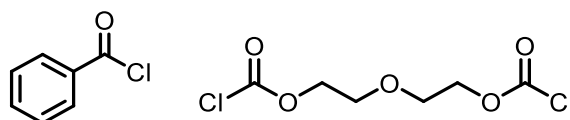
Scheme 24: Structures of benzoyl chloride (left) and diethylene glycol bis-chloroformate (right).

Table 9: Duration until solidification of stabilized 4,4'-MDI in DMPU through the addition of acidic additives.

Treatment of DMPU	Concentration DIBIS/ ppm	Time until solidified (RT)/ d	Time until solidified (50 °C)/ d
Untreated	0	< 1	-
	10	< 1	< 1
	100	2	< 1
	1000	2	< 1
Distilled	0	< 1	-
Molecular sieve	0	< 1	-
	50	1	< 1
	100	3	< 2
	250	5	< 2
Distilled from CaH₂	250	10	-

The solvents also affected the achievable molecular weight. Sulfolane was selected as the more suitable solvent compared to DMPU because higher molecular weight polymers could be obtained under similar conditions without additives to prevent the trimerisation of isocyanate. Kinetic differences may have contributed to the lower molecular weights in DMPU, but more likely, side reactions have impacted the stoichiometry and, consequently, the molecular weight.

For this investigation, polymerisations were carried out at a high temperature of 185 °C (Table 10). BMPC was mixed with epoxide and 85% of the total solvent, similar to the model system.

Stabilised DMPU (distilled over CaH_2) was used to prevent solvent-induced trimerisation. The equimolar monomer mixture was added together with the residual over 90 minutes (monomer dosing approach). The reaction mixture with a final index of 98 was cooled down after 4.5 h reaction time.

Table 10: Molecular weights achieved in DMPU or sulfolane at different solid contents.

Solvent	Solid content/ $g \cdot g^{-1}$	M_n/ $g \cdot mol^{-1}$	M_w/ $g \cdot mol^{-1}$
DMPU	23	16900	36100
Sulfolane	23	23800	73300

Significantly higher molecular weight polymers were obtained by utilising an altered process in which the majority of solvent was added over time (solvent & monomer dosing). The addition profile proved to be one of the key factors in suppressing side reactions. The higher reaction rate (Chapter 5.2) at increased concentration is the reason for the reduced extent of isocyanate-based side reactions; thus, the stoichiometry remained closer to one. Higher molecular weights were obtained consequentially.
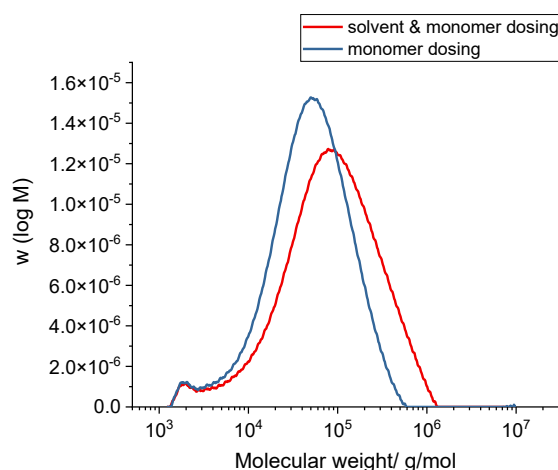
Figure 32: Molecular weight distribution of the products in case of the monomer addition only (blue) or the monomer and sulfolane addition over time (red).

High reactant concentrations were crucial for a fast conversion, according to the kinetic study (Equation 3). This was accomplished by adding the solvent as a second feed. The initially reduced use of solvent significantly increased the catalyst and monomer concentrations. The difference in time-dependent monomer concentration between both approaches is significant (Figure 33). Higher, plateau-like theoretical monomer concentrations will be obtained after a brief initial phase of about 20 minutes in the case of solvent and monomer dosing. The use

of less solvent was avoided to reduce the risk of non-ideal mixing of the reactants in the quite viscous reaction mixture.
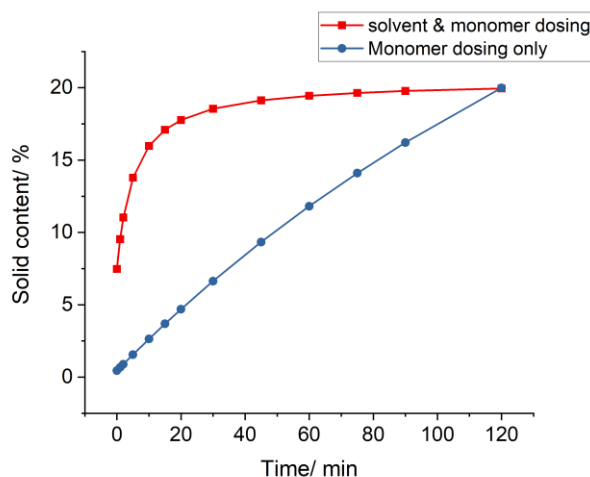
Figure 33: Time-dependent solid content for solvent & monomer dosing (red) or monomer dosing only (blue) protocols.

Increased final solid contents and thus higher reactant concentrations, led to a shift to a higher degree of polymerisation (Figure 34). Fewer side products were formed because of the higher reaction rate to poly(oxazolidine-2-one). The trend is similar for DMPU (Figure 77). A solid content of 22 % in sulfolane was identified as the upper limit. A WEISSENBERG effect was observed above this limit while stirring the reaction mixture.
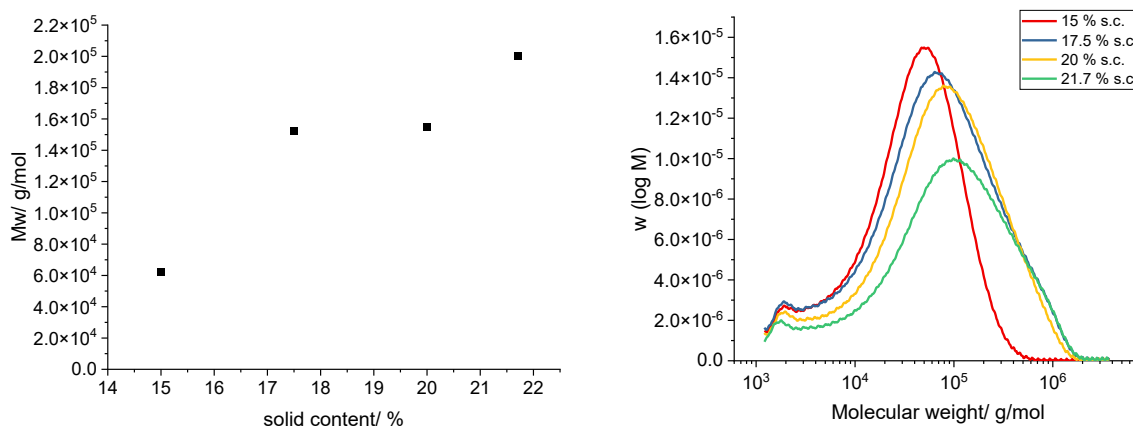
Figure 34: Weight-average molecular weight of the polymers plotted against the final solid contents in sulfolane. The molecular weight distributions are shown (right).

Low molar mass material of 1000 g·mol^{-1} to 2750 g·mol^{-1} was detected as a shoulder in SEC (Figure 32 and Figure 34) measurements. This feature in step growth polymerisations is typically interpreted in terms of the presence of cyclic oligomers, consisting of two to five repeating

units. Cycles can form at low monomer concentrations according to the RUGGLI-ZIEGLER dilution principle. The probability of intramolecular reactions, such as cyclisations, is independent of the concentration, whereas the probability of intermolecular reactions, i.e., the polyreaction, decreases with increasing dilution. Linear polymers are therefore favoured at higher concentrations.[83]
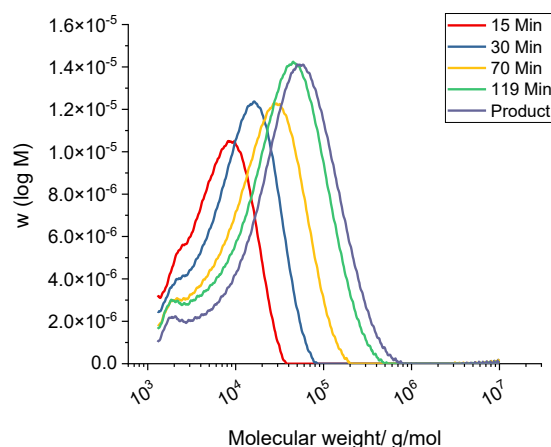
Figure 35: Time-dependent SEC of an experiment according to the improved process.

The formation of the shoulder in SEC determinations was observed even when using the solvent and monomer dosing approach. The cycles predominantly formed during the initial stage of the reaction. The molecular weight is low at the early stage of the reaction. Oligomers of about 2000 g·mol^{-1} have a higher probability of an intramolecular ring closure at this stage. The necessary solvent for dissolving the catalyst makes this dilution inevitable. Cyclisation became less prominent in a later stage of the polyreaction. The number of cycles was calculated as the integral ratio of cyclic molecules peak (1000 g·mol^{-1} to 2750 g·mol^{-1}) to the main polymer peak. The cycle-to-product ratio decreased after the monomer addition due to ongoing polymerisation.

Table 11: Integral ratio of cycles to polymer of an exemplarily reaction.

Time/ min	Integral ratio cycle/polymer /%
15	24.5
30	13.9
70	9.2
119 (end of monomer addition)	6.9
180 (product)	5.0

A high solid content throughout the reaction is favourable for obtaining high molecular weight polymers with a minimum number of cycles. The upper limit for the solid content was 22%. The experimental procedure (improved standard reaction) was modified to include the solvent and monomer addition process using a catalyst solution of BMPC, 1,3-di-*p*-tolylurea as a co-catalyst and 5% of the total solvent.

5.3.3. **Catalyst system and load**

The oxazolidinone-forming reaction using BMPC as a catalyst exhibited a lower reaction rate compared to a BMPC:urea catalyst system but a higher chemoselectivity in the model system (Chapter 5.1.5). In the polymer system, the isocyanate band at 2270 cm^{-1} was only observed during the addition with the pure BMPC catalyst. The *in-situ* generation of urea through the addition of water or 1,3-di-*p*-tolylurea accelerated the oxazolidinone formation reaction and reduced both the free isocyanate and the amount of trimer formed. The initial addition of urea was preferred because water-initiated side reactions are avoided and the urea amount could be precisely defined. The minimum and optimal urea content required to increase the chemoselectivity in the polymer system was found to be 0.5 mol% with respect to the total molar amount of isocyanate.
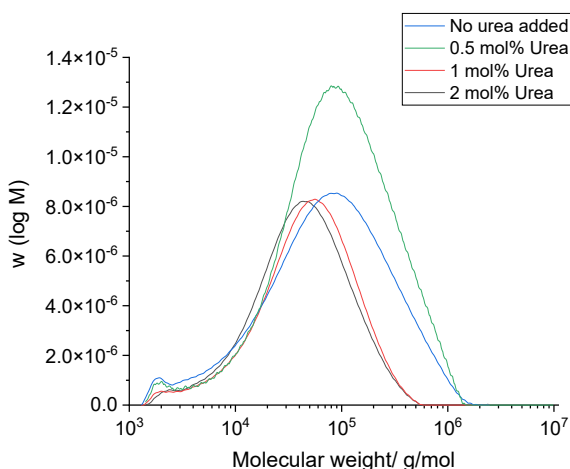
Figure 36: Size exclusion chromatograms of reaction products in which the co-catalyst (1,3-di-p-tolylurea) amount was varied.

Table 12: Weight-average molecular weight of the synthesised polymers using different amounts of urea co-catalyst.

Amount of 1,3-di-*p*-tolylurea/ mol%	M_w/ g·mol^{-1}
0	159.000
0.5	172.000
1	73.500
2	67.100

Amounts exceeding 0.5 mol% urea co-catalyst resulted in a shorter chain length. A possible reason for this is that amines formed in the urea epoxide reaction (Scheme 21) might form terminal groups with reduced reactivity, such as urea and β-amino alcohols. Both functional groups are, in principle, eligible for oxazolidinone formation (Chapter 3.3).
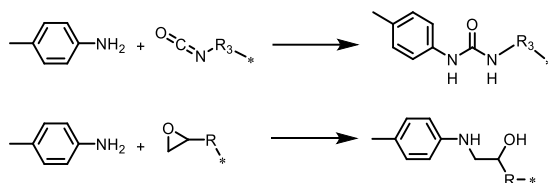
Scheme 25: Chain termination through the reaction of mono-functional amine (i.e. p-toluidine) with reactive chain ends.

Polyurea formation is another conceivable reason for the lower M_w at higher urea contents. Polyurea is obtained from the reaction of diisocyanate with *in-situ* formed MDI-based amines (Scheme 26). The resulting imbalanced stoichiometry leads to lower molecular weight polymers. An attack by the second urea nitrogen on the epoxide would lead to the desired chain growth under release of an amine. Urea can be regenerated from the amine-isocyanate reaction.
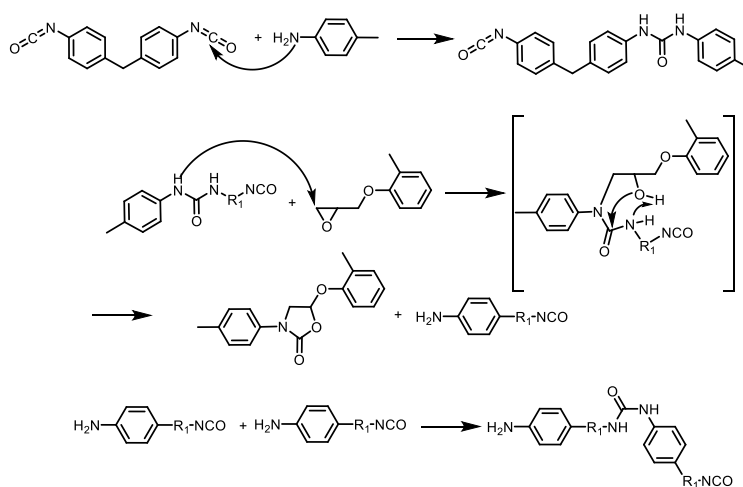
Scheme 26: Formation of an MDI-based urea or MDI-based amine similar to Scheme 21. The resulting isocyanate-containing amine may be capable of forming polyurea (bottom).

The reduction in cyclic oligomers and the increase in chain length using 0.5 mol% 1,3-di-*p*-tolylurea are probably caused by an alteration in the reaction mechanism (Scheme 21 and Scheme 26) compared to reactions without urea. The use of 2.5 mol% BMPC and 0.5 mol% 1,3-di-p-tolylurea as a catalyst system proved to yield products with a low cycle content and high molecular weight.

5.4.   **Scale-Up**

Sample quantities of up to 130 g of poly(oxazolidine-2-one) were obtained using a scaled-up procedure with optimized parameters from the lab-scale synthesis at an index of 100 (Chapters 5.3.2 and 5.3.3). The final solid content was reduced to 17% to prevent the WEISSENBERG effect in the reactor.

5.4.1. **Index-dependent molecular weight control**

The stoichiometry, as expressed by the isocyanate index, determines the molecular weight of the polymer. Index variation is a convenient method for controlling molecular weight, particularly when lower M_n values are desired. Higher molecular weight polymers can be obtained, for example, by an increase in conversion. The theoretical molecular weight can be calculated using the CAROTHERS equation (Equation 6). An excess of one of the monomers fundamentally results in a decrease in the maximum degree of polymerisation X_n (Chapter 3.1). The theoretical M_n was calculated by multiplying the mass of the repeating unit with the X_n calculated from the Carothers equation at an assumed conversion level of 98%. The calculated M_n values are in good agreement with the experimentally determined values (Figure 37). The assumed conversion of 98% implies a loss of ca. 2% of a functionality with respect to an initially equimolar stoichiometry. Side reactions account for this loss of presumably isocyanate. NMR spectroscopic analysis indicated that the urea formation was more prominent than the isocyanurate formation. An amount of 2 -3.5 mol% urea relative to the oxazolidinone unit was calculated using NMR data, which is higher than in the small-scale syntheses with up to 2.0 mol%. Urea was probably formed from isocyanate and water during the transfer of monomers, as the hydrophilic solvent picked up some water from the reactor. Polyreactions with indices above 100 were not performed because of undesired isocyanate reactions, such as isocyanurate formation.
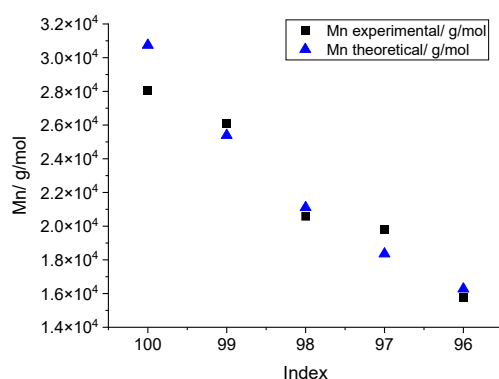
Figure 37: Molecular weight M_n (from SEC) from an equimolar (index 100) ratio of monomers to an epoxide excess of 4% excess (equals an index of 96).

The molecular weight calculated from NMR spectroscopic analysis ranged in a similar magnitude to the M_n obtained from SEC. The calculation of M_n from NMR spectra was based on the ratio of the methine signal of the polymer backbone to the remaining methylene signal of the terminal oxirane rings (Equations 27 and 28). NMR spectral analysis enabled the calculation of the absolute value of M_n, whereas SEC gives a relative M_n. The procedure only allowed for an estimation of the absolute M_n because the signal of the end group (methine proton) usually appeared as a shoulder on the larger sulfolane signal, potentially leading to a larger integral and resulting in a lower calculated M_n. Lower M_n might be obtained from NMR calculations because the cyclic content could not be excluded per se.

Table 13: M_n obtained from SEC and NMR calculations.

Polymer	M_n/ g·mol^{-1} SEC	M_n/ g·mol^{-1} NMR
PFR120	$3.5 \cdot 10^4$	$2.7 \cdot 10^4$
PFR111	$3.9 \cdot 10^4$	$2.7 \cdot 10^4$
PFR115	$6.5 \cdot 10^4$	$3.2 \cdot 10^4$

5.4.2. **Reaction temperature**

Elevated temperatures may decrease the isocyanurate content by accelerating oxazolidinone formation and increasing the decomposition of the trimer moieties, ultimately resulting in longer polymers. The average molecular weights (M_n, M_w), however, were not significantly impacted by the reaction temperature. No decomposition of functional entities was evident.
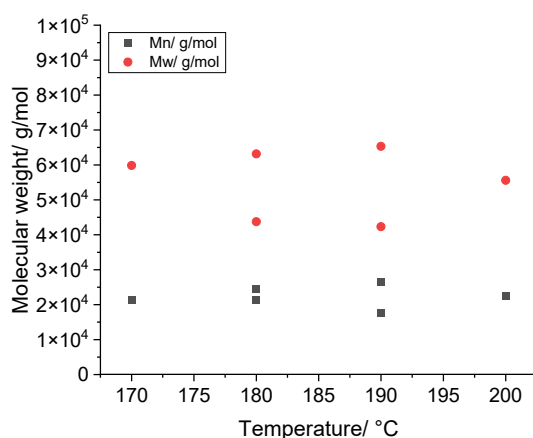
Figure 38: Influence of the reaction temperature on the average molecular weights M_n and M_w.

More oligomeric cycles were formed with increasing temperatures. This could result from an increased reaction rate for cyclisation in the initial phase of the addition due to the high dilution (Chapter 5.3.2). The formation of cyclic entities is an entropy-reducing reaction, which should be more favourable and faster at higher temperatures (by Eyring transition state theory considerations) relative to polymerisation.[84] An increase in cyclisation was also reported before and is in agreement with findings from Chapter 3.3.2.[61]
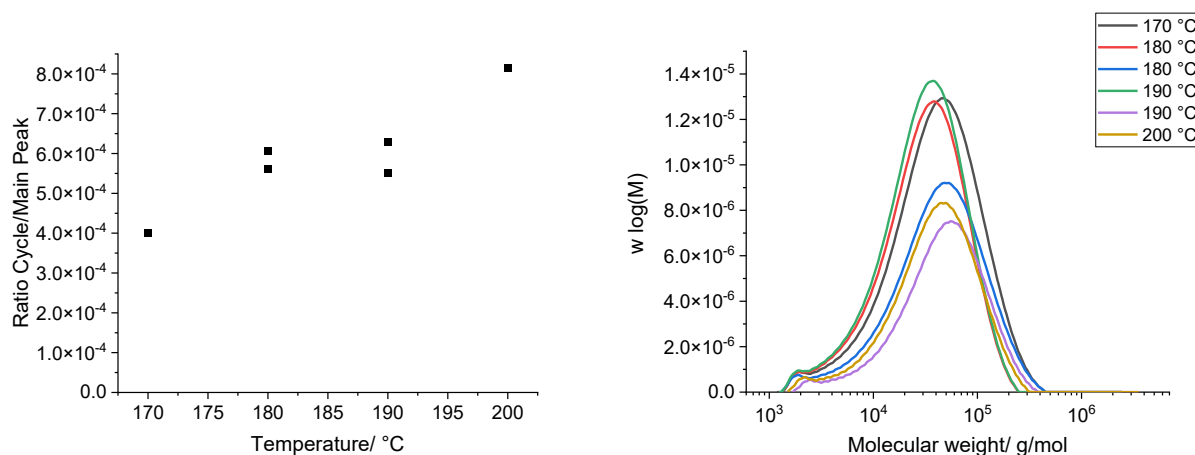
Figure 39: Cycle/main peak ratio with temperature (left); Molecular weight distributions of the prepared polymers in scale up (right).

The influence of temperature on the chemo- and regioselectivity of the mono-functional model system was investigated in Chapter 5.1.6. The optimal reaction temperature for molecular weight build-up in the procedure used is between 170 °C and 180 °C.

5.5. **Polymer properties**

5.5.1. **Work-up of polymers**

NMR analysis of the polymers revealed that they possess epoxide end-groups, even though an equimolar ratio (index 100) of reactants was used. The M_n can be calculated from the epoxide end-groups using NMR analysis (Chapter 716.3.2). Isocyanate-based side reaction products (urea, isocyanurate, oxazolidine imine) are probably responsible for the excess in epoxide and epoxide-termination of the polymer. The reactive epoxide end-groups could crosslink chains through an etherification reaction at elevated temperatures, i.e., in an extruder. Etherification was observed in the model system (Chapter 5.1.5). Crosslinking negatively impacts the thermoplastic characteristics and properties of the polymers. This stability issue can be addressed by converting the epoxide into a non-reactive end group.

An end-capping of the epoxide-terminated oxazolidinone polymers was attempted through a reaction with a monofunctional isocyanate (*p*-TI) or a carbodiimide (1,3-di-*p*-tolylcarbodiimide) with the objective of generating an oxazolidinone moiety and an oxazolidine imine moiety. These reactants were selected because the resulting products resemble the structural motif of the polymer. A 3.3-fold excess of *p*-TI or a 3-fold excess of 1,3-di-*p*-tolylcarbodiimide relative to the epoxide end-groups was sufficient to convert the epoxide end-groups. The termination by isocyanate was faster than that by carbodiimide and is, therefore, preferred. Full conversion of end-groups at 160 °C was observed after one hour using isocyanate and after six hours using the carbodiimide (Figure 40). This aligns with findings about the reaction rate from Chapter 5.1.8. The conversion was observed through the disappearance of the terminal epoxide signal at 2.7 ppm.
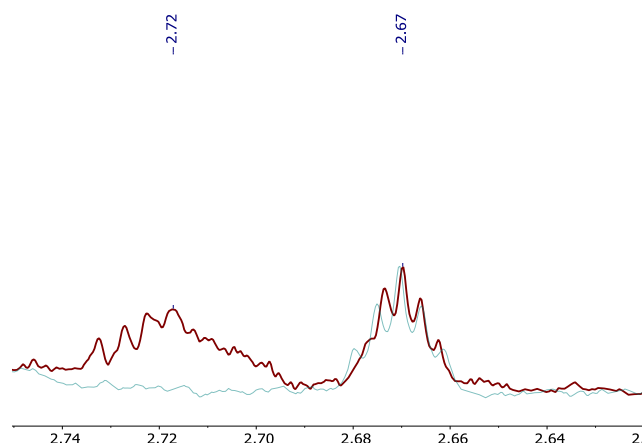
Figure 40: Detail of NMR spectra of an untreated polymer product (red) and the same product reacted with a 3.3-fold excess of p-TI after 1 hour.

The precipitation of the polymeric products from the solvent sulfolane (83 wt%) in an ethanol:water mixture was successfully achieved. Residual amounts of sulfolane ranging from 1.5 to 0.5 mol% in the polymer powder were indicated by 1H NMR using the optimal precipitation conditions. An absolute quantification, similar to that in Chapter 5.1.2, indicated that effectively only 0.1 wt% sulfolane was present in the polymer powder. Dilution of the reaction mixture was necessary to achieve lower viscosities and minimise the polymer-sulfolane interaction for this result. Dichloromethane (DCM) was chosen for the dilution because of its ability to dissolve the polymer, its low boiling point and high volatility. The end-capped polymerizates were diluted to a solid content of 3% for optimal results and precipitated in a mixture of ethanol and water (4:1). A minimum seven-fold excess of the precipitant ethanol was necessary to prevent the redissolution or swelling of the polymer. The fundamental reason for this elaborate process is the high affinity of sulfolane for poly(oxazolidine-2-one), hampering their separation. A fine white to beige powder was obtained that was eligible for further analysis and processing (Figure 41).
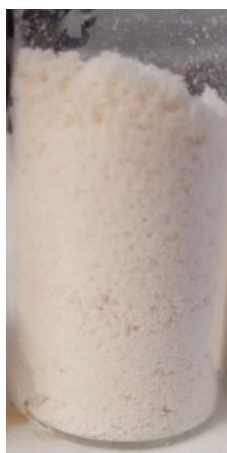
Figure 41: Polymer powder obtained after precipitation with a sulfolane content of 0.1 wt%.

The analysis of an end-capped, precipitated polymer, prepared according to the improved standard procedure (i.e., PFR111), confirmed the presence of poly(oxazolidine-2-one) as the predominant species of the product by ^{1}H and ^{13}C IGATED NMR. DMSO-d6 accounts for the two major peaks at 2.5 and 3.3 ppm. The two small peaks at 3.0 ppm and 2.3 ppm originate from the residual sulfolane.
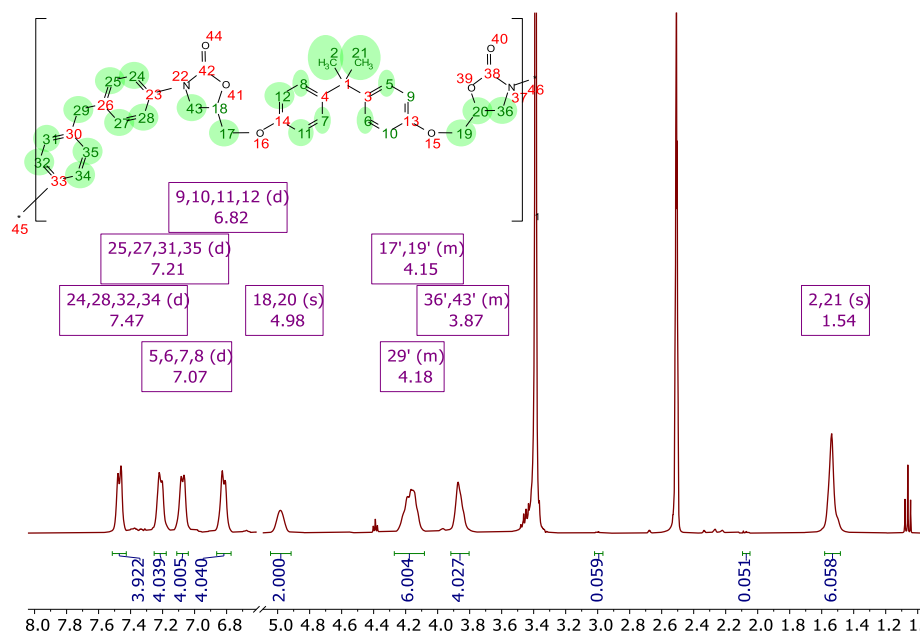
Figure 42: NMR spectrum with assignments of the precipitated, end-capped polymer PFR111.

No side products could be quantified in the ^{13}C-IGATED NMR analysis. This implies that the isocyanurate content (signal at 149 ppm.[51]) is favourably low. The signal at 70.9 ppm originates from the methine proton of the 5-substituted poly(oxazolidine-2-one). The two methylene signals at 46.5 ppm (C-N of oxazolidinone ring) and 68.0 ppm (C-O-C$_{arom}$) also belong to the 5-substituted poly(oxazolidine-2-one). No signals of the 4-substituted poly(oxazolidine-2-one) could be observed (expected at 65.9, 65.0 and 55.9 ppm).[51]
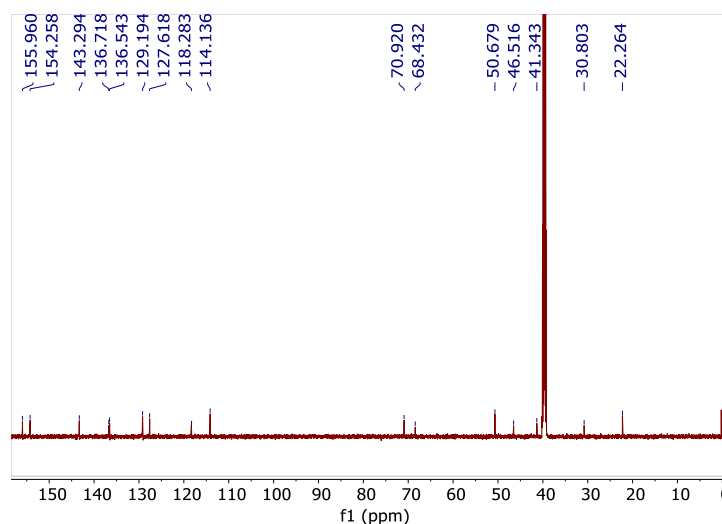
Figure 43: ^{13}C-IGATED NMR spectrum of a precipitated polymerisation product.

The signal at 98 ppm in ^{15}N HMBC spectroscopy could be assigned to the nitrogen atom of poly(oxazolidine-2-one). The corresponding signal of the nitrogen atom in the mono-oxazolidinone end-capped moiety was observed at 97 ppm. No other signals were detected.
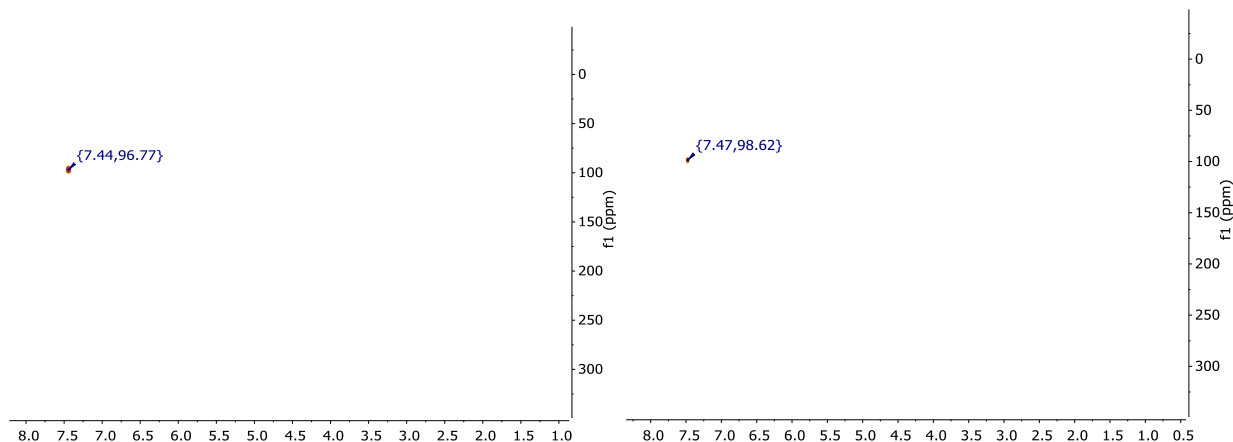
Figure 44: ^{15}N-HMBC spectra of a precipitated mono-(left) and poly(oxazolidine-2-one) (right).

The polymers exhibited thermoplastic properties because they could be melted, solidified and remelted again. All three polymer products from the scale-up experiments were dissolvable in DMSO.

5.5.2. **Properties of the poly(oxazolidine-2-one)**

The molar mass of the repeating unit of poly(oxazolidine-2-one) was confirmed by MALDI-MS at 590.2 g·mol^{-1}. It was performed using dithranol and sodium iodide as a matrix for a polymer powder (PFR115). Only oligomers were detected; therefore, the complete molecular weight distribution obtained from SEC measurements could not be verified. X_n values of up to eight were observed. The molecular weights increased by a mass of 23 due to the attached sodium ([M+Na]).
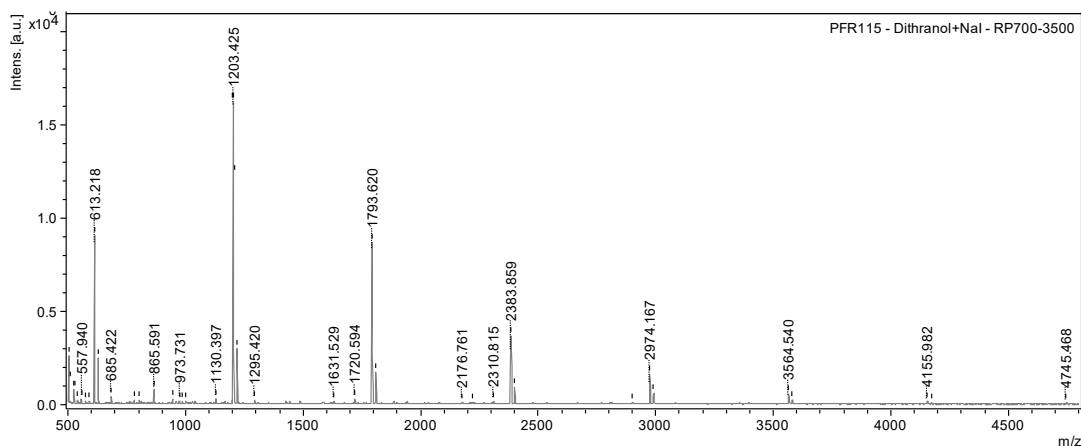
Figure 45: MALDI-MS of a polymer powder (PFR115) using Dithranol and sodium iodide as matrix.
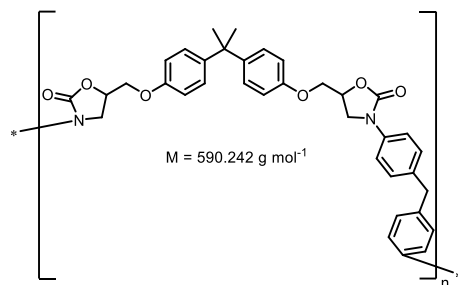
Scheme 27: Repeating unit of the formed POX as confirmed by MALDI-MS.

The polymer powder was amorphous, as indicated by the broad reflex around 20 ° in a powder X-Ray diffraction (PXRD) analysis. No other significant sharp reflexes were observed (Figure 46). Literature suggests that unsymmetrical repeating units in *d-* and *l-* configurations might prevent the crystallisation.[38]
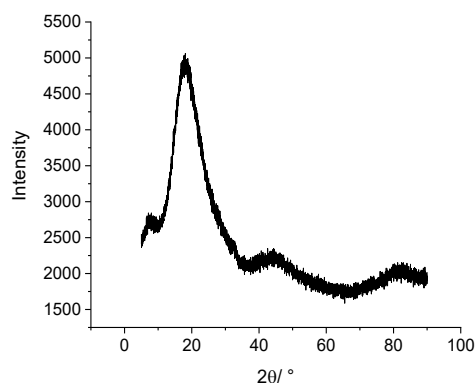
Figure 46: Powder XRD (PXRD) of the precipitated, end-capped PFR111.

The T_g is a function of the free volume of the polymer. It is governed by the chain ends because of their greater volume requirements at this range of degree of polymerisation. The chain ends account for a smaller proportion as molecular weights increase, resulting in a higher T_g. The operation temperature is typically defined as the region below the alpha transition or T_g, respectively. This is particularly true if the material's strength and stiffness are critical to the application. The T_g must not be mistaken with the decomposition temperature. The integrity of the polymer remains intact even at temperatures exceeding the alpha transition. The polymer can be used up to its decomposition T_d or ceiling temperature. [85]

The empirical FLORY-FOX equation describes the relationship between T_g and molecular weight. This enables the determination of the fundamental glass transition temperature $T_{g,\infty}$ that hypothetical polymers of infinite M_n possess. *L* is an empirical parameter dependent on the

polymer, which is related to the free volume of the polymer. The $T_{g,\infty}$ of the synthesised poly(oxazolidine-2-one) was 183 °C.

$$T_g = T_{g,\infty} - \frac{L}{M_n}$$
(13)

A value of $4.7 \cdot 10^5$ mol·g^{-1} for L was determined by a linear fit. L can be extracted from the slope of the plot of T_g against M_n^{-1} and ranges in the same magnitude of data published by Flory and Fox.[86,87]
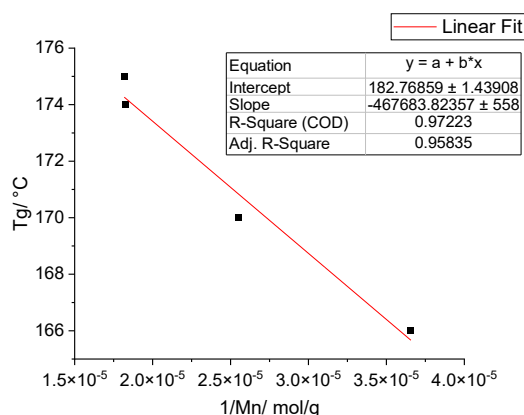
Figure 47: Inverse number-average molecular weight M_n against the glass transition temperature T_g.

Table 14: Molecular weights of selected, partially end-capped, polymer powders.

Polymer	M_n/ g·mol^{-1}	M_w/ g·mol^{-1}	End-capped	Crystallinity
PFR103	$5.5 \cdot 10^4$	$2.0 \cdot 10^5$	No	-
PFR111	$3.9 \cdot 10^4$	$7.5 \cdot 10^4$	Yes	Amorphous
PFR114	$2.7 \cdot 10^4$	$4.8 \cdot 10^4$	No	-
PFR115	$6.5 \cdot 10^4$	$1.6 \cdot 10^5$	Yes	-
PFR119	$5.5 \cdot 10^4$	$1.5 \cdot 10^5$	No	-
PFR120	$3.5 \cdot 10^4$	$6.2 \cdot 10^4$	Yes	-

The glass transition temperature T_g of the polymer powders (Table 15) was determined using Differential Scanning Calorimetry (DSC). The samples were heated to 200 °C, cooled to 25 °C and then re-heated to 200 °C at a specified heating rate of 10 K·min^{-1}. The measured glass transition temperatures T_g were taken from the second heating cycle. The glass transition temperatures and consequently the operating temperatures, were observed to be between 166 °C and 175 °C, regardless of the end-capping. Higher T_g were observed with increasing molecular

weight. The T_g of POX was significantly lower than that of commercial PES (T_g 220 °C).[50] POX with a T_g of 160 °C (BADGE; 4,4'-MDI) and 179 °C (BADGE, 2,4-TDI) has been reported in literature, leading to the conclusion that similar or higher molecular weight polymers were obtained.[29,30]

Table 15: Thermal properties of the polymers using DSC and TGA.

Polymer	T_g/ °C	T_{d_onset} / °C	T_d/ °C	$T_{g\infty}$/ °C
PFR103	175	330	400	
PFR111	170	330	400	
PFR114	166	330	400	
PFR115	174	-	-	183
PFR119	174	330	400	
PFR120	169	-	-	

The decomposition of poly(oxazolidinone) was observed to start from 330 °C, regardless of whether inert gas or air (T_{d_onset}) was used during the TGA. The samples were heated to a final temperature of 600 °C at a heating rate of 10 K·min^{-1}. The decomposition temperatures T_d were determined as the temperature at the maximum slope of decomposition. The thermal decomposition temperature T_d of all polymers was approximately 400 °C. The measured T_{d_onset} of 330 °C exceeds the T_{d_onset} reported in the literature, which ranged from 240 °C to 300 °C. Thermodynamically more stable isocyanurate is reported to decompose at about 400 °C.[13,15,88]

No difference between end-capped and non-end-capped POX was detected by TGA. It was postulated that carbon dioxide is the main product of the decomposition of the oxazolidinone ring (first decomposition step). The similarity of the T_{d_onset} with or without nitrogen purging gas indicates that this is a non-oxidative decomposition process. Amines, compounds containing C=C and C=N double bonds and aniline were reportedly detected by IR as further decomposition products.[15] These decomposition products may react with atmospheric oxygen, leading to a second oxidative decomposition step at about 450 °C (Figure 48). Similar T_d values were reported for poly(oxazolidine-2-one) synthesised from TDI and BADGE.[30] Poly(oxazolidine-2-one) exhibits higher decomposition temperatures compared to conventional polyurethanes made from aromatic isocyanates and an aliphatic polyol. The T_{d_onset} of polyurethane is usually around 200 °C (Chapter 3.2), with their T_d around 300 °C.[89] The decomposition temperature T_d of PES is significantly higher (about 500 °C) than that of the prepared poly(oxazolidine-2-one).[90]
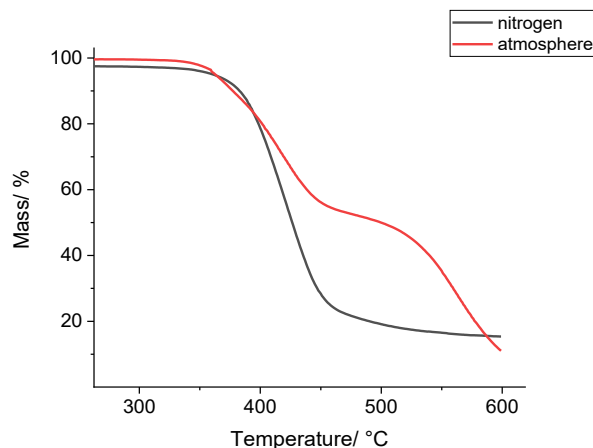
Figure 48: Zoom-in of TGA curves showing a second thermal decomposition step under atmospheric conditions.

5.6.   **Summary**

Polymers with molecular weights M_w up to $2.0 \cdot 10^5$ g·mol^{-1} were obtained through semi-batch polymerisations in sulfolane using a catalyst system of 2.5 mol% BMPC and 0.5 mol% 1,3-di-*p*-tolylurea at 180 °C on lab-scale. The majority of the solvent was added with the monomers to achieve high solid contents early in the process. Reduced side product quantities and higher molar masses were obtained compared to dosing the monomer only. Sulfolane was preferred over DMPU as a solvent because of the higher molecular weights achieved and the absence of solvent-induced side reactions. The variation of the index allowed for the tuning of the molar mass. The M_n aligned with predictions based on the Carothers equation at an assumed conversion of 98%. The optimal reaction temperature for the selected procedure of monomer and solvent addition was between 170 and 180 °C.

Reactive chain-ends were capped using *p*-tolyl isocyanate. Solvent removal was achieved by precipitation of the reaction mixture after dilution with DCM into a mixture of ethanol and water (4:1). The expected repeating unit of the polymer was confirmed by MALDI spectrometry and the amorphous state was verified by PXRD measurements. Amorphous, thermoplastic poly(oxazolidine-2-one) had a T_g of about 170 °C, a T_{d_onset} at 330 °C and a decomposition temperature T_d of ca. 400 °C. They range between thermoplastic polyurethane and high-performance polymers like PES. POX could not outperform PES, which has a higher T_g of about 220 °C and a higher decomposition temperature T_d of ca.500 °C.

6. Experimental

6.1.   Instruments

Fourier-Transformation Infrared Spectroscopy (FT-IR)

FT-IR measurements were performed at room temperature using a Bruker Vertex 70 equipped with an A225 platinum diamond ATR unit and *OPUS* software. Data were recorded in the range of 450-4000 cm^{-1} using 32 scans and a resolution of 4 cm^{-1}.

Nuclear magnetic resonance spectroscopy (NMR)

NMR spectra were recorded in chloroform-*d* (model products) or in DMSO-*d6* (polymers) with tetramethyl silane (TMS) as an internal standard using a Bruker AVANCE 400 MHz and 500 MHz (frequencies for ^{1}H-NMR) spectrometer. The data was evaluated using *MestReNova* 10.0. A Whittaker Smoother baseline correction was applied to the spectra of the model system before the calculation of the chemo- and the regioselectivity.

Mass spectrometry

ESI-MS and LC-MS were performed on an Agilent 6224 ESI-TOF connected to an Agilent HPLC 1200 series with a direct injection or an LC-MS inlet. The samples were dissolved in acetone. MALDI-MS analysis was conducted on a Bruker UltrafleXtreme fitted with a Smartbeam II Laser and a TOF-TOF detector. Dithranol and sodium iodide served as the matrix.

Column chromatography

Column chromatography was used for the separation of the reaction products from the oxazolidinone low-molar-mass model reaction. Basic, activated aluminum oxide (Brockmann activity I) was used as the stationary phase. Toluene and ethyl acetate (6:1) were chosen as the eluent.

Automatic titration for EEW determination

The automatic titration was conducted using a Schott TA 20 titrator equipped with a pH-electrode. A 0.1 M potassium hydroxide solution in ethanol was used as a titrant. The automatic titrator was controlled through the software TitriSoft 2.73.

Size exclusion chromatography (SEC)

The SEC system consisted of a Kontron 422 pump set to a nominal flow rate of 0.7 mL/min, a SpectraSYSTEM AS1000 autosampler and a Schambeck RI 2000 RI-detector. A MZ-Gel SDplus linear column (5 µm, 300x8 mm) and two MZ-Gel SDplus guard columns (50 Å, 100 Å, 50x8 mm each) were utilized for the separation. HPLC-grade DMF, containing 0.01 mol·L^{-1} LiBr, served as a mobile phase. The measurements were performed at 60 °C. *Chromatographica V1.0.25* was used for the evaluation. The calibration was performed using PS-standards of various molecular weights with a narrow molecular weight distribution.

Powder X-ray diffraction (PXRD)

PXRD measurements were performed using a Panalytical MPD X'Pert Pro equipped with a copper anode and a BRAGG-BRENTANO geometry. Data were recorded from 5 ° to 90 °.

Differential Scanning Calorimetry (DSC)

DSC was performed using a Mettler Toledo DSC 1. The measurements were conducted using a program that included heating from 25 °C to 200 °C, cooling to 25 °C and a second heating to 200 °C at a heating and cooling rate of 10 K·min^{-1}.

Thermogravimetric analysis (TGA)

TGA was performed on a Netzsch TGA 209 F1 Iris at a heating rate of 10 K·min^{-1}. Measurements were conducted from 25°C to 600°C under either nitrogen or atmospheric conditions using ceramic aluminum oxide pans. Approximately 5 mg of the samples was used per measurement.

6.2.   Chemicals

OCGE (Grilonit RV1805) was distilled under reduced pressure prior to use and stored under inert gas over molecular sieve 4 Å. The epoxide equivalent weights ranged from 168.7 g·mol^{-1} to 172.7 g·mol$^{-1,}$ corresponding to a purity of 95% to 97%. *p*-Tolyl isocyanate was purchased from ABCR, stored under inert gas and was used as received. BMPC and 1-Ethyl-3-methylimidazolium acetate (EMIM acetate) were purchased from IoLiTech. TBAB, lithium chloride, anhydrous zinc chloride, bismuth chloride and iron chloride were purchased from Merck. All catalysts were stored under inert gas and used without further purification. The phosphane ligands TPPO, TOPO and TBPO were purchased from Sigma Aldrich and used as received. Sulfolane, 1,2-Dichlorobenzene, mesitylene and NMP were purchased from Merck. DMI was bought from TCI Chemicals. DMPU

was obtained from BASF SE and distilled prior to use. DMI, DMPU and Sulfolane were stored under inert gas and dried over molecular sieve 4 Å. The other solvents were used as received.

BADGE (DER 332), DMPU and 4,4'-MDI (Lupranat MES) were obtained from BASF SE. The required amounts of BADGE were stored at 50 °C to reduce viscosity and ease handling. 4,4'-MDI was stored at -28 °C and liquefied at 50 °C shortly before use. Sulfolane and DMPU were dried over molecular sieve 4 Å, unless stated otherwise. Chloroform-*d* and DMSO-*d6* were dried on molecular sieve 4 Å and used without further treatment. The CDCl$_3$ contained a strip of elemental silver as a stabilizer.

Synthesis of metal halide phosphane oxide complexes

All metal halide complexes were synthesised using the identical procedure described in the literature.[91] An exemplary description is given for ZnCl$_2$(TPPO)$_2$.
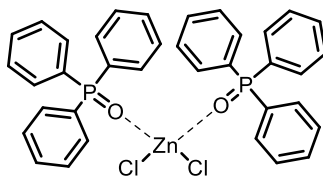
Scheme 28: Structure of the synthesised ZnCl$_2$(TPPO)$_2$ complex.

Triphenyl phosphine oxide (TPPO, 5.63 g, 20.2 mmol) was dissolved in 50 mL dry ethanol. Zinc (II) chloride (1.31 g, 10.0 mmol) was added to this solution while stirring. A white precipitate formed after one minute. The solution was stirred for an additional 20 h to complete the reaction. The suspension was filtered and the precipitate was subsequently dried in vacuum. The product was used without further purification.
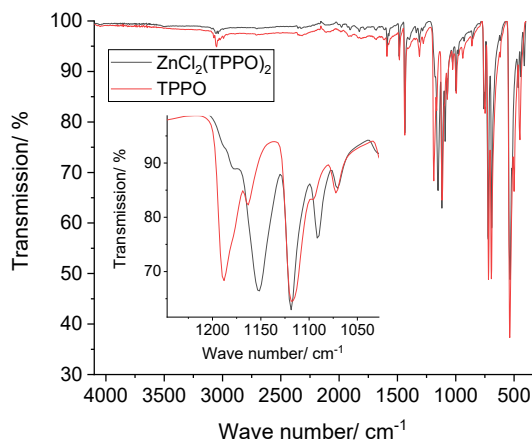
Figure 49: IR spectrum of the ZnCl2(TPPO)2 (black) and the pure ligand TPPO (red). [92]

The most significant difference in the IR spectrum is the P=O stretching vibration occurring between 1190 cm^{-1} and 1240 cm^{-1} in pure TPPO. A shift in the signal because of complexation was observed.[93] A band at 449 cm^{-1} appeared in the product spectrum (Zn-O vibration).

IR: 1437 cm^{-1} (m, P-Ar, aromatic in-plane stretching vibration), 1190 cm^{-1} (s, TPPO, P=O stretching vibration), 1151 cm^{-1} (s, ZnCl$_2$(TPPO)$_2$, P=O stretching vibration), 1119 cm^{-1} (s, P=O stretching vibration), 719 cm^{-1} (s, CH arom). 694 cm^{-1} (s, ring vibration), 536 cm^{-1} (vs, ring vibration), 449 cm^{-1} (w, ZnCl$_2$(TPPO)$_2$, Zn-O vibration).[93]

No precipitate formed when using tributyl phosphine oxide (TBPO). An oily product was obtained after evaporating the solvent and drying under vacuum. A molar ratio of ligand to metal halide of 3 to 1 was selected when using iron (III) chloride and bismuth (III) chloride.

Determination of epoxide equivalent weight (EEW)

The EEW of the *o*-cresyl glycidyl ether (OCGE) was determined using a back titration method according to Jung and Kleeberg.[94] A solution of hydrochloric acid in butanone (3%) was prepared by mixing 10 mL hydrochloric acid (37%) with 300 mL butanone. The OCGE (0.31 g, 1.9 mmol) was weighed into a 50 mL Erlenmeyer flask. Hydrochloric acid solution (5 mL) and 10 mL butanone were added. The solution was stirred for at least 30 minutes. Deionised water was boiled to remove CO_2 and prevent the formation of carbonic acid, which can falsify the result. Pretreated water (5 mL) was added to the epoxide solution to dissolve the potassium chloride that formed during the titration. Titration was conducted with a 0.1 M potassium hydroxide solution in ethanol. The titre was determined using an aqueous solution of 0.26 g (1.3 mmol) potassium hydrogen phthalate. Blank tests for reference were performed three times. The EEW titration was repeated three times to minimize the experimental error. The EEW was determined according to Equation 14. All volumes *V* (in mL) represent the average consumption of the three titrations.

$$EEW = \frac{1000 \cdot m_{epoxide}}{(V_{blind} - V_{Epoxide}) \cdot c_{KOH} \cdot titer} \tag{14}$$

The determination of the EEW for BADGE was based on a method from Garcia and Soares.[95] ^{1}H-NMR spectra of BADGE in CDCl$_3$ were recorded and employed to quantify the ratio of epoxide rings to the aromatic backbone of the BADGE. The integrals of the methine (3.32 ppm) and methylene protons (2.72 ppm and 2.86 ppm) were summed and denominated as I_1. The integrals I_2 of the aromatic peaks (approx. 6.82 ppm and 7.11 ppm) were summed as representatives of the backbone.

$$R_b = \frac{I_2}{I_1} \qquad (15)$$

The R_b value represents the ratio of the aromatic backbone to the oxirane protons. This ratio amounts to 1.33 for neat BADGE. The degree of polymerisation X_n of BADGE was calculated by subtracting the theoretical value from the measured value and dividing by 1.33.

$$X_n = \frac{R_b - 1.33}{1.33} \qquad (16)$$

The EEW of the supplied BADGE is calculated by the multiplication of X_n with the molar mass of the repeating unit (142 g·mol^{-1}) and subsequent addition to the theoretical EEW of BADGE (170.2 g·mol^{-1}).

$$EEW = 142 \frac{g}{mol} \cdot X_n + 170.2 \frac{g}{mol} \qquad (17)$$

The EEW was used to calculate the stoichiometry (the index) of the reaction instead of the molecular mass.

6.3. Analysis and calculations

6.3.1. IR analysis

The reaction was monitored using IR spectroscopy. The formation of oxazolidinone was indicated by an increase in the C=O band at approx. 1750 cm^{-1} and isocyanurate was detected at about 1710 cm^{-1}. The conversion of the isocyanate was observed as a decrease in the NCO vibration at 2270 cm^{-1}.
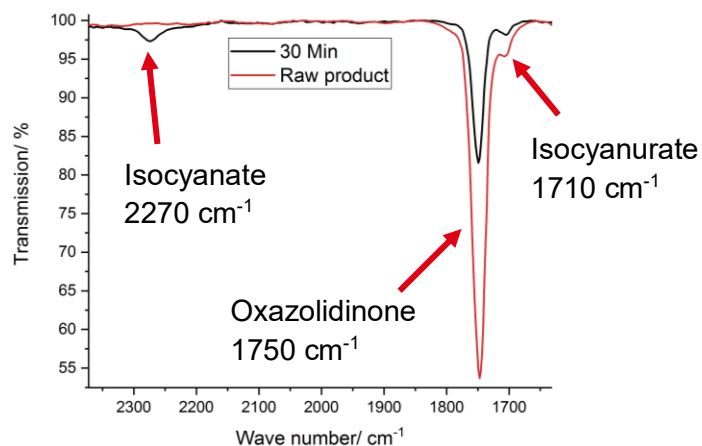
Figure 50: Zoom-in of an exemplary IR spectrum, highlighting the monitored signals during the reaction.

6.3.2. **NMR analysis**

NMR was the most important method for identifying and quantifying the reaction products. The starting compounds in the model system both contained an aromatic methyl group, which shifted depending on the chemical environment. The compounds' methyl signals were used for quantification because they allow easy assignment and show minimal overlap with other signals. The methyl group of p-TI appeared at 2.31 ppm, that of OCGE at 2.25 ppm and the sulfolane methylene groups were observed at about 2.22 ppm (pentet) and at 3.03 ppm (triplet). The methyl moiety originating from the epoxide shifted to 2.13 ppm and that of the isocyanate to 2.33 ppm in the mono-oxazolidinone. The methyl groups of isocyanurate were found at 2.38 ppm (Figure 51).

The calculations for the side product ratio were conducted using the integral ratio per proton $I_{\text{per proton}}$. The relevant integrals were divided by their respective number of protons to yield the $I_{\text{per proton}}$ (Equation 18). The integral ratio per proton of the relevant signals was divided by the total integral ratios per proton of the side product and the oxazolidinone signal at 2.33 ppm (Equation 19) for the side product quantification.

$$I_{\text{per proton}}=\frac{\text{integral}}{\text{number of protons}} \tag{18}$$

$$side\ product\ ratio = \frac{I_{\text{per proton}}(CH_3\ \text{of side product})}{I_{\text{per proton}}(CH_3\ \text{of oxazolidinone at 2.33 ppm})+I_{\text{per proton}}(CH_3\ \text{of side product})} \tag{19}$$
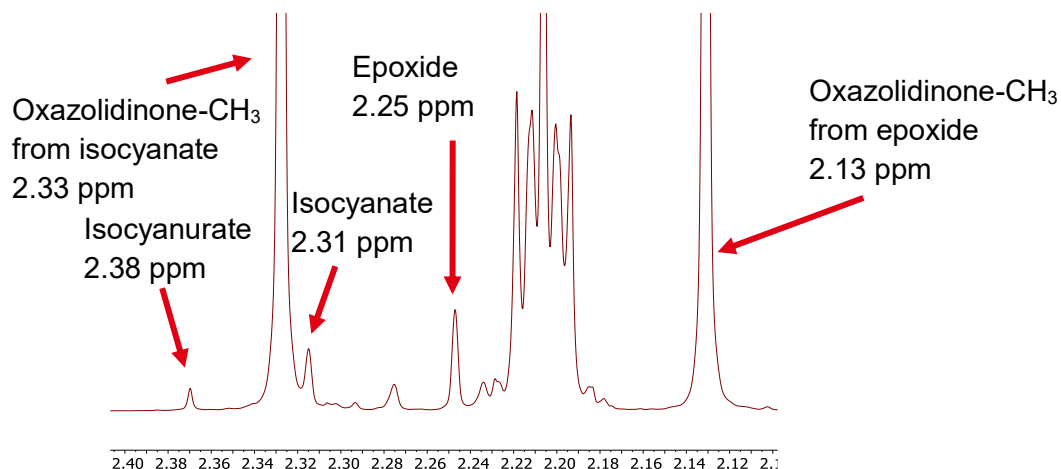
Figure 51: Detail of an NMR spectrum of an exemplary product from the model reaction. The most relevant signals have been assigned. The pentet at 2.22 ppm originates from sulfolane.

The ring-opening of the epoxide can occur in two different ways. Two isomers of the oxazolidinone can be formed, the 3-(p-tolyl)-4-((o-tolyloxy)methyl)oxazolidine-2-one (4-isomer) and the

3-(p-tolyl)-5-((o-tolyloxy)methyl)oxazolidine-2-one (5-isomer; Scheme 10 and Scheme 29). The isomers can be distinguished by NMR because of the different shifts of their methine protons. The CH-signal of the 4-isomer appears at about 4.7 ppm and that of the 5-isomer at about 5.0 ppm (Figure 52). The regioselectivity was calculated as the ratio of the 4-isomer to the 5-isomer (Equation 20). It was governed by the regioselectivity of the epoxide ring-opening (Scheme 29).
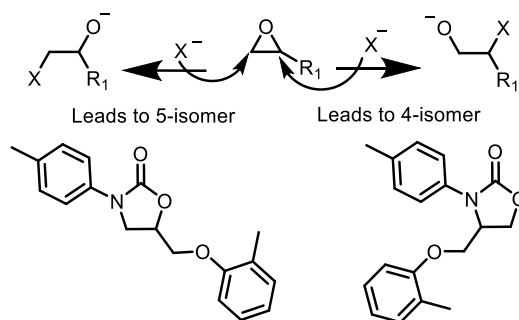
Scheme 29: Scheme of the two possible pathways of the epoxide opening leading to the 3-(p-tolyl)-4-((o-tolyloxy)methyl)oxazolidine-2-one or the 3-(p-tolyl)-5-((o-tolyloxy)methyl)oxazolidine-2-one of the oxazolidinone.

$$\text{Regioselectivity}=\frac{I\left(\text{CH}_{3\text{-}(p\text{-tolyl})-4\text{-}((o\text{-tolyloxy})\text{methyl})\text{oxazolidine-2-one}}\right)}{I\left(\text{CH}_{3\text{-}(p\text{-tolyl})-5\text{-}((o\text{-tolyloxy})\text{methyl})\text{oxazolidine-2-one}}\right)} \tag{20}$$

CH proton of the 3-(*p*-tolyl)-5-((*o*-tolyloxy)methyl)oxazolidine-2-one 4.98 ppm

CH proton of the 3-(*p*-tolyl)-4-((*o*-tolyloxy)methyl)oxazolidine-2-one 4.71 ppm
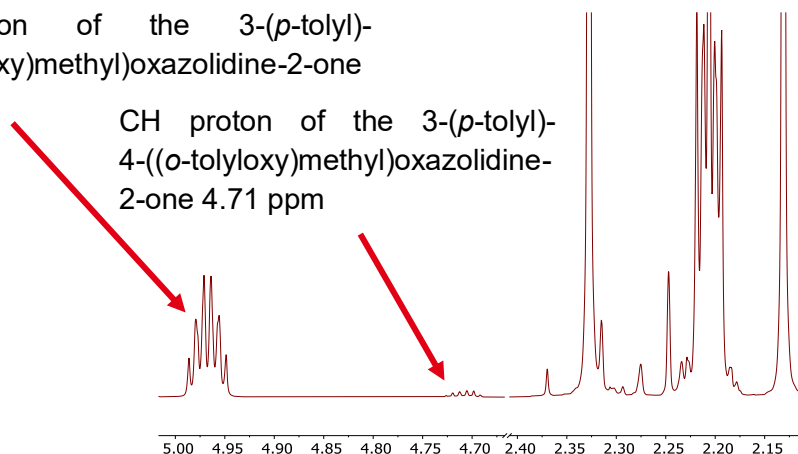
Figure 52: Detail of an NMR spectrum of an exemplary product showing the shift of the methine proton in the 3-(p-tolyl)-4-((o-tolyloxy)methyl)oxazolidine-2-one and the 3-(p-tolyl)-5-((o-tolyloxy)methyl)oxazolidine-2-one, respectively.

An example of time-resolved monitoring of side product selectivity and regioselectivity for a reaction conducted according to the general model synthesis procedure can be found in Chapter 5.1.2 (Figure 8).

The absolute quantification of isocyanurate was conducted using the following calculations. The mass of each sample was weighed and a specified amount of phenanthrene was added. The

integral per mole phenanthrene was calculated (Equation 21). The integral was divided by two because two protons **a** give the signal at 8.7 ppm.

$$\frac{integral}{mol} = \frac{integral_{\text{phenanthrene}}}{2 \cdot n_{\text{phenanthrene}}} = I_{\text{mol}} \tag{21}$$

The signal at 2.3 ppm was assigned to the nine protons of the methyl groups of *p*-tolylisocyanurate **b**.
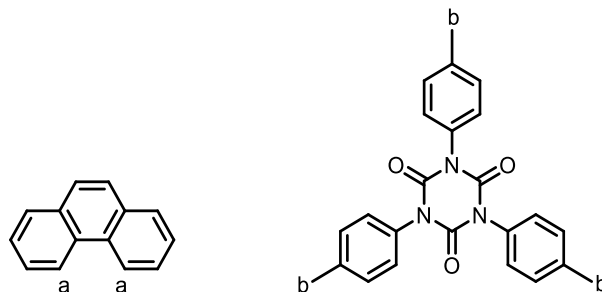
*Scheme 30: Structures of phenanthrene (left) and p-tolylisocyanurate (right). The protons used for the quantification are marked with **a** and **b**.*

The integral per proton was calculated using Equation 22.

$$integral_{\text{proton(isocyanurate)}} = \frac{integral_{\text{isocyanurate}}}{Number\ of\ protons_{\text{isocyanurate}}} = \frac{integral_{\text{isocyanurate}}}{9} \tag{22}$$

The mass of isocyanurate present in the sample was calculated using Equation 23 in which the molecular mass of isocyanurate is denoted as $M_{\text{Isocyanurate}}$.

$$m_{\text{isocyanurate}} = \frac{integral_{\text{proton(isocyanurate)}}}{I_{\text{mol}}} \cdot M_{\text{isocyanurate}} \tag{23}$$

The absolute weight percent of isocyanurate was calculated by dividing the mass of isocyanurate ($m_{\text{isocyanate}}$) by the total mass (m_{total}) of epoxide, isocyanate and solvent weighed in for the NMR experiment (g·g^{-1}; Equation 24).

$$isocyanurate_{\text{absolute}} = \frac{m_{\text{isocyanurate}}}{m_{\text{total}}} \tag{24}$$

The integral per proton of oxazolidinone was calculated using the methine group at 5.0 ppm (Equation 15). The relative amount of isocyanurate to oxazolidinone (mole·mole^{-1}) was calculated from Equation 26.

$$\text{integral}_{\text{proton(oxazolidinone)}} = \frac{\text{integral}_{\text{oxazolidinone}}}{1} \tag{25}$$

$$\text{isocyanurate}_{\text{relative}} = \frac{\text{integral}_{\text{proton(isocyanurate)}}}{\text{integral}_{\text{proton(oxazolidinone)}}} = \frac{n_{\text{Isocyanurate}}}{n_{\text{Oxazolidinone}}} \tag{26}$$

The NMR of the polymers allowed an estimation of the M_n. The X_n was calculated using the ratio of the integral per proton of the backbone to that of the oxirane end-groups. The X_n was multiplied by the mass of the repeating unit and the molecular weight of the end-groups (2.7 ppm) was added. The integral of the methine group (5.0 ppm) in the backbone was set to an integral of two for all calculations based on NMR, as this corresponds to the number of methine protons per repeating unit.
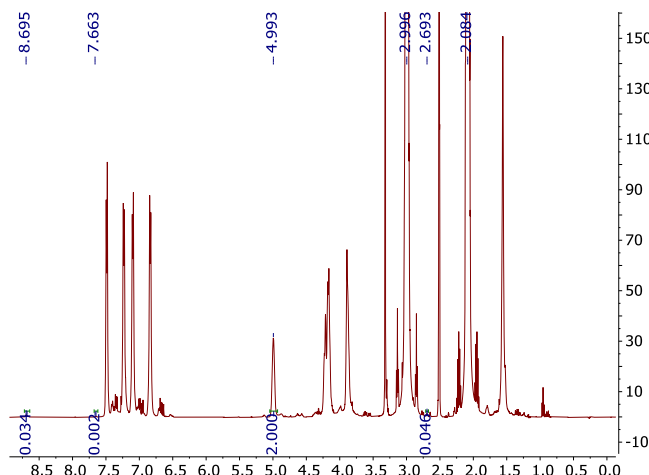
Figure 53: NMR of a reaction product of a polymerisation. The signals of the oxazolidine imine (7.7 ppm) and of urea (8.7 ppm) could be observed as well as of sulfolane at 2.1 ppm and 3.0 ppm.

$$X_n = \frac{I_{\text{per proton}}(\text{CH backbone})}{I_{\text{per proton}}(\text{CH}_2 \text{ oxirane})} \tag{27}$$

$$M_n = X_n \cdot M_{\text{repeating unit}} + M_{\text{endgroup}} = X_n \cdot 590.68 \frac{g}{\text{mol}} + 340.17 \frac{g}{\text{mol}} \tag{28}$$

The amount of residual solvent after precipitation was calculated using the integral per proton of the solvent after the precipitation. The solvent content was calculated for both methylene signals of sulfolane at 2.1 ppm and 3.0 ppm individually. The methine proton of poly(oxazolidine-2-one) at about 5.0 ppm was set to two for reference.

$$\text{Residual solvent} = \frac{I_{\text{CH2 of sulfolane}}}{4} \tag{29}$$

The urea content was calculated as a ratio of the integral per proton of the NH signal at 8.6 ppm to the sum of the integrals per proton of the methine signal from the poly(oxazolidine-2-one) backbone and urea itself.

$$\text{Urea content (\%)} = \frac{I_{\text{per proton}}(\text{Urea-NH})}{I_{\text{per proton}}(\text{POX-CH}) + I_{\text{per proton}}(\text{Urea-NH})} \tag{30}$$

6.4. Procedures using the model system

General procedure for model reactions

An exemplary reaction describes the general procedure for the preparation of 2-oxazolidinone. The conditions were slightly adapted depending on the investigation.
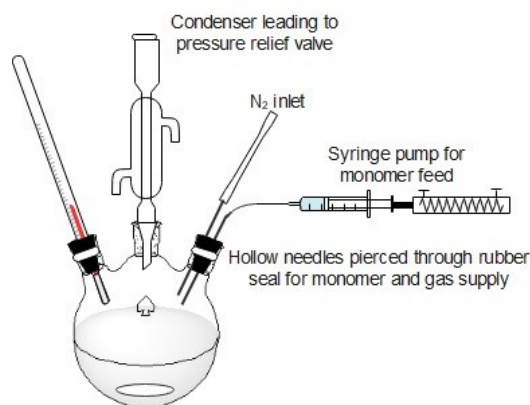
Figure 54: Drawing of the reaction setup used for the model reactions.

BMPC (1 mol% calculated on the total molar amount of epoxide, viz. 0.062 g, 0.31 mmol) and 5.0 g of the solvent sulfolane were weighed into a three-necked flask equipped with a magnetic stirrer bar, a rubber seal, a condenser and a thermometer. The flask was evacuated and purged with inert gas. OCGE (2 wt% of the total amount of epoxide, 0.11 mL, 0.12 g, 0.70 mmol) was added using a syringe that was inserted through the rubber seal. An index 98 mixture of 5.65 g (33.9 mmol) OCGE and 4.35 g (32.7 mmol) *p*-tolyl isocyanate was taken up into a 10 mL syringe under inert gas atmosphere and used as monomer feed. The three-necked flask was inserted into the oil bath at 173 °C and the monomer addition was started after 2 min using a Razel R-99 syringe pump. The addition took 90 min (0.11 g·min^{-1} or 5.95 mL·h^{-1} respectively). The reaction mixture was stirred with a stirrer bar at 750 rpm and the reaction temperature was maintained at approximately 160 °C. The final solid content of the reaction was 67 wt%. Aliquots of 0.1 mL were periodically taken from the closed vessel during the monomer addition using a

syringe inserted through the rubber seal. IR and NMR spectroscopy were employed to analyze the samples. The solution was maintained for an additional hour at the selected reaction temperature after completing the monomer addition. The reaction mixture was cooled to approximately 20 °C using cold water. In Chapters 5.1.5, 5.1.7 and 5.1.8, the addition time, catalyst and induction time were varied but all other parameters were kept constant.

A small amount of both monomers was added to the reaction vessel before the reaction began in the experiments in Chapters 5.1.4 and 5.1.6. The amounts of isocyanate and epoxy added were 2.5 and 2 wt%, respectively, of the total required amount.

The addition of isocyanate to epoxy, instead of using a mixture of epoxide and isocyanate, was tested in Chapter 5.1.7. BMPC (0.090 g, 0.47 mmol), OCGE (8.55 g, 50.3 mmol) and sulfolane (7.5 g) were weighed into a two-necked flask. The flask was evacuated and purged with inert gas. The reaction mixture was heated to 160 °C. *p*-TI (6.44 g, 48.4 mmol) was added by syringe over 84 minutes while the mixture was stirred at 250 rpm. The reaction mixture was maintained at 160 °C for additional 65 minutes. It was cooled subsequently to room temperature using an ice bath.

An excess epoxide or isocyanate was added to the catalyst solution prior to the start of the monomer addition experiments in Chapters 5.1.4 and 5.1.6. The procedure was the same for all tested catalysts. The experiment using Ph_4PBr is given as an example. Tetraphenylphosphonium bromide (0.136 g, 0.324 mmol) and *p*-TI (0.41 mL, 0.43 g, 3.2 mmol) were weighed into a three-necked flask under inert gas and heated to 160 °C. A mixture of 5.44 g (31.7 mmol) OCGE, 3.70 g (27.8 mmol) *p*-TI and 5.44 g sulfolane was added over 93 minutes. The solution was kept at 160 °C for another hour before cooling to room temperature.

The addition protocol for the reaction process in Chapter 5.1.7 was modified and conducted as schematically represented in Figure 55.
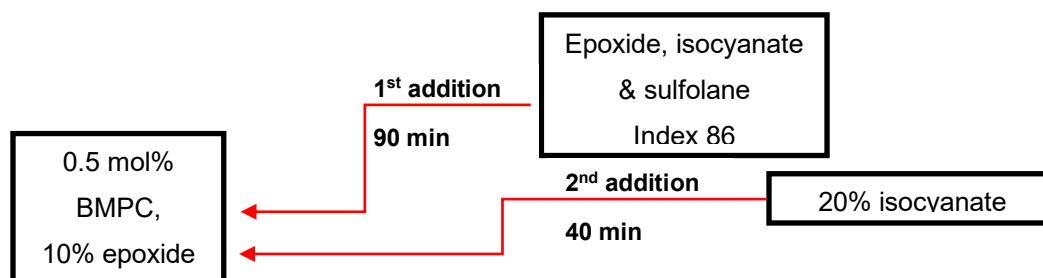
Figure 55: Flow chart for the process attempting a reduction in instantaneous isocyanate concentration.

O-Cresyl glycidyl ether (10 wt% of the required amount of epoxide, 0.55 mL, 3.5 mmol) and BMPC (0.051 g, 0.26 mmol) were placed in the flask prior to the reaction start. A mixture of OCGE (5.08 g, 30.2 mmol), *p*-TI (3.42 g, 25.7 mmol) and 5.0 g sulfolane was added over a period of 90 min reaching the reaction temperature of 160 °C. The molar ratio of epoxide to isocyanate was 76 to 100. An additional 0.86 g *p*-TI (6.5 mmol) was added over 40 min after the first addition was completely to achieve the final ratio of isocyanate to epoxide of 96 to 100.

Doping the catalyst solution with 50 wt% of the total required amount of epoxide prior to the start was tested in the same chapter. The temperatures, addition times and stirring rates were identical to those in the general procedure. The three-necked flask was charged with 0.064 g (0.33 mmol) BMPC and 2.90g (16.9 mmol) OCGE. The flask was evacuated and purged with inert gas. The mixture was heated to ca. 160 °C. A monomer mixture with an index of 146 consisting of 2.85 g (16.6 mmol) OCGE, 4.25 g (31.9 mmol) *p*-TI and 4.99 g sulfolane was added over 91 minutes. The index at the end of the addition was 96, which was identical to the other reactions.

Isocyanurate or carbodiimide replaced 30 wt% of the total amount of isocyanate in Chapter 5.1.8. They were added to the catalyst solution before the monomer addition. An exemplary reaction with 1,3-di-*p*-tolylcarbodiimide is described. BMPC (0.065 g, 0.34 mmol), OCGE (0.11 mL, 0.12 g, 0.69 mmol), 1,3di-*p*-tolylcarbodiimide (2.17 g, 9.76 mmol) and 4.99 g sulfolane were weighed into a three necked flask. The flask was evacuated, purged with inert gas and heated to 160 °C. An index 70 mixture of 5.65 g (32.9 mmol) OCGE and 3.06 g (23.0 mmol) *p*-TI was taken up in a 10 mL syringe under inert gas. The index 70 mixture was added over 84 minutes and a final index of 98 was obtained. The reaction mixture was maintained at 160 °C for another 60 minutes before cooling to room temperature.

Reaction with additional oxazolidinone as a co-catalyst

General procedure: A previously prepared reaction product (3.75 g) was added to the catalyst solution before the reaction commenced. The reaction product consisted of 1.25 g sulfolane, 2.5 g oxazolidinone and 0.01 g BMPC (0.05 mmol). The quantities of sulfolane and catalyst in the product were included in the monomer/catalyst calculation. Only 0.05 g (0.26 mmol) of fresh BMPC was added to the product prior to the addition. OCGE (5.74 g, 34.1 mmol), *p*-TI (4.25 g, 31.9 mmol) and 3.75 g of sulfolane were added over 90 minutes at 160 °C. Total amounts of 0.06 g BMPC (0.31 mmol), 5.0 g of sulfolane and 10.0 g monomers were used, which was identical to the standard procedure. The mixture was maintained at 160 °C for one more hour after the addition was completed and then cooled to room temperature.

Reactions with additional alcohol

The reaction was conducted similarly to the general procedure; however, in this case, 10 mol% of alcohol relative to the total amount of isocyanate was added before the reaction. An increase in index was necessary because the in situ formed urethane did not completely decompose. The index was adjusted to 105, which would be equivalent to an index of 95 in the event of full urethane decomposition. The reaction using 2-ethylhexanol is provided as an example.

The flask was charged with 0.066 g (0.34 mmol) BMPC, 0.438 g (3.7 mmol) 2-ethylhexanol, 0.11 mL (0.70 mmol) OCGE and 5.08 g sulfolane and heated to 180 °C. A mixture of 5.53 g (32.2 mmol) OCGE and 4.49 g (33.7 mmol) *p*-TI was added over a period of 89 minutes. The mixture was stirred for one more hour at 180 °C after the addition was completed and then cooled to room temperature.

Reactions with additional urea

The reaction was conducted similarly to the general procedure, but in this instance, 0.5 mol% urea (calculated relative to+ the total molar amount of isocyanate) was added to the catalyst solution as a co-catalyst. The addition time was reduced from 90 minutes to 30 minutes. The reaction using 1,3-diethyl-1,3-diphenylurea is given as an example.

The flask was charged with 0.068 g (0.34 mmol) BMPC, 0.044 g 1,3-diethyl-1,3-diphenyl-urea (0.16 mmol), 0.124 g (0.74 mmol) OCGE and 5.01 g sulfolane. The reaction solution was heated to 160 °C. A mixture of 5.63 g (33.5 mmol) OCGE and 4.37 g (32.8 mmol) *p*-TI was added over a period of 86 minutes. The mixture was stirred for one more hour at 160 °C after the completion of the addition and then cooled to room temperature.

Preparation of urethanes

Urethanes were synthesised from the alcohols 1-octanol, 2-ethylhexanol and Triton X 100 with *p*-TI. The synthesis procedure was identical for all three urethanes. 1-Octanol (2.24 g, 17.2 mmol) was weighed into a flask under a counter-current inert gas flow. The flask was closed with a rubber seal and heated to 60 °C. The alcohol was stirred at 400 rpm using a magnetic stirrer bar. *p*-TI (2.24 g, 16.8 mmol) was added over 5 minutes. The solution was cooled to room temperature after 250 minutes at 60 °C and analysed by IR and NMR.
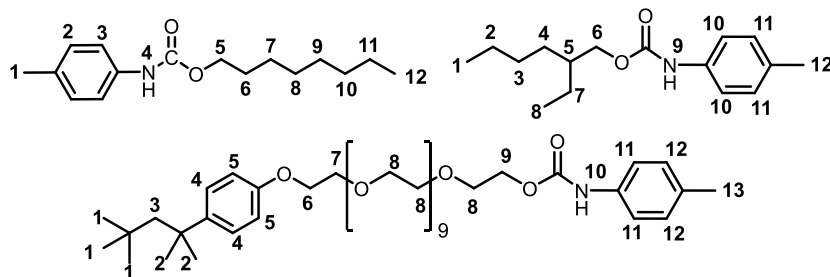
Figure 56: Structure of the p-TI-1-octanol urethane (top left), p-TI-2-ethylhexanol urethane (top right) and the p-TI Triton X-100 urethane (bottom).
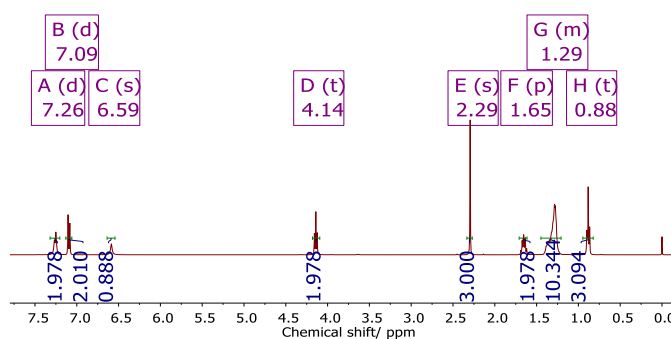
Figure 57: NMR spectrum of the p-TI-1-octanol urethane.

^{1}H NMR (400 MHz, Chloroform-d) δ 7.26 (d, ^3J = 6.8 Hz, 2H, **3**, CH arom.), 7.09 (d, ^3J = 8.2 Hz, 2H, **2**, CH arom.), 6.59 (s, 1H, **4**, NH), 4.14 (t, ^3J = 6.7 Hz, 2H, **5**, CH$_2$), 2.29 (s, 3H, **1**, CH$_3$), 1.65 (p, ^3J = 7.6, 6.8, 6.8 Hz, 2H, **6**), 1.43-1.20 (m, 10H, **7-11**, CH$_2$), 0.88 (t, ^3J = 6.8 Hz, 3H **12**, CH$_3$).

Further signals: 0.00 (s, TMS).
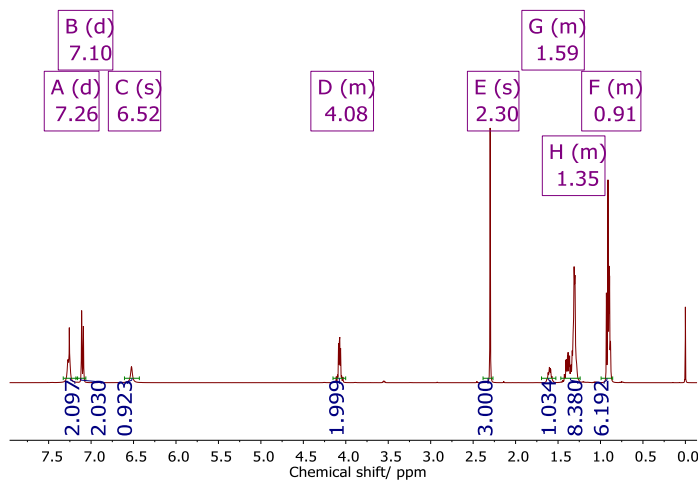
Figure 58: NMR spectrum of the p-TI-2-ethylhexanol urethane.

^{1}H NMR (400 MHz, Chloroform-*d*) δ 7.26 (d, ^3J = 6.6 Hz, 2H, **10**, CH arom.), 7.10 (d, ^3J = 8.3 Hz, 2H, **11**, CH arom.), 6.52 (s, 1H, **9**, NH), 4.14 – 4.01 (m, 2H, **6**, CH$_2$), 2.30 (s, 3H, **12**, CH$_3$), 1.67 – 1.53 (m, 1H, **5**; CH), 1.45 – 1.26 (m, 8H, **2, 3, 4, 7**, CH$_2$), 0.96 – 0.86 (m, 6H, **1, 8**, CH$_3$).

Further signals: 0.00 (s, TMS).
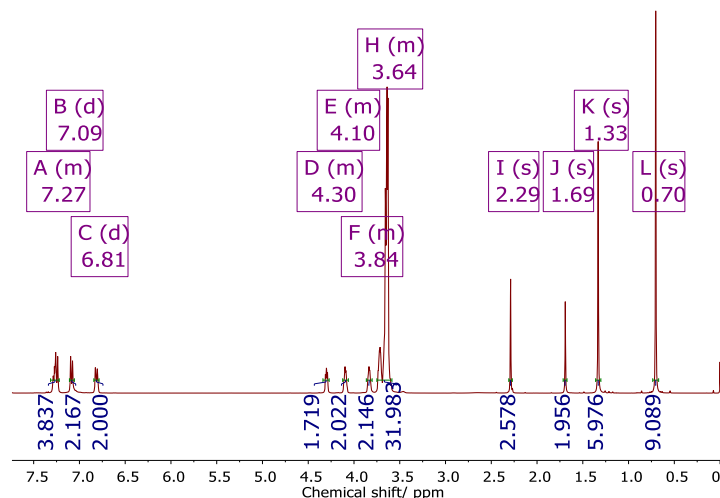
Figure 59: NMR spectrum of the p-TI-Triton X 100 urethane.

^{1}H NMR (400 MHz, Chloroform-*d*) δ 7.30 – 7.21 (m, 4H, **4,5**, CH arom.), 7.09 (d, ^3J = 8.1 Hz, 2H, **11**, CH arom.), 6.81 (d, ^3J = 8.9 Hz, 2H, **12**, CH arom.), 4.34 – 4.27 (m, 2H, **9**, CH$_2$), 4.14 – 4.05 (m, 2H, **6**, CH$_2$), 3.88 – 3.79 (m, 2H, **7**, CH$_2$), 3.69 – 3.58 (m, 32H, **8**, CH$_2$), 2.29 (s, 3H, **13**, CH$_3$), 1.69 (s, 2H, **3**, CH$_2$), 1.33 (s, 6H, **2**, CH$_3$), 0.70 (s, 9H, **1** CH$_3$).

Further signals: 0.00 (TMS).

Catalyst-monomer reactivity tests

The potential side reactions of the catalysts with neat monomers (epoxide or isocyanate) were investigated in Chapter 5.1.5. A flask was charged with 0.5 mol% Ph$_4$PCl (0.029 g, 0.075 mmol) and 2.56 g (15 mmol) OCGE for the test with epoxide. It was evacuated and purged with nitrogen. The flask was then fitted with a condenser with a pressure relief valve and placed into an oil bath at 173 °C to achieve a temperature of 160 °C. A flask was charged with 0.030 g (0.080 mmol) Ph$_4$PCl and 2.13 g (16 mmol) *p*-TI for the test with isocyanate. It was sealed with a stopper. Both experiments were stopped after 24 h of reaction, allowed to cool to room temperature and analysed using IR and NMR. The procedure was identical for the other tested catalysts.

Precipitation of mono-oxazolidinone

5-[(2-methylphenoxy)methyl]-3-(4-methylphenyl)-2-oxazolidinone, hereinafter abbreviated as **mono-oxazolidinone,** prepared according to the general procedure, was isolated by precipitation in a mixture of ethanol and water (4:1). Its structure was confirmed by NMR, IR and ESI-MS.
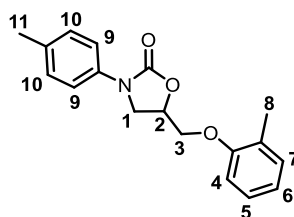
Scheme 31: Structure of the desired mono-oxazolidinone.
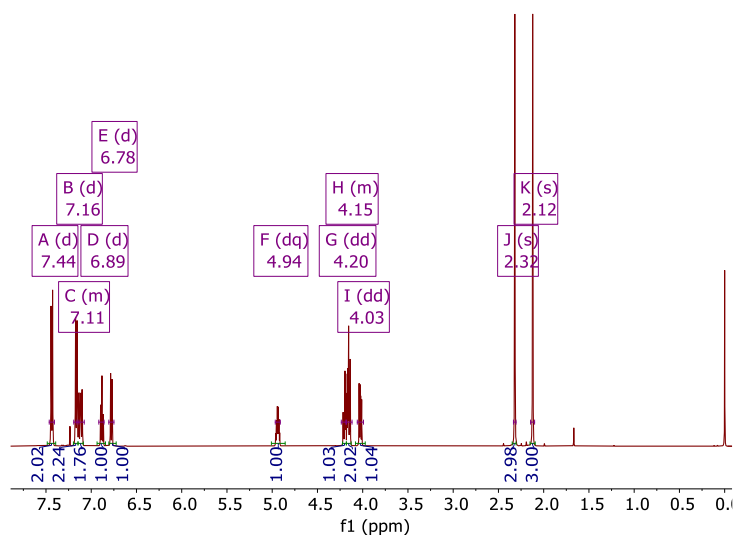
Figure 60: NMR spectrum of the synthesised and precipitated oxazolidinone.

^{1}H NMR (500 MHz, Chloroform-*d*) δ 7.44 (d, [3]*J* = 8.6 Hz, 2H, **9**), 7.16 (d, [3]*J* = 8.4 Hz, 2H, **10**), 7.14 – 7.09 (m, 2H, **5, 7**), 6.89 (d, [3]*J* = 7.4 Hz, 1H, **6**), 6.78 (d, [3]*J* = 8.1 Hz, 1H, **4**), 4.94 (dq, [3]*J* = 9.1, 4.2 Hz, 1H, **2**), 4.20 (dd, [3]*J* = 10.2, 4.4 Hz, 1H, **1'**), 4.19 – 4.12 (m, 2H, **3**), 4.03 (dd, [3]*J* = 8.8, 5.4 Hz, 1H, **1''**), 2.32 (s, 3H, **11**), 2.12 (s, 3H, **8**). Further signals: 7.24 (CDCl$_3$), 1.56 (water), 0.00 (TMS).
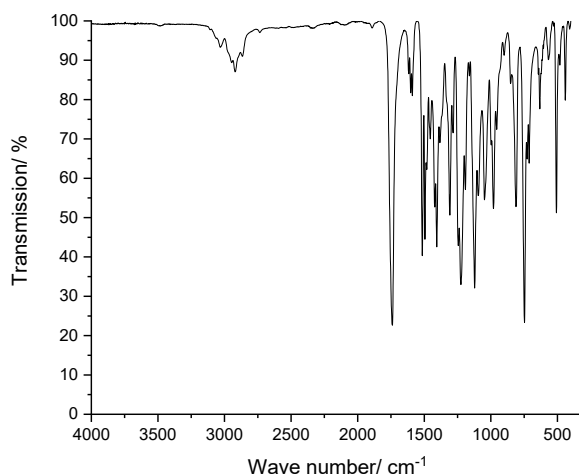
Figure 61: IR spectrum of the synthesised, precipitated and molten oxazolidinone.

IR: 2921 cm^{-1} (w, CH_3/CH_2 vibration), 1740 cm^{-1} (vs, C=O vibration), 1515 cm^{-1} (s, N-C vibration), 1225 cm^{-1} (s, C-O stretching vibration), 1121 cm^{-1} (s, C-O stretching vibration), 810 cm^{-1} (C-C skeletal vibration), 747 cm^{-1} (s, phenoxy C-H out of plane deformation), 507 cm^{-1} (s, aromatic in or out of plane deformation).[68,93]

ESI-MS: m/z [Da] 298.147 [$C_{18}H_{19}NO_3$+H] (calculated M+H 298.144), 617.266 [$C_{36}H_{38}N_2O_6$+Na] (calculated 2M+Na 617.263).

Catalyst-monomer reactivity tests

Possible side reactions of the catalysts with the neat monomer (epoxide or isocyanate) were investigated in Chapter 5.1.5. A flask was charged with 0.5 mol% Ph_4PCl (0.029 g, 0.075 mmol) and 2.56 g (15 mmol) OCGE for the test with epoxide. It was evacuated and purged with nitrogen. The flask was then fitted with a condenser with a pressure relief valve and placed into an oil bath at 173 °C to achieve a reaction temperature of 160 °C. A separate flask was charged with 0.030 g (0.080 mmol) Ph_4PCl and 2.13 g (16 mmol) *p*-TI for the test with isocyanate. It was sealed with a stopper. Both experiments were terminated after 24 h of reaction, allowed to cool to room temperature and analysed using IR and NMR. The procedure was the same for the other tested catalysts.

6.5. General procedure for the kinetic analysis of the polymerisation

The software DesignExpert® was used to set up the experimental plan for the DoE. A cubic experimental approach was employed to determine the partial orders and reaction rate. Two concentration levels were set for each reactant. An excess of epoxide was used to prevent isocyanate-based side reactions. The concentrations were expressed as molality b (mol·g^{-1}) to eliminate volume and density effects. The catalyst concentrations were chosen to facilitate the experimental determination of the initial 20% to 30% isocyanate conversion. The residual parameters were chosen to avoid side reactions. The conversion was monitored by ^{1}H-NMR and IR.
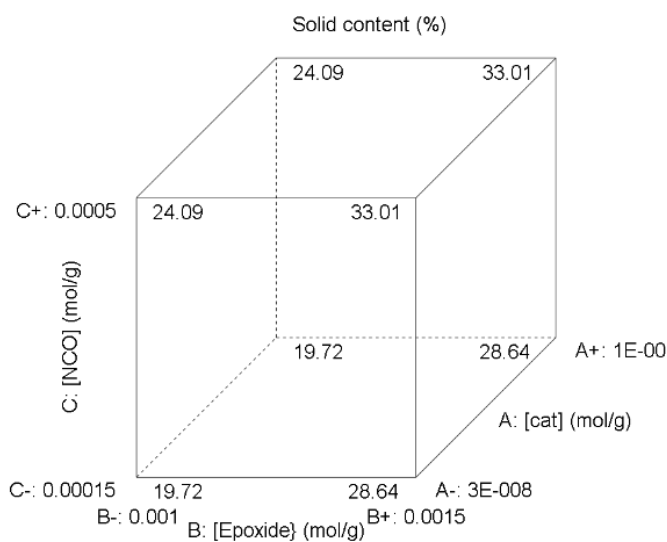
Figure 62: Cubic design of experiments involving three parameters: catalyst, epoxide and isocyanate concentration. The resulting solid contents (in %) are displayed as well.

All reaction vessels were made of glass, evacuated and purged with nitrogen before use. BADGE was dried over molecular sieve 4 Å. The sulfolane was dried over calcium hydride, distilled and stored over molecular sieve 4 Å under nitrogen.

Reactions were conducted according to the outlined procedure. A catalyst solution of 0.121 g BMPC in 15.8 g dichloromethane (DCM) was prepared and a clear, yellow solution was obtained. BADGE (17.76 g, 0.100 mol) was weighed into a nitrogen-purged, three-necked flask. Sulfolane (47.44 g) was added using a syringe to prevent contamination with water. A fraction of the catalyst solution (0.050 g, equal to 3.8 mg or 2.0·10^{-6} mol BMPC) was added by syringe. The

flask was evacuated, removing the DCM and then purged with nitrogen. Frozen 4,4'-MDI (3.47 g, 0.0277 mol) was weighed into a separate purged flask equipped with a stirrer bar. The flask was evacuated and purged with nitrogen again. The isocyanate was gently heated with a heat gun until a clear liquid was obtained. Sulfolane (3.47 g) was added by syringe. The solution was stirred and evacuated, accompanied by a noticeable removal of volatile compounds. It was purged with nitrogen after the gas release had stopped.

The flask containing the catalyst and the epoxide was equipped with a pressure relief valve, a rubber seal and a moon-shaped stirrer made from PTFE and PEEK under counter-current flow of nitrogen gas. The agitator shaft was made from stainless steel. A Pt100 thermocouple was inserted through the rubber seal. The flask was placed in an oil bath at 197 °C and the temperature of the reaction mixture was maintained at 180 °C. The MDI-sulfolane mixture (2.49 g, i.e., 1.25 g MDI, 0.010 mol) was injected at once through the rubber seal. Samples of 0.2 mL were taken periodically and analysed by ^{1}H-NMR and IR. The NMR sample was immediately quenched with an excess of methanol to prevent uncontrolled isocyanate side reactions. Residual methanol was removed under reduced pressure and NMR analysis using DMSO-*d6* was performed. The conversion of isocyanate was estimated using the ratio of the peak height of the isocyanate signal at 2270 cm^{-1} divided by the initial peak height. The reaction was terminated when about 20 to 30% of the isocyanate was consumed.

The amount of solvent and its integrals of the NMR signals remained constant throughout the reaction. The initial integral value of the signal at 2.08 ppm was defined using a sample taken immediately after MDI injection. The integral of the solvent was set to this reference in all subsequent samples. The residual isocyanate was converted with methanol to form a urethane. The integral of the methyl peak at 3.65 ppm was utilized to calculate the isocyanate conversion (Equation 31). The epoxide conversion was quantified using the oxirane methylene signal at 2.70 ppm. The ratio of the current to the initial samples decreases because of the reaction. The conversion is determined by subtracting the ratio from the initial 100% monomers.

$$conversion_{\text{NCO/epoxide}} = 1 - \frac{integral_{\text{current sample}}}{integral_{\text{first sample}}} \qquad (31)$$

The conversion to oxazolidinone was calculated using the integral of the methine signal at 5.00 ppm (Equation 32). The integral per proton ratios were determined for the urethane (3.65 ppm) and the oxazolidinone by dividing their integrals by three (urethane) or two (OXA). The isocyanate, respectively its quenched analogue, the urethane, was chosen as a reference because it was the limiting monomer in the OXA formation.

$$conversion_{\text{oxazolidinone}} = \frac{oxazolidinone\ integral_{\text{per proton current sample}}}{urethane\ integral_{\text{per proton 1st sample}}} \tag{32}$$

The conversions were plotted against time [min] and fitted using linear regression. The slope provided the rate of OXA formation per minute. The response value for generating the model, the molar conversion rate, was determined by multiplying the conversion rate by the initial molality.

6.6.   **Polymerisations**

DMPU required the addition of an inhibitor to prevent the trimerisation of the 4,4'-MDI. Tests were conducted using benzoyl chloride and DIBIS. A stock solution of DMPU with the corresponding additive was utilized. DMPU (10 g) was doped with 11 mg DIBIS or 41 mg benzoyl chloride, resulting in a 1000 ppm (DIBIS) or 3800 ppm (BzCl) solution. The solutions were diluted with DMPU to obtain the tested additive concentrations. About 2 mL of the diluted DMPU-additive solution was pipetted into a glass vial and five drops of molten 4,4'-MDI were added. The vial was sealed with a PP stopper and stored at room temperature or at 50 °C. The samples stored at 50 °C were fitted with a pierced rubber stopper to release the observed pressure. The sample stored under nitrogen was weighed into a glass flask and sealed with a glass stopper.

The possibility of BADGE homopolymerisation was tested. Catalyst (1 to 1.3 mol% on the total molar amount of epoxide groups) was utilized. An example using BMPC is provided. BMPC (0.017 g, 0.09 mmol) and BADGE (1.16 g, 6.8 mmol) were weighed into a sealable glass vial. The vial was placed in an oil bath at 195 °C for 6 h. The solutions were stirred with a magnetic stirrer bar. The mixtures were cooled to room temperature after 6 h and analysed using NMR and IR.

6.6.1. **Polymerisation on lab scale**

The conditions used in the model study required adaptation. The solid content was reduced to 16 to 35 wt% to account for the increased viscosities resulting from the formation of high molecular weight polymers. The solid content (s.c.) was determined by the ratio of the amount of solid material obtained after the solvent removal. Solids are defined as catalysts, monomers, polymers and potential side products. The amount of catalyst was increased from 1 mol% to 2 mol%, referring to the total epoxide. This higher catalyst concentration was necessary to prevent the accumulation of isocyanate. The mixture of monomers was diluted with solvent to achieve a sufficiently low viscosity for the monomer addition and to prevent the crystallisation of the 4,4'-MDI.

A three-necked flask was charged with 2.0 mol% BMPC (relative to the total molar amount of epoxide, 0.293 g, 1.53 mmol) and 52.51 g sulfolane under countercurrent nitrogen flow. BADGE (0.268 g, 1.53 mmol) was added, corresponding to 2 mol% of the total epoxide amount. The flask was evacuated to remove impurities and purged with inert gas. The flask was equipped with a condenser fitted with a pressure relief valve, a rubber seal and a halfmoon-shaped stirrer made from PTFE and PEEK, under counter-current flow of nitrogen using a hollow needle that was punched through the rubber seal. The agitator shaft was made from stainless steel. A Pt100 thermocouple was inserted through the rubber seal. The flask was placed in an oil bath. The oil temperature was adjusted to reach the desired reaction temperature in the vessel, e.g., 180 °C. The stirrer was set to 300 rpm. The monomer mixture, consisting of 13.1 g (75.1 mmol) BADGE, 9.40 g (75.2 mmol) 4,4'-MDI and 22.5 g sulfolane, was degassed, stored under inert gas and then added over 90 minutes to the catalyst solution using a 50 mL syringe. The final solid content (s.c.) was 23%. The mixture was maintained at the reaction temperature for an additional 60 minutes before cooling to room temperature. This reaction setup was utilized to compare DMPU and sulfolane in Chapter 5.3.2.
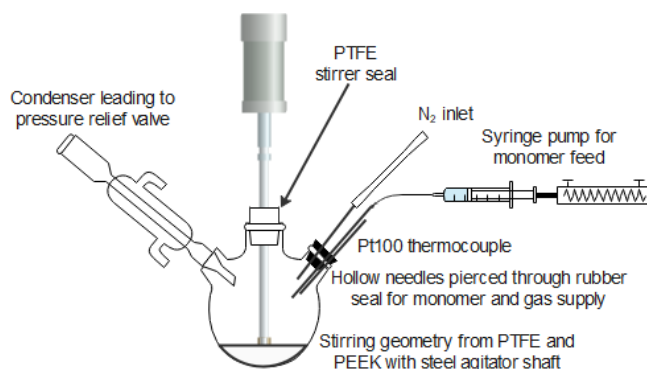
Figure 63: Setup of the polymerisation reactions on the lab scale in a 250 mL three-necked flask.

Polymerisations with solvent addition (solvent and monomer dosing approach) using urea followed a different procedure. A three-necked flask was charged with 0.49 g (2.5 mmol) BMPC, 0.13 g (0.56 mmol) 1,3-di-*p*-tolylurea and 6.0 g sulfolane. The flask was evacuated and purged with nitrogen. It was equipped with two rubber seals and a moon-shaped stirrer made from PTFE and PEEK under counter-current nitrogen gas flow. The catalyst solution was heated to 180 °C and stirred at 450 rpm. A mixture of 19.10 g (111 mmol) BADGE, 13.91 g (111 mmol) 4,4'-MDI and 14.1 g sulfolane was prepared, degassed and weighed into a 50 mL syringe. A second and a third 50 mL syringe were each filled with 51.70 g sulfolane. The monomers and the solvent were added over 120 minutes at addition rates of 17.4 mL·h^{-1} and 40.2 mL·h^{-1}, respectively. The first solvent syringe was empty after 58 minutes and was immediately replaced with the next solvent-

filled syringe. Monomer and solvent were added through two separate rubber seals. The reaction mixture was maintained at reaction temperature for another 60 minutes before cooling to room temperature.

6.6.2. **Polymerisation in the 1 L stainless steel reactor**

A 1 L pressurizeable Juchheim stainless steel reactor was utilized. It featured an oil-filled heating jacket connected to a Juchheim JU 75 2S thermostat with 2 kW heating power. The reactor was equipped with a U-shaped anchor stirrer with 2 crosspieces, two gauge glasses, a closed pipe inlet for a thermocouple, a syringe inlet, a bottom valve and a stirrer seal. The oil-lubricated stirrer seal featured an extra gas inlet. This inlet was linked to a three-way valve to apply vacuum or nitrogen gas to the closed reactor. An overpressure relief valve was also installed, allowing the nitrogen flow to be monitored during the reaction. The thermocouple was connected to a USB data logger with a data writing frequency of 15 seconds. The syringe inlet consisted of a pipe leading into the reactor and a screw-on rubber seal on top. A Heidolph Hei Torque 200 served as a stirrer. The addition of the monomer into the reactor was performed using a Razel R-99 syringe pump equipped with 50 mL syringes, plasticizer-free PVC tubing (Tygon 2001) and a hollow needle. A LongerPump LSP02-1B equipped with two 50 mL syringes, plasticizer free PVC tubing (Tygon 2001) and a hollow needle was used for the solvent addition. Three needles were inserted through the screw-on rubber seal leading into the reactor. The syringes had to be replaced during the addition. Three monomer syringes and seven solvent syringes were utilized for the addition in total.
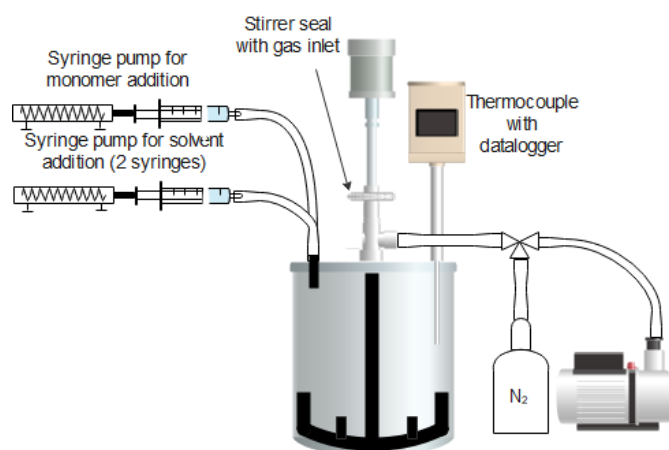
Figure 64: Setup of the 1 L stainless steel reactor.

The index and temperatures were varied, but all reactions were performed using the same process. The reactor was evacuated and purged with nitrogen. A catalyst solution was prepared

containing 2.03 g (0.016 mol) BMPC, 0.524 g (2.18 mmol) 1,3-di-*p*-tolylurea and 83.0 g sulfolane. The flask was evacuated and purged with nitrogen. The catalyst solution was filled into the reactor through an open inlet under a counter-current nitrogen gas flow. Catalyst particles were washed into the reactor with an additional 10.0 g of sulfolane. The inlet was sealed afterwards with the screw-on rubber seal. The solution was stirred at 200 rpm. The reactor was evacuated, purged with nitrogen and a constant flow of nitrogen was maintained. The monomer mixture (index 100, 70 wt% monomer), consisting of 72.47 g (422.1 mmol) BADGE, 52.78 g (422.2 mmol) molten 4,4'-MDI and 53.48 g sulfolane, was prepared. The monomer solution was degassed, purged with nitrogen and filled into three 50 mL syringes. Seven syringes, each containing 67.72 g sulfolane, were prepared and stored at 50 °C to prevent crystallisation.

The reactor was heated to the desired reaction temperature of e.g., 180 °C. The stirring rate was increased to 400 rpm and monomers and solvent were added. The addition time for one monomer syringe was about 40 minutes. The addition time for each syringe with solvent was set to 17 minutes or 34 minutes when two syringes were used simultaneously. The PVC tubing for the solvent was occasionally heated with a heat gun to prevent crystallisation of the solvent. Samples were periodically collected using the bottom valve to monitor the progress of the reaction and analysed using IR and ^{1}H-NMR. The syringes were removed after the addition was completed and the solution was maintained at the set reaction temperature for an additional 60 minutes. The reactor was cooled to approximately 60 to 100 °C and the hot product was released into a bottle using the bottom valve. The emptied reactor was filled with about 100 mL DMF and heated to 150 °C for 10 minutes for cleaning purposes. The reactor was cooled to room temperature, opened and the DMF was removed. Residues were cleaned manually.

6.7.   **Polymer processing**

End-capping

The required amount of chain stopper was calculated based on the remaining quantity of oxirane groups, which show a signal at 2.7 ppm in NMR. The integral ratio of the methylene signal of unreacted oxirane to that of the methine proton of the backbone at about 5.0 ppm provided the molar amount of terminal epoxides ($r_{non-converted\ epoxide}$). The mass of terminal epoxides was calculated using the sample amount, the solid content (s.c.), the ratio of residual terminal epoxides and the ratio of initial epoxide to the sum of initial epoxide and isocyanate (g·g^{-1}, equation 34).

$$r_{\text{non-converted epoxide}} = \frac{I_{\text{per proton}}(\text{oxirane-CH}_2)}{I_{\text{per proton}}(\text{backbone-CH})} \tag{33}$$

$$m_{\text{terminal epoxide}} = m_{\text{sample}} \cdot s.c. \cdot \frac{r_{\text{non-converted epoxide}}}{\dfrac{m_{\text{epoxide}}}{m_{\text{total monomer}}}} \tag{34}$$

The molar amount of terminal epoxides was determined using the calculated mass and the EEW of the terminal epoxide moiety. The necessary molar amount of reactant was calculated based on the molar amount of terminal epoxide. Full conversion of the epoxide groups was indicated by the disappearance of the characteristic oxirane methylene signal at 2.7 ppm. This peak partially interfered with the satellite signals of the deuterated DMSO.

$$n_{\text{terminal epoxide}} = \frac{m_{\text{terminal epoxide}}}{\text{EEW}_{\text{epoxide}}} \tag{35}$$

$$n_{\text{reactant}} = n_{\text{terminal epoxide}} \cdot \text{excess}_{\text{reactant}} \tag{36}$$

A three-necked flask was charged with 60.57 g polymerizate (equivalent to 12.11g polymer), which had a solid content of 20% and the flask was equipped with a condenser, a stopper and a rubber seal. A ratio $r_{\text{non-converted epoxide}}$ of 1.85 mol% of remaining epoxide groups relative to the initial epoxide amount was calculated based on NMR data. The polymer product was heated to 160 °C and a 3.8-fold excess of p-TI (0.382 g, 2.87 mmol) was added through the rubber seal over 20 min. This temperature was maintained for an additional 60 minutes to complete the reaction. The mixture was then cooled to room temperature and analysed using NMR.

Precipitation

The precipitations were conducted by diluting the end-capped polymerizate (18.88 g) with a solid content of 20% using 107.0 g of dichloromethane to yield a solution with a solid content of 3%. It was taken up in 50 mL syringes. The precipitant consisted of ethanol (0.75 L) and water (0.185 L) in a volume ratio of 4:1. The precipitant was mixed vigorously at room temperature using a disk-shaped mixer at 900 rpm. The syringe containing the polymerizate was positioned as high as possible above the beaker. An increased drop height enhanced the fineness of the dispersion. The addition rate of the polymerizate was set to 1 mL·min^{-1}. A white to beige precipitate was obtained. Insufficient dilution with DCM led to incomplete precipitation. Solidified droplets with a high solvent content (up to 35 mol% sulfolane relative to the polymer) were obtained.

Figure 65: Polymer obtained after precipitation using a too concentrated polymerizate (left) and using optimum conditions (3% s.c., right).

The precipitate was filtered under reduced pressure using a Büchner funnel and a water-jet vacuum pump. It was washed twice with ethanol and acetone. It was redispersed in approximately 1 L of water at 1000 rpm to remove any remaining residues of sulfolane. The dispersion was filtered and washed again using the previously described procedure. The precipitate was transferred into a flask and pre-dried at 60 °C with a membrane vacuum pump. Drying was then completed using a rotary vane vacuum pump capable of achieving a better vacuum. The resulting powder was analysed using NMR, MALDI-MS and PXRD.

Thermoplastic properties

The precipitated polymer powders were fully soluble in DCM at room temperature (23 °C). A single piece weighing approximately 100 mg was placed into a 50 mL bottle with a screw cap and then 30 mL of DCM was added. The specimen initially broke down into small pieces before fully dissolving.

6.8.   Synthesis of side products

Side products were synthesised to determine their chemical shifts (NMR) and IR bands. The ESI-MS spectra are included in the supporting information (Chapter 8).

1,3,5-tris(4-methylphenyl)-1,3,5-triazine-2,4,6(1H,3H,5H)-trione, hereinafter abbreviated as ***p*-tolylisocyanurate or isocyanurate**, was prepared by adding three drops of 1-Ethyl-3-methyl-imidazolium acetate (EMIM acetate) to 20.0 g (0.15 mol) *p*-TI while stirring. The flask was cooled using cold tap water. Fumes escaped from the flask during this strong exothermic reaction and the reaction product turned yellow. The reaction was finished after 20 minutes and a yellow solid was obtained. The solid was dispersed in ethanol and a fine powder was obtained after filtration.

The powder was suspended in acetone. A white, fine-grained powder was obtained after solvent removal by filtration and its structure was confirmed by NMR and IR analysis.
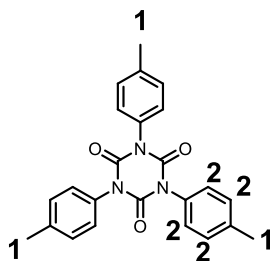
Scheme 32: Structure of p-tolylisocyanurate.
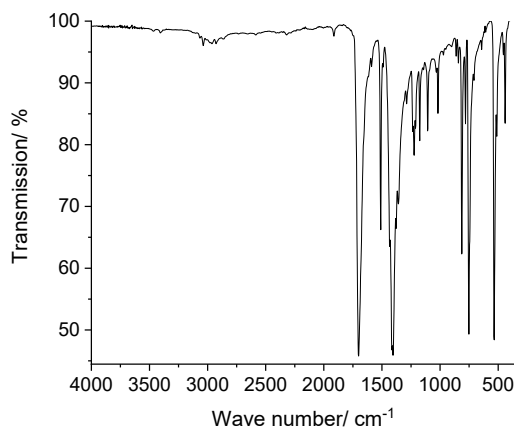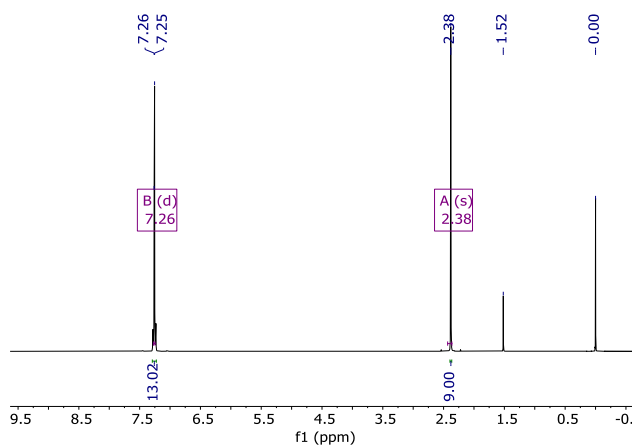
Figure 66: NMR and IR spectra of p-tolylisocyanurate. The dominant absorption at 1701 cm^{-1} (C=O vibration) was described for isocyanurates.[96]

^{1}H NMR (400 MHz, Chloroform-d) δ 7.26 (d, ^3J = 3.0 Hz, 12H, **2**, H arom.), 2.38 (s, 9H, **1**, CH$_3$). Further signals: 1.56 (s, H$_2$O), 0.00 (s, TMS).

IR: 1701 cm^{-1} (vs, C=O stretching vibration), 1510 cm^{-1} (vs, amide vibration), 1404 cm^{-1} (vs, symmetrical NCO stretching vibration), 752 cm^{-1} (vs, CH arom.), 534 cm^{-1} (vs, ring vibration).[93,96]

ESI-MS: m/z [Da] 400.166 [$C_{24}H_{21}N_3O_3$+H] (calculated M+H 400.166), 821.305 [$C_{48}H_{22}N_6O_6$+Na] (calculated 2M+Na 821.306).

1,3-di-*p*-Tolylcarbodiimide was synthesised from isocyanate using phosphane oxide as a catalyst following literature procedures.[71] *p*-TI (61.1 g, 0.459 mol) was weighed into a nitrogen-filled flask equipped with a condenser and a pressure relief valve. A 25 wt% solution of 3-Methyl-1-phenyl-2-phospholene-1-oxide in triethyl phosphate (0.237 g, 0.308 mmol) was added. The mixture was placed in an oil bath at 140 °C for 4 hours, during which strong gas evolution was initially observed. The product was recrystallised from cold diethyl ether, yielding long, colourless to slightly brownish needles and the structure was confirmed by IR and NMR analysis.
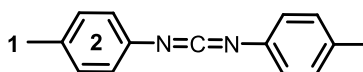
Scheme 33: Structure of the synthesised 1,3-di-p-tolylcarbodiimide.
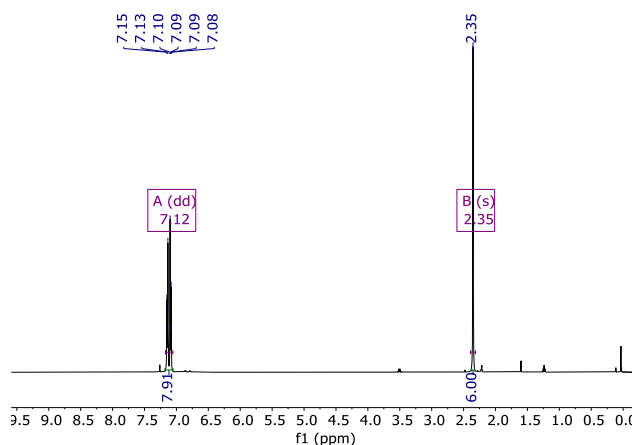
Figure 67: NMR spectrum of the synthesised 1,3-di-p-tolylcarbodiimide.

^{1}H NMR (500 MHz, Chloroform-d) δ 7.08 (dd, ^3J = 25.1, 8.3 Hz, H arom., 8H, **2**), 2.32 (s, CH3, 6H, **1**).

Further signals: 7.26 ($CDCl_3$), 3.51 (q, CH_2, 4H, diethyl ether), 1.24 (s, CH_3, 6H, diethyl ether), 1.56 (s, H_2O), 0.00 (s, TMS).
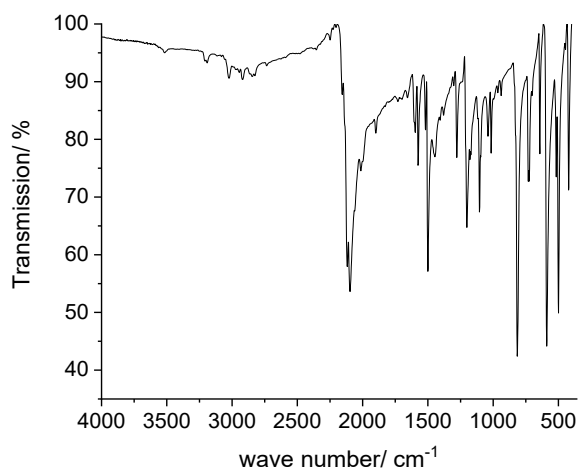
Figure 68: IR spectrum of the synthesised 1,3-p-tolylcarbodiimide.

IR: 2096 cm^{-1} & 2117 cm^{-1} (s, N=C stretching vibration), 1500 cm^{-1}(s, C-H arom), 1105 cm^{-1} (vs, aromatic C-H in plane deformation), 815 cm^{-1} (vs, CH arom.), 590 cm^{-1} (vs).[93]

ESI-MS: m/z [Da] 223.123 [C$_{25}$H$_{26}$N$_2$O$_2$+H] (calculated M+H 223.123).

***N*-3-di-*p*-tolyl-4-((*o*-tolyloxy)methyl)oxazolidin-2-imine**, hereinafter abbreviated as **oxazolidine imine**, was synthesised by weighing 0.119 g (0.62 mmol) BMPC, 2.3 mL (15 mmol) OCGE and 3.55 g(15 mmol) 1,3-*p*-tolylcarbodiimide into a nitrogen-filled flask. The amount of BMPC corresponds to 2 mol% relative to epoxide. The mixture was stirred under nitrogen and heated to 160 °C for 8 hours. The resulting product was a brown, brittle solid with a melting point of approximately 100 °C. Its structure was verified by IR, NMR and ESI-MS analysis.
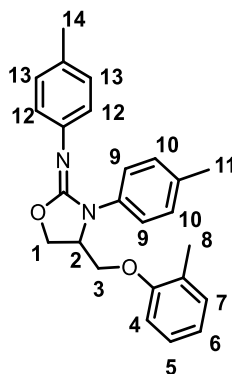
Scheme 34: Structure of the synthesised oxazolidine imine (N,3-di-p-tolyl-4-((o-tolyloxy)methyl)oxazolidin-2-imine).
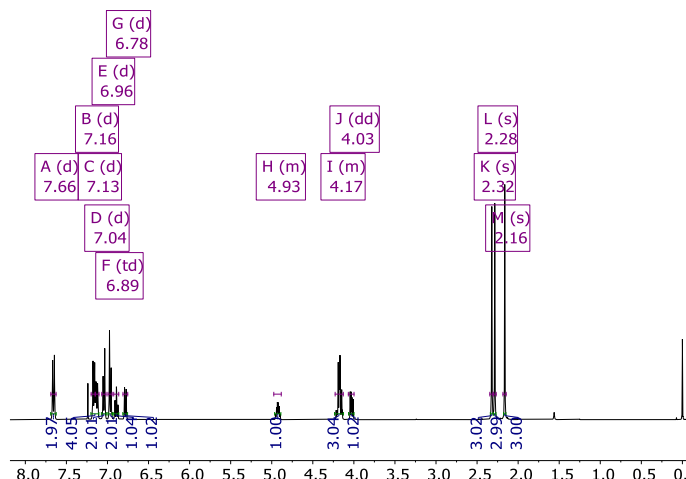
Figure 69: NMR spectrum of the synthesised N,3-di-p-tolyl-4-((o-tolyloxy)methyl)oxazolidin-2-imine.

^{1}H NMR (400 MHz, Chloroform-d) δ 7.66 (d, ^3J = 9.1 Hz, H arom., 2H, **9**), 7.16 (d, ^3J = 8.4 Hz, H arom., 2H, **13**), 7.13 (d, ^3J = 7.5 Hz, H arom., 2H, **10**), 7.04 (d, ^3J = 8.1 Hz, H arom., 2H, **5,7**), 6.96 (d, ^3J = 8.6 Hz, H arom., 2H, **12**), 6.89 (td, ^3J = 7.4, 1.1 Hz, H arom., 1H, **6**), 6.78 (d, ^3J = 7.9 Hz, H arom., 1H, **4**), 4.98 – 4.88 (m, CH, 1H, **2**), 4.23 – 4.13 (m, CH$_2$, 2H, **1''; 3**), 4.03 (dd, ^3J = 8.7, ^2J = 5.2 Hz, CH$_2$, 1H, **1'**), 2.32 (s, CH$_3$, 3H, **14**), 2.28 (s, CH$_3$, 3H, **11**), 2.16 (s, CH$_3$, 3H, **8**).

Further signals: 7.24 (CDCl$_3$), 1.56 (s, H$_2$O), 0.00 (s, TMS).
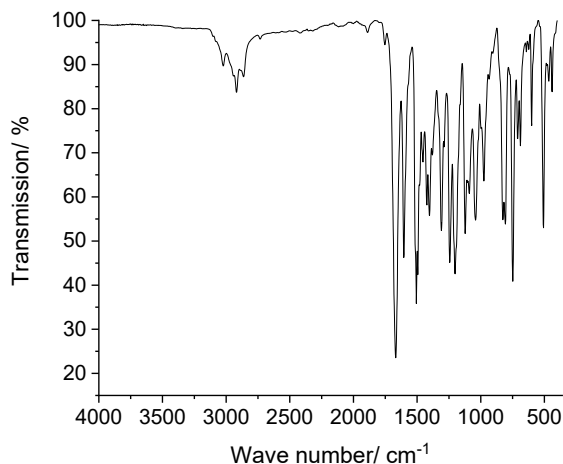
Figure 70: IR spectrum of the synthesised N,3-di-p-tolyl-4-((o-tolyloxy)methyl)oxazolidin-2-imine.

IR: 2918 cm^{-1} (w, CH$_3$/CH$_2$ vibration), 1668 cm^{-1} (vs, N=C vibration), 1604 cm^{-1} (vs, C=N stretching vibration), 1506 cm^{-1} (s, amide vibration), 1243 cm-1 (m, C-O stretching vibration), 1201 cm-1 (m, C-O stretching vibration), 748 cm-1 (m, CH arom), 507 cm-1 (m, ring vibration).[68,93]

ESI-MS: m/z [Da] 387.249 [C$_{25}$H$_{26}$N$_2$O$_2$+H] (calculated M+H 387.207).

1,3-di-*p*-Tolylurea was synthesised by reacting *p*-toluidine with *p*-TI. *p*-Toluidine (1.11 g, 10.3 mmol) was dissolved in 10 mL THF. *p*-TI (1.3 mL, 1.37 g, 10.3 mmol) was added to the stirred amine solution over a period of 15 min. A colourless to slightly yellowish precipitate was formed. It was further diluted with another 80 mL of THF. The precipitate was dried in vacuum after filtration and washed with THF. The product structure was confirmed by NMR and IR analysis.
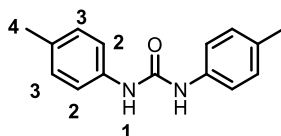
Scheme 35: Structure of the synthesised 1,3-di-p-tolylurea.
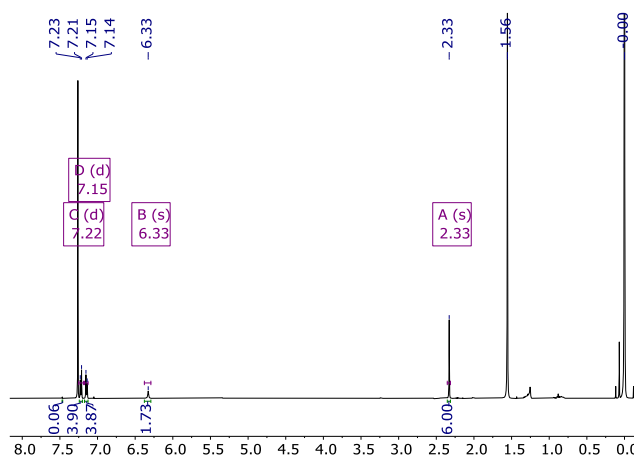
Figure 71: NMR spectrum of the synthesised 1,3-p-tolylurea.

^{1}H NMR (500 MHz, Chloroform-d) δ 7.22 (d, ^3J = 8.4 Hz, H arom., 4H, **2**), 7.15 (d, ^3J = 8.1 Hz, H arom.,4H, **3**), 6.33 (s, NH, 2H, **1**), 2.33 (s, CH₃, 6H, **4**).

Further signals: 7.26 (CDCl₃), 1.56 (s, H2O), 0.00 (s, TMS).
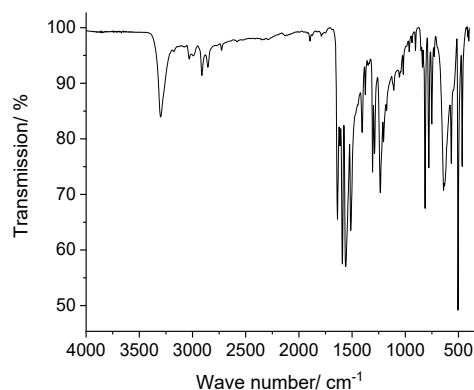
Figure 72: IR spectrum of the synthesised 1,3-di-p-tolylurea.

IR: 3300 cm^{-1} (m, NH stretching vibration), 2912 cm^{-1} (w, CH$_3$/CH$_2$ vibration), 1637 (s, C=O stretching vibration amide), 1591 cm^{-1} & 1560 cm^{-1} & 1514 cm^{-1} (s, urea amide band), 1234 (m, C-O stretching vibration), 813 cm^{-1} (m, CH arom.), 505 cm^{-1} (s, ring vibration).

7. Literature

[1]   S. Okumoto, S. Yamabe, *J Comput Chem* **2001**, *22*, 316–326.

[2]   G. Odian, *Principles of Polymerisation*, Wiley Interscience, Hoboken, **2004**.

[3]   P. J. Flory, *Principles of Polymer Chemistry*, Cornell University Pres, Ithaca, **1953**.

[4]   H. R. Kricheldorf, G. Schwarz, *Macromol Rapid Commun* **2003**, *24*, 359–381.

[5]   Y. Song, J. B. Fan, S. Wang, *Mater Chem Front* **2017**, *1*, 1028–1040.

[6]   E. L. Wittbecker, P. W. Morgan, *Journal of Polymer Science* **1959**, *40*, 289–297.

[7]   M. J. T. Raaijmakers, N. E. Benes, *Prog Polym Sci* **2016**, *63*, 86–142.

[8]   L. Abele, G. Avar, A. Awater, G. Baatz, R. Bock, H. Boden, *Kunststoff Handbuch Polyurethane*, Hanser, **1993**.

[9]   M. F. Sonnenschein, *Polyurethanes: Science, Technology, Markets, and Trends*, John Wiley & Sons, Inc., New Jersey, **2015**.

[10]   B. Eling, T. AbiSaleh, M. Anderson, G. Biesmans, J. Bosman, D. Daems, K. Dedecker, J. Deschaght, J. Dobbs, N. Duggan, B. Fogg, A. Hamilton, N. Hernandez, M. Jeffs, V. Kapasi, S. Lee, N. Limerkens, P. Mackey, S. O'Nien, A. Parfondry, C. Phanopoulos, W. Pille-Wolf, D. Randall, S. N Singh, D. Sparrow, D. Thorpe, G. Verhelst, J. Wilfrod-Brown, R. I. Zimmermann, *The Polyurethanes Book*, Huntsman International LLC, **2002**.

[11]   Douglas A.Wicks, Z. W. W. Jr., *Prog Org Coat* **1999**, *36*, 148–172.

[12]   J. Simon, F. Barla, A. Kelemen-Haller, F. Farkas, M. Kraxner, *Chromatographia* **1988**, *25*, 99–106.

[13]   N. Polyurethane, E. Delebecq, J. Pascault, B. Boutevin, U. De Lyon, F. Ganachaud, *Chem. Rev* **2013**, *113*, 80–118.

[14]   A. P. Gies, W. H. Heath, R. J. Keaton, J. J. Jimenez, J. J. Zupancic, *Macromolecules* **2013**, *46*, 7616–7637.

[15]   D. Braun, J. Weinert, *Die Angewandte Makromolekulare Chemie* **1979**, *78*, 1–19.

[16]   J. J. Monagle, *Journal of Organic Chemistry* **1962**, *27*, 3851–3855.

[17]   F. Parodi, *Comprehensive Polymer Science and Supplements* **1989**, *6*, 387–412.

[18]   N. Adam, G. Avar, H. Blankenheim, W. Friederichs, M. Giersig, E. Weigand, M. Halfmann,
       F.-W. Wittbecker, D.-R. Larimer, U. Maier, S. Meyer-Ahrens, K.-L. Noble, H.-G. Wussow,
       in *Ullmann's Encyclopedia of Industrial Chemistry*, Wiley-VCH Verlag GmbH & Co. KGaA,
       Weinheim, Germany, **2005**, pp. 603–611.

[19]   J. O. Akindoyo, M. D. H. Beg, S. Ghazali, M. R. Islam, N. Jeyaratnam, A. R. Yuvaraj, *RSC
       Adv.* **2016**, *6*, 114453–114482.

[20]   M. E. Dyen, D. Swern, *Chemical Reviewse* **1967**, *2*, 197–246.

[21]   Ikeda, Sakuji, Soga, Kazuo, *Verfahren Zur Herstellung von 2~Oxazolidon Und Seinen
       Derivaten*, **1977**, DE2713063A1.

[22]   T. E. Müller, C. Gürtler, S. Basu, C. Rangheard, D. Rivillo, W. Leitner, B. Köhler, *PROCESS
       FOR THE SYNTHESIS OF POLYOXAZOLIDINONE COMPOUNDS WITH HIGH
       STABILITY*, **2016**, WO2016128380A1.

[23]   T. E. Müller, C. Gürtler, *PROCESS FOR THE SYNTHESIS OF POLYOXAZOLIDINONE
       COMPOUNDS WITH HIGH STABILITY*, **2016**, WO2016/128380.

[24]   T. E. Müller, C. Gürtler, S. Basu, C. Rangheard, A. Weber, H. Vogt, W. Leitner,
       CATALYSTS FOR THE SYNTHESIS OF OXAZOLIDINONE COMPOUNDS, **2015**,
       WO15173110.

[25]   T. E. Müller, C. Gürtler, S. Basu, I. Latorre, C. Rangheard, W. Leitner, *CATALYSTS FOR
       THE SYNTHESIS OF OXAZOLIDINONE COMPOUNDS*, **2015**, WO1517311 1 A1.

[26]   G. P. G. Speranza, W. J. Peppel, *J Org Chem* **1958**, *23*, 1922–1924.

[27]   A. Sendijarević, V. Sendijarević, K. C. Frisch, *J Polym Sci A Polym Chem* **1987**, *25*, 151–
       170.

[28]   M. Žilić, A. Sendijarević, V. Sendijarević, K. C. Frisch, *J Polym Sci A Polym Chem* **1989**,
       27, 1843–1851.

[29]   J. S. Senger, I. Yilgor, J. E. McGrath, R. A. Patsiga, *J Appl Polym Sci* **1989**, *38*, 373–382.

[30] A. Prokofyeva, H. Laurenzen, D. J. Dijkstra, E. Frick, A. M. Schmidt, C. Guertler, C. Koopmans, A. Wolf, *Polym Int* **2017**, *66*, 399–404.

[31] V. Sendijarevic, A. Sendijarevic, H. H. Lekovic, H. H. Lekovic, K. C. Frisch, *Journal of Elastomers and Plastics* **1996**, *28*, 63–83.

[32] S. R. Sandler, F. Berg, G. Kitazawa, *J Appl Polym Sci* **1965**, *9*, 1994–1996.

[33] S. R. Sandler, *J Polym Sci A1* **1967**, *5*, 1481–1485.

[34] N. S. Gromakov, V. G. Khozin, V. A. Voskresenskii, *Khimiya i Khimicheskaya Tekhnologiya* **1976**, *19*, 440–443.

[35] S. Ghrab, L. Aroua, M. Beji, *J Heterocycl Chem* **2017**, *54*, 2397–2404.

[36] H. Šehović, A. Sendijarević, V. Sendijarević, K. C. Frisch, *J Polym Sci A Polym Chem* **1987**, *25*, 2729–2736.

[37] M. J. Galante, R. J. J. Williams, *J Appl Polym Sci* **1995**, *55*, 89–95.

[38] J. E. Herweh, W. Y. Whitmore, *J Polym Sci A1* **1970**, *8*, 2759–2773.

[39] A. Berkessel, E. Ertürk, *Adv Synth Catal* **2006**, *348*, 2619–2625.

[40] H. J. Thomas, M. Schuette, B. Eling, P. Matt, *Polyoxazolidone Und Deren Herstellung*, **2018**, WO2018/149844 A1.

[41] M. Uribe, K. A. Hodd, *Thermochim Acta* **1984**, *77*, 367–373.

[42] D. Caille, J.-P. Pascault, L. Tighzert, *Polymer Bulletin* **1990**, *24*, 31–38.

[43] B. Guenther Soares, S. Livi, J. Duchet-Rumeau, J. F. Gerard, *Polymer (Guildf)* **2012**, *53*, 60–66.

[44] B. Eling, H. J. Thomas, P. Deglmann, J. Hengelsberg, T. Pelzer, G. A. Luinstra, *VERFAHREN ZUR HERSTELLUNG VON OXAZOLIDINONGRUPPEN AUFWEISENDEN VERBINDUNGEN*, **2018**, WO2018/167228A1.

[45] C. Holtgrewe, H. Küster, T. Bachon, A. Ferencz, O. Lammerschop, R. Schönfeld, C. Mai, *OXAZOLIDINON- UND ISOCYANURAT-VERNETZTE MATRIX FÜR FASERVERSTARKTES MATERIAL*, **2016**, WO 2016/102359 A1.

[46] M. Flores, X. Fernández-Francos, J. M. Morancho, À. Serra, X. Ramis, *J Appl Polym Sci* **2012**, *125*, 2779–2789.

[47]   H. J. Thomas, P. Desbois, *Bulkpolymerisierung von Polyoxazolidon*, **2020**, WO 2020/016276 A1.

[48]   Covestro, "Desmopan 1050D Properties," can be found under https://solutions.covestro.com/en/products/desmopan/desmopan-1050d_79939078-05122320?SelectedCountry=DE#hazardsacc.toeuclp, **2018**.

[49]   Covestro, "Desmopan 3072D Properties," can be found under https://solutions.covestro.com/en/products/desmopan/desmopan-3072d_00943174-00002792?SelectedCountry=DE#hazardsacc.toeuclp, **2018**.

[50]   BASF SE, "Ultrason ® E, S, P (PESU, PSU, PPSU)," can be found under https://www.basf.com/global/documents/en/products-and-industries/car-interior-ideal/2019/BASF_Ultrason_brochure.pdf, **2021**.

[51]   H. J. Altmann, M. Clauss, S. König, E. Frick-Delaittre, C. Koopmans, A. Wolf, C. Guertler, S. Naumann, M. R. Buchmeiser, *Macromolecules* **2019**, *52*, 487–494.

[52]   R. M. Mathur, K. Prajapati, A. Varshney, C. Lines, S. Kanpur-india, **2012**, *3*, 2553–2560.

[53]   H. J. Altmann, M. Clauss, S. König, E. Frick-Delaittre, C. Koopmans, A. Wolf, C. Guertler, S. Naumann, M. R. Buchmeiser, *Macromolecules* **2019**, *52*, 487–494.

[54]   R. R. Dileone, *J Polym Sci A1* **1970**, *8*, 609–615.

[55]   O. Nuyken, S. D. Pask, *Polymers (Basel)* **2013**, *5*, 361–403.

[56]   T. Endo, R. Hoogenboom, *Handbook of Ring-Opening Polymerisation*, Wiley-VCH Verlag GmbH & Co. KGaA, Weinheim, **2009**.

[57]   T. Pelzer, B. Eling, H. J. Thomas, G. A. Luinstra, *Eur Polym J* **2018**, *107*, 1–8.

[58]   H. C. Chitwood, B. T. Freure, *J Am Chem Soc* **1946**, *68*, 680–683.

[59]   Y. Gao, Y. Qin, X. Zhao, F. Wang, X. Wang, *Journal of Polymer Research* **2012**, *19*, 9878.

[60]   R. J. Young, P. A. Lovell, *Introduction to Polymers*, CRC Press, Boca Raton, **2011**.

[61]   J. P. Pascault, R. J. J. Williams, *Handbook of Polymer Synthesis, Characterisation, and Processing* **2013**, 519–533.

[62]   T. Liu, B. Han, L. Zhang, M. Wu, A. Xing, X. Miao, Y. Meng, X. Li, *RSC Adv* **2016**, *6*, 14211–14221.

[63] T. K. L. Nguyen, S. Livi, B. G. Soares, S. Pruvost, J. Duchet-Rumeau, J. F. Gérard, *ACS Sustain Chem Eng* **2016**, *4*, 481–490.

[64] A. J. Bloodworth, A. G. Davies, *Journal of the Chemical Society (Resumed)* **1965**, 6858.

[65] E. Delebecq, J. Pascault, B. Boutevin, *Chem Rev* **2013**, *113*, 80–118.

[66] E. Vowinkel, P. Gleichenhagen, *Tetrahedron Lett* **1974**, 143–146.

[67] Dr. phil. habil. H. Arnold, Dr. R. Rebling, *Verfahren Zur Herstellung von Imidazolidonen*, **1963**, DE1226589B.

[68] A. Baba, K. Iwamoto, H. Matsuda, *特願平3-20921*, **1991**, 特開平4-261164.

[69] H. Ulrich, *Journal of Polymer Science: Macromolecular Reviews* **1976**, *11*, 93–133.

[70] M. G. González, J. C. Cabanelas, J. Baselga, M. Gonzlez, J. Carlos, J. Baselg, *Infrared Spectroscopy - Materials Science, Engineering and Technology* **2012**, 2, 261–284.

[71] W. Neumann, P. Fisher, *Angewandte Chemie International Edition in English* **1962**, *1*, 621–625.

[72] N. Wiberg, *Lehrbuch Der Anorganischen Chemie*, Wiley-VCH Verlag GmbH & Co. KGaA, **2007**.

[73] S. Dahi, A. Zilkha, *Eur Polym J* **1980**, *16*, 471–473.

[74] T. E. Müller, C. Gürtler, S. Basu, W. Leitner, *Method for the Production of Oxazolidinone Compounds*, **2014**, WO2014076024A1.

[75] Y. Iwakura, S. Izawa, *J Org Chem* **1964**, *29*, 379–382.

[76] D. A. Wicks, Z. W. Wicks, *Prog Org Coat* **2001**, *41*, 1–83.

[77] F. Wang, C. Xu, Z. Li, C. Xia, J. Chen, *J Mol Catal A Chem* **2014**, *385*, 133–140.

[78] C. Betti, D. Landini, A. Maia, *Synlett* **2006**, *2006*, 1335–1338.

[79] W. Cheng, Q. Su, J. Wang, J. Sun, F. Ng, *Catalysts* **2013**, *3*, 878–901.

[80] SigmaAldrich, "MSDS DMPU," can be found under https://www.sigmaaldrich.com/DE/de/product/aldrich/41661, **n.d.**

[81] A. L. Silva, J. C. Bordado, *Catal Rev Sci Eng* **2004**, *46*, 31–51.

[82]   J. F. Coetzee, in *Recommended Methods for Purification of Solvents and Tests for Impurities*, Elsevier, **1982**, pp. 16–18.

[83]   S. Kubik, in *Römpp [Online]* (Eds.: F. Böckler, B. Dill, U. Dingerdissen, G. Eisenbrand, F. Faupel, B. Fugmann, T. Gamse, R. Matissek, G. Pohnert, G. Sprenger), Thieme Gruppe PP - Stuttgart, **2004**.

[84]   M. G. Evans, M. Polanyi, *Transactions of the Faraday Society* **1935**, *31*, 875–894.

[85]   K. P. Menard, *Dynamic Mechanical Analysis*, CRC Press, Boca Raton, **2008**.

[86]   T. G. Fox, P. J. Flory, *J Appl Phys* **1950**, *21*, 581–591.

[87]   T. G. Fox, P. J. Flory, *Journal of Polymer Science* **1954**, *14*, 315–319.

[88]   M. Kitayama, Y. Iseda, F. Odaka, S. Anzai, K. Irako, *Rubber chemistry and technology* **1992**, *53*, 1–13.

[89]   J. Chambers, J. Jiricny, C. B. Reese, *Fire Mater* **1981**, *5*, 133–141.

[90]   M. Lai, J. Liu, *J Therm Anal Calorim* **2004**, *77*, 935–945.

[91]   D. C. Batesky, M. J. Goldfogel, D. J. Weix, *J Org Chem* **2017**, *82*, 9931–9936.

[92]   L. Li, Z. P. Wang, G. R. Tian, X. Y. Song, S. X. Sun, *J Cryst Growth* **2008**, *310*, 1202–1205.

[93]   M. Hesse, H. Meier, B. Zeeh, *Spektroskopische Methoden in Der Organischen Chemie*, Thieme, Stuttgart, **2005**.

[94]   B. Dobinson, W. Hofmann, B. P. Stark, *Determination of Epoxide Groups*, Pergamon Press, London, **1969**.

[95]   F. G. Garcia, B. G. Soares, *Polym Test* **2003**, *22*, 51–57.

[96]   J. S. Senger, I. Yilgor, J. E. McGrath, R. A. Patsiga, *J Appl Polym Sci* **1989**, *38*, 373–382.

8. Appendix

8.1.   List of hazardous substances according to GHS

The chemicals used in this work are listed with safety instructions (Table 16).

Table 16: Safety information according to the individual material safety data sheets. Safety informations and waste disposal

Substance	GHS pictogram	Hazard phrases	Precaution phrases
1,3,5-tris(4-methylphenyl)-1,3,5-triazine-2,4,6(*1H,3H,5H*)-trione (*p*-tolylisocyanurate)	No classification according to GHS.		
1,3-Diethyl-1,3-diphenylurea	GHS07 **Warning**	H302, H412	P273
1,3-di-*p*-tolylcarbodiimid	GHS07 **Warning**	H302, H312, H315, H319, H332, H335	P261, P280, P305+P351+P338
1,3-di-*p*-tolylurea	GHS07 **Warning**	H302, H312, H332	P261, P264, P270, P271, P280, P304+P340+P312, P301+P330, P305+P353+P363, P501
1-Ethyl-3-methyl-imidazolium-acetat (EMIM Acetate)	Non-hazardous substance according to GHS.		
1-Methyl-2-pyrrolidon (NMP)	GHS07, GHS08 **Danger**	H315, H319, H335, H360FD	P201, P202, P261, P302+P352, P305+P351+P338, P308+P313

Substance	GHS pictogram	Hazard phrases	Precaution phrases
1-Octanol	GHS07 **Warning**	H319, H412	P273, P305+P351+P338
2-Ethyl-1-hexanol	GHS07 **Warning**	H315, H319, H332, H335	P302+P352, P304+P340+P312, P305+P351+P338
4,4'-MDI	GHS07, GHS08 **Danger**	H315, H317, H319, H332, H334, H335, H351, H373	P260, P280, P305+P351+P338, P342+P311
5-[(2-methyl-phenoxy)methyl]-3-(4-methylphenyl)-2-oxazolidinone (model oxazolidinone)	No classification according to GHS.		
BADGE (DER 332)	GHS07 **Warning**	H315, H317, H319	P280, P305+P351+P338
Benzoyl chloride	GHS05, GHS06 **Danger**	H302+H312, H314, H317, H331	P280, P301+P312+P330, P301+P330+P331, P303+P361+P353, P304+P340+P311, P305+P351+P338
BiCl$_3$	GHS07 **Warning**	H315, H319	P302+P352, P305+P351+P338
BiCl$_3$(TPPO)$_3$	No classification according to GHS.		
BMPC	No classification according to GHS.		

Substance	GHS pictogram	Hazard phrases	Precaution phrases
Chloroform-*d*	GHS06, GHS08 **Danger**	H315, H319, H331, H351, H361d, H372	P260, P280, P301+P312+P330, P304+P340+P311, P305+P351+P338, P403+P233
Dicyclohexylcarbodiimide (DCC)	GHS05, GHS06 **Danger**	H302, H311, H317, H318	P280, P301+P312+P330, P302+P352+P312, P305+P351+P338+ P310
DCM	GHS07, GHS08 **Warning**	H315, H319, H336, H351	P201, P302+P352, P305+P351+P338, P380+P313
DIBIS	GHS05, GHS07, GHS09 **Warning**	H302, H315, H318, H411	P202, P273, P305+P351+P338, P301+P310, P405, P501
DMF	GHOS02, GHS07, GHS08 **Danger**	H226, H312+H332, H319, H360D	P210, P280, P303+P361+P353, P304+P340+P312, P305+P351+P338, P308+P313
DMI	GHS05, GHS07, GHS08 **Danger**	H302, H318, H361, H373	P280, P305+P351+P338
DMPU	GHS05, GHS07, GHS08 **Danger**	H302, H317, H318, H361	P280, P305+P351+P338
DMSO	Non-hazardous substance according to GHS.		

Substance	GHS pictogram	Hazard phrases	Precaution phrases
DMSO-*d6*	Non-hazardous substance according to GHS.		
Ethanol	GHOS02, GHS07 **Danger**	H225, H319	P210, P240, P305+P351+P338, P403+P233
Ethyl acetate	GHOS02, GHS07 **Danger**	H225, H319, H336	P210, P261, P305+P351+P338
FeCl$_3$	GHS05, GHS07 **Danger**	H290, H302, H315, H318	P234, P264, P280, P301+P312, P302+P352, P305+P351+P338
FeCl$_3$(TPPO)$_3$	No classification according to GHS yet.		
LiCl	GHS07 **Warning**	H302, H315, H319	P301+P312+P330, P302+P352, P305+P351+P338
Mesitylene	GHOS02, GHS07, GHS08, GHS09 **Danger**	H226, H304, H315, H332, H335, H411	P210, P273, P301+P310+P331, P302+P352, P304+P340+P312
Methanol	GHS02, GHS05, GHS08 **Danger**	H225, H301+H311+H331, H370	P210, P233, P280, P301+P310, P303+P361+P353, P304+P340+P311
MPPO	GHS07, GHS08 **Warning**	H302, H351, H412	P201, P273, P301+P312+P330, P308+P313

Substance	GHS pictogram	Hazard phrases	Precaution phrases
N,3-di-*p*-tolyl-4-((*o*-tolyloxy)methyl)oxazolidin-2-imine (model oxazolidine imine)	No classification according to GHS.		
o-cresyl glycidyl ether (OCGE)	GHS07, GHS08, GHS09 **Warning**	H315, H317, H341, H411	P201, P273, P280, P308+3P13, P391
o-dichloro benzene	GHS07, GHS09 **Warning**	H302+H332, H315, H317, H319, H335, H410	P273, P280; P301+312+P330, P302+P352, P304+P340+P312, P305+P351+P338
Ph₄PBr	Non-hazardous substance according to GHS.		
Ph₄PCl	Non-hazardous substance according to GHS.		
Phosphoric acid (85%)	GHS05, GHS07 **Danger**	H290, H302, H314	P234, P270, P280, P301+P312, P303+P361+P353, P305+P351+P338
Poly(oxazolidine-2-one)	No classification according to GHS.		
***p*-TI urethanes**	No classification according to GHS.		
p-tolylisocyanate (*p*-TI)	GHS07, GHS08 **Danger**	H302+H312+H332, H315, H319, H334, H335	P261, P280, P305+P351+P338, P342+P311
Sulfolane	GHS07 **Warning**	H302	P301+P312+P330
TBAB	GHS07 **Warning**	H302, H319, H412	P273, P301+P312+P330, P305+P351+P338

Substance	GHS pictogram	Hazard phrases	Precaution phrases
TBPO	GHS05, GHS07 **Danger**	H302, H312, H314, H332	P280, P305+P351+P338, P310
TEP	GHS07 **Warning**	H302, H319	P301+P312+P330, P305+P351+P338
Toluene	GHS02, GHS07, GHS08 **Danger**	H225, H304, H315, H336, H361d, H373, H412	P201, P210, P273, P301+P310+P331, P302+P352, P308+P313
TOPO	GHS05 **Danger**	H315, H318, H412	P273, P280, P305+P351+P338+ P310
TPPO	GHS07 **Warning**	H302, H315, H319, H335	P261, P305+P351+P338
Triton X100	GHS05, GHS07, GHS09 **Danger**	H302, H315, H318, H410	P273, P280, P301+P312+P330, P302+P352, P305+P351+P338, P310
ZnCl$_2$	GHS05, GHS07, GHS09 **Danger**	H302, H314, H410	P260, P280, P301+P312+P330, P303+P361+P353, P304+P340+P310, P305+P351+P338
ZnCl$_2$(TBPO)$_2$	No classification according to GHS.		
ZnCl$_2$(TOPO)$_2$	No classification according to GHS.		
ZnCl$_2$(TPPO)$_2$	No classification according to GHS.		

The CMR substances are listed in Table 17.

Table 17: List of the CMR substances used.

Substance	CAS number	Procedure	Used amount	Category
101-68-8	4,4'-MDI	Monomer for polymerisation	5 kg	C2
865-49-6	Chloroform-d	NMR solvent	750 mL	C1B, M2, R2
75-09-2	DCM	Solvent used in precipitation	5 L	C2
68-12-2	DMF	Cleaning	2 L	R1B
80-73-9	DMI	Solvent for synthesis	100 mL	R2
7226-23-5	DMPU	Solvent for synthesis	7 L	R2
707-61-9	MPPO	Catalyst for carbodiimide formation	0.15 g	C2
872-50-4	NMP	Solvent for synthesis	20 mL	R1B
2210-79-9	OCGE	Monomer model system	1.2 kg	M2
108-88-3	Toluene	Liquid chromatography solvent	2 L	R2

8.2.   **Supporting figures**

Only low quantities of oxazolidine imine were obtained after column chromatography of a product from a model system reaction, which explains the low signal-to-noise ratio. The main impurities were the eluents toluene and ethyl acetate, along with traces of p-tolylisocyanurate and oxazolidinone that were also detected.
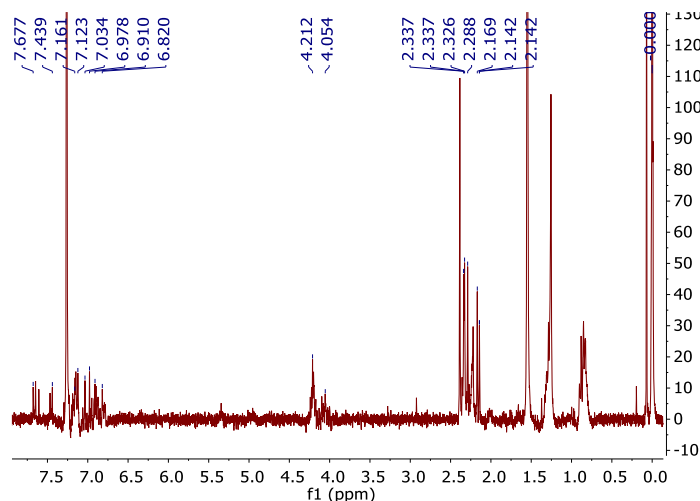
Figure 73: NMR spectrum of the fraction containing the oxazolidine imine isolated by column chromatography from the oxazolidinone formation product.
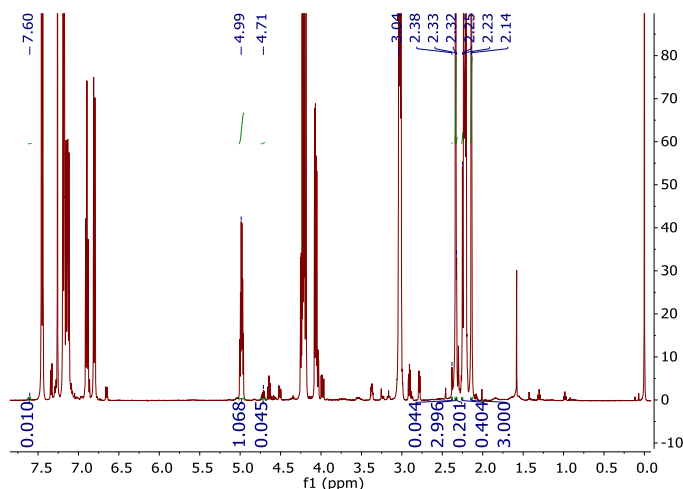
Figure 74: NMR spectrum of an untreated product of a mono-oxazolidinone formation experiment conducted according to general procedure.

The LiCl-induced polyether formation was observed by the CH_2 signals, which appeared around 4 ppm. The oxirane signal at 2.7 ppm, in contrast, almost disappeared, indicating the ring-opening. The appearance of the broad OH-band from 3200 to 3600 cm^{-1} and the broad C-O-C ether band from 1060 to 1100 cm^{-1} indicated the formation of polyether.
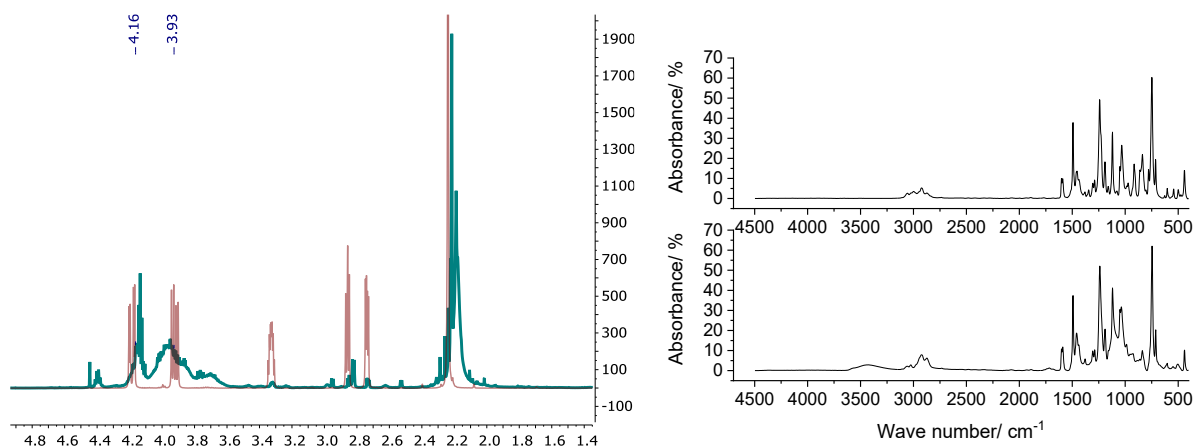
Figure 75: NMR and IR of the reaction product of OCGE and 1 mol% LiCl after 24 h at 160 °C (blue). The neat OCGE is shown for reference (red). The IR spectra of neat OCGE (right top) and of the reaction product after 24 h (right bottom) are shown.
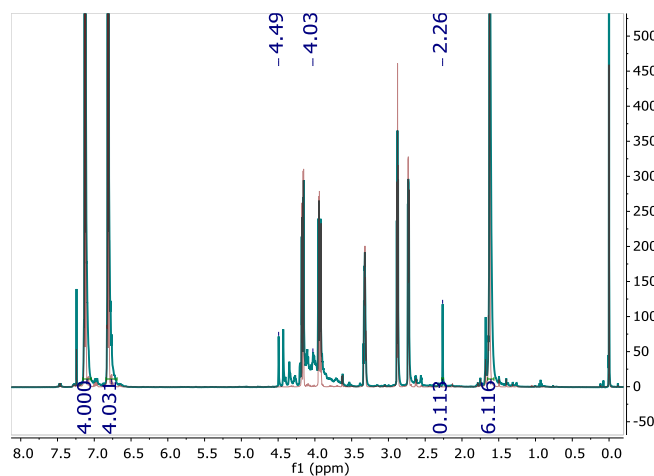

Figure 76: Full spectrum of neat BADGE (red) and BADGE with 1 mol% BMPC for 6 h at 190 °C.
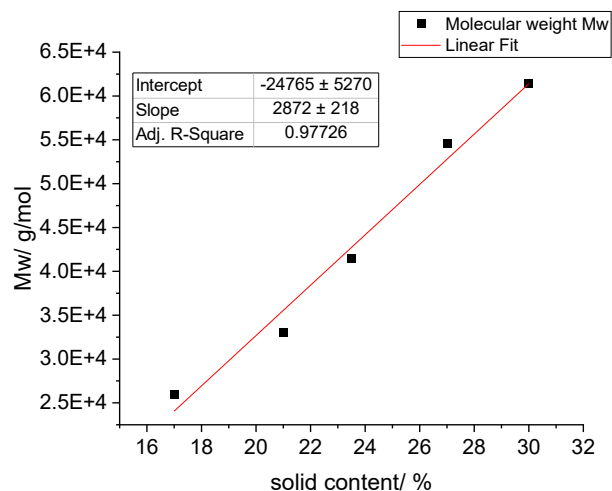

Figure 77: Weight-average molecular weight M_w of the final products yielded in DMPU plotted against the final solid contents achieved. The increase in M_w with increasing solid content is obvious.
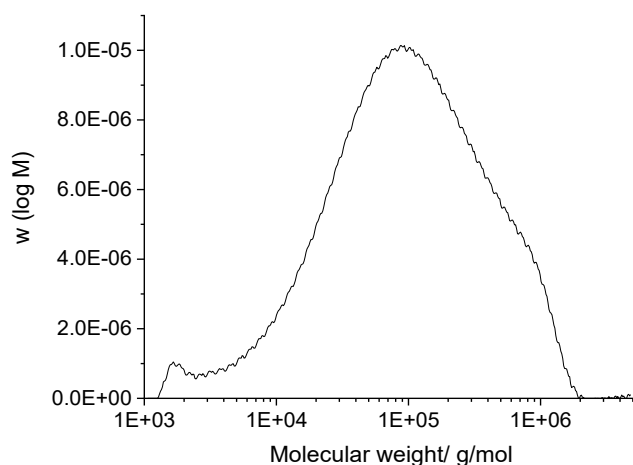
Figure 78: Molecular weight distribution of a polymerisation using water as co-catalyst. The tailing is obvious. It is most likely caused by the polyurea formation and the resulting branching or crosslinking.

The isocyanate band at 2270 cm-1 (left) appears in the experiment with a dosing time of 60 minutes, becoming evident after 15 minutes and 30 minutes. No free isocyanate was in the final product.
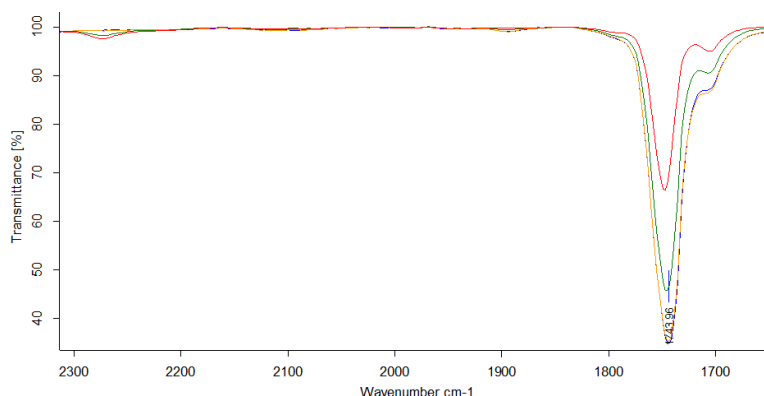

Figure 79: Zoom-In of an exemplarily IR spectra of the proceeding reaction when a dosing time of 60 min was used. The colours show the reaction time; 15 min (red), 30 min (green), 60 min (orange, end of feed) and the final product at room temperature (blue).

The oxazolidine imine formation reaction was carried out by reacting OCGE with 1,3-di-p-tolyl carbodiimide. The two aromatic protons (7.6 ppm) used for quantification are visible on the left side. The three distinct methyl groups can be observed on the right, ranging from 2.16 ppm to 2.31 ppm.
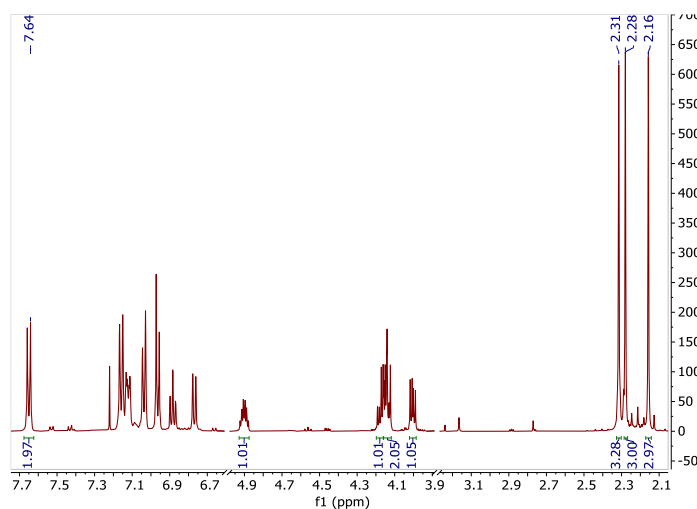
Figure 80: NMR spectrum of the reaction product of 1,3-p-tolyl carbodiimide and OCGE yielding oxazolidine imine.
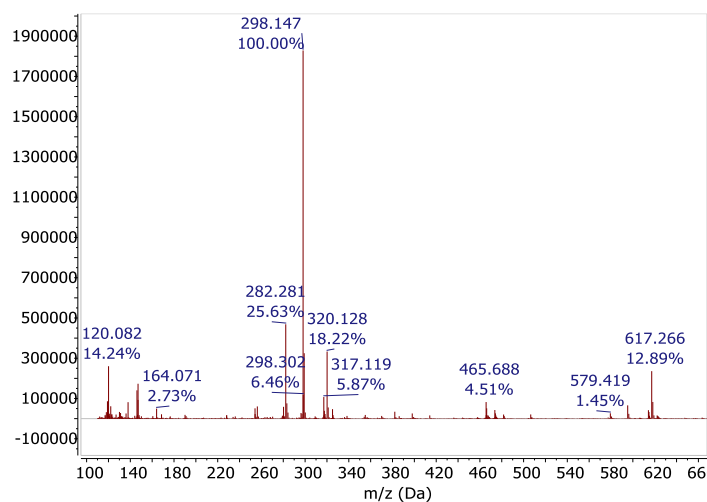

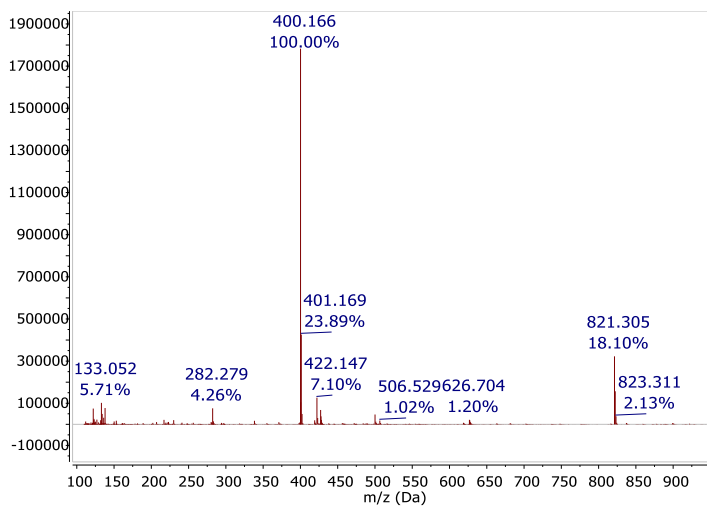*Figure 81: ESI-MS spectrum of the precipitated mono-oxazolidinone.*

Figure 82: ESI-MS spectrum of the synthesised p-tolylisocyanurate.
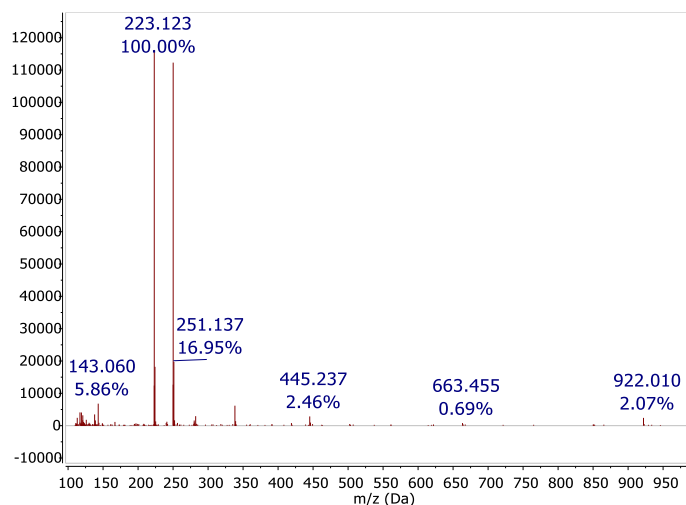
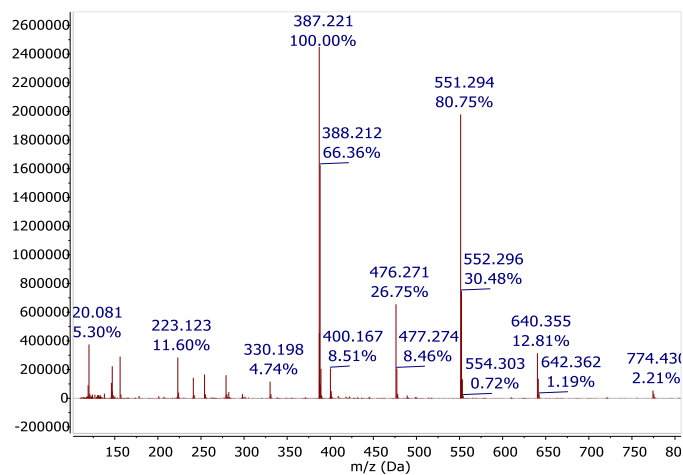*Figure 83: ESI-MS of the synthesised 1,3-p-tolylcarbodiimide.*

Figure 84: ESI-MS spectrum of the reaction product of carbodiimide and epoxide yielding the oxazolidine imine.
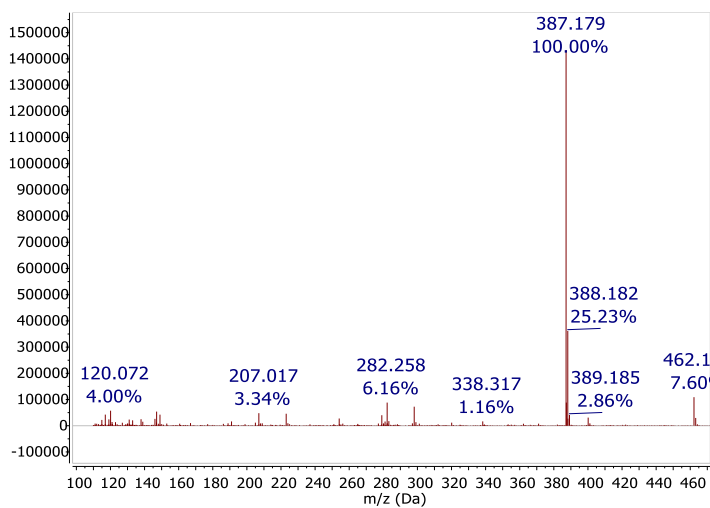

Figure 85: ESI-MS spectrum of the fraction containing the oxazolidine imine isolated by column chromatography from the oxazolidinone formation product.

9. Acknowledgements

Besonders danken möchte ich allen voran meiner langjährigen Partnerin und besten Freundin Marlena Gaul. Ferner möchte ich mich bei allen Mitgliedern des Arbeitskreises Luinstra für die gute und kollegiale Zusammenarbeit danken. Hier seien vor allem meine Büro- und Laborkommilitonen Yannick Wencke, Niklas Voigt, Mengyu Zhang, Tim Beermann sowie Jessica Redmann und Wolf Ammann genannt. Berend Eling möchte ich für die zahlreichen, fruchtbaren Besprechungen, die maßgeblichen Einfluss auf die Arbeit hatten sowie das Thema explizit bedanken. Herrn Gerrit Luinstra danke ich für die Aufnahme in den Arbeitskreis und die Übernahme der Betreuung meiner Arbeit.

10.   Declaration of oath

Hiermit versichere ich an Eides statt, die vorliegende Dissertationsschrift selbst verfasst und keine anderen als die angegebenen Quellen und Hilfsmittel benutzt zu haben. Sofern im Zuge der Erstellung der vorliegenden Dissertationsschrift generative Künstliche Intelligenz (gKI) basierte elektronische Hilfsmittel verwendet wurden, versichere ich, dass meine eigene Leistung im Vordergrund stand und dass eine vollständige Dokumentation aller verwendeten Hilfsmittel gemäß der Guten wissenschaftlichen Praxis vorliegt. Ich trage die Verantwortung für eventuell durch die gKI generierte fehlerhafte oder verzerrte Inhalte, fehlerhafte Referenzen, Verstöße gegen das Datenschutz- und Urheberrecht oder Plagiate.